

**Effects of Urban Development on the Hydrology and Water Storage
Capacity of Isolated Depressional Wetlands**

(EPA#L CD-95417909-0)

FINAL REPORT SUBMITTED TO
U.S. Environmental Protection Agency

PRINCIPAL INVESTIGATORS:

Matthew J. Cohen, Ph.D.
University of Florida, School of Forest Resources and Conservation

Daniel L. McLaughlin, Ph.D.
University of Florida, School of Forest Resources and Conservation

EXECUTIVE SUMMARY

Growing appreciation of the myriad ecosystem services provided by wetlands has prompted large scale conservation, regulation, and mitigation efforts. However, two relevant questions continue to be debated: 1) should isolated wetlands be under federal jurisdiction, and 2) do condition assessments used in mitigation sufficiently represent wetland function? This research evaluated the hydrology of 11 isolated wetlands, specifically north Florida cypress domes, to determine functions of isolated wetlands that span a gradient of wetland condition. Understanding how disturbance affects hydrologic regime and flows provided salient insights regarding important functions of isolated wetlands that may remain, or are even amplified, in systems with impaired condition. We monitored wetland stage in our 11 sites for over two years to document hydrologic regime and groundwater and evapotranspiration (ET) fluxes. Accurate quantification of ET and groundwater fluxes, however, required methodological considerations, which resulted in refinement and novel applications of the White (1932) method. Chapters 1 and 2 focus on these methodological refinements, which are then used in Chapters 3 to explore the distinction between wetland condition and function. Chapter 4 presents a landscape-scale hydrologic model motivated by results in Chapter 3. This model simulates the effect of isolated wetland area and density on regional water table dynamics and thus the variation in stream flow at the landscape scale.

White Method for Wetland ET and Groundwater Exchange

The White method has been routinely used to estimate phreatophyte transpiration (i.e., groundwater uptake from deep rooted vegetation) from diurnal groundwater variation, but can also yield total ET and groundwater exchange in wetland systems. Applications in surface water systems, including flooded wetlands, have been extremely rare due to two constraints, namely

the need for high resolution stage data and an accurate specific yield (S_y) of flooded conditions. S_y , a key parameter of the White method, determines the water level change that is induced by ET or rain fluxes. S_y of surface waters is assumed to be near 1.0, whereas S_y of groundwater systems is much lower (ca. 0.1 – 0.3), which amplifies groundwater decline from ET fluxes resulting in a response far easier to detect with less accurate water level recorders. Pressure transducers with requisite accuracy and resolution to detect diurnal variation in surface waters are now available but require compensation for barometric pressure variation. Typically, barometric pressure transducers are installed in the head space of monitoring wells where they are exposed to a slightly but significantly different thermal regime than the down-well transducers. In Chapter 1, we demonstrate the sensitivity of these transducers to temperature and the large errors in water levels and subsequent inferences of ET and groundwater exchange that result when they are installed in ambient thermal conditions. For example, uncorrected ET rates can be as much as 2 – 4 times actual values, with particularly significant errors arising in the winter months where diel temperature variation is largest in north Florida. A simple correction, namely installing dry wells where the barometric pressure transducers experience a buffered thermal regime, corrects for these errors and facilitates the use of the White Method for ET and groundwater flow measurements in surface water systems. This new sensor protocol was used throughout this work, and was published in the journal *Water Resources Research*.

The few studies that have applied the White method in flooded wetlands assumed S_y to be 1.0, but rapid equilibration with exposed wetland areas may reduce S_y with decreasing stage. In Chapter 2, we document the occurrence of this rapid equilibration that creates stage-dependent variation in S_y ; we give the function describing this relationship the term ecosystem specific yield (ESY). Two approaches were investigated to obtain site-specific ESYs, both of which

resulted in reasonable ET rates across all stage while assuming S_y of 1.0 overestimated ET at low to intermediate stage (by as much as a factor of 14). The methodological refinements provided by this work along with those of Chapter 1 (i.e., proper installation of barometric pressure transducers) allow accurate application of the White method in wetlands, where it simultaneously provides empirical, low cost measurements of ET and groundwater exchange. The implications of these methodological refinements are difficult to overstate: the ability to quickly, and at low cost, evaluate several ecosystem services (water storage, water use, microclimate regulation, groundwater recharge) of individual wetlands can readily be incorporated into regional wetland assessment efforts.

Wetland Condition versus Function

In Chapter 3, we document hydrologic regime (i.e., mean and variation in daily stage and flooding duration) and, using the White method and site-specific ESY relationships, quantify ET and groundwater exchange in our 11 cypress domes. These domes spanned a gradient of land use intensity and assessed wetland condition (via Florida's Uniform Mitigation Assessment Method; UMAM) allowing us to compare hydrologic regime and fluxes across a disturbance gradient. Surprisingly, there was no systematic variation in hydrologic regime with increased land use intensity. The land use effects on ET rates, however, were clear with increased ET in higher land use intensities. Increases in ET were concordant with increases in leaf area index (LAI), indicating amplified wetland productivity (perhaps due to nutrient enrichment, preclusion of grazing, and exclusion of fire) and water use in urban and agriculture settings. The fact that functions related to ET (latent heat exchange) and productivity (C-sequestration, support of biogeochemical cycles) remain and may even be amplified in systems with low assessed condition critically questions how we currently value "working wetlands". Moreover, frequent

reversals in groundwater flow direction were observed at all sites; this source/sink behavior of isolated wetlands likely buffers water table dynamics, providing an important function at the regional scale.

Isolated Wetlands as Water Storage Capacitors to Buffer Regional Water Table

The source/sink function of isolated wetlands documented in Chapter 3 motivated development of a landscape-scale hydrologic model to simulate the effect of isolated wetland area and density on regional water table dynamics. In Chapter 4, we integrate models of soil moisture, upland water table, and wetland stage dynamics to simulate daily water table depth as a function of wetland area and density. The hydraulic influence of isolated wetlands was clear, where increasing wetland area or density decreased the frequency of both high and low water table events. As such, isolated wetlands buffer water table response to wet and dry periods and act as water storage capacitors in the landscape. That is, even without a direct connection (via surface or subsurface pathways) to other water bodies, there is a strong and predictable influence of isolated wetlands on the surficial aquifer and the regional surface waters it supports. In short, we found an indirect, but nonetheless significant nexus between isolated wetlands and downstream water bodies.

Conclusion

Hydrology is the primary determinant of wetland processes, and understanding the functions of isolated wetlands thus requires thorough hydrologic investigations. This work alleviated the constraints that have limited applications of the White method in wetlands, which yields integrated measurements of ET and groundwater exchange across heterogonous systems. Applying the method in 11 north Florida cypress domes that spanned a land use gradient clarified the distinction between wetland condition and function, with critical implications to

current wetland regulation and mitigation. Further, our empirical and modeling results demonstrate the ability of “isolated” wetlands to exert hydraulic control on the regional water table and ultimately the downstream water bodies it supports, questioning the current notion of no significant nexus between isolated wetlands and traditional waters of the United States.

The findings of this work, and their regulatory implications, have and will continue to be disseminated in multiple venues. The four chapters represent four stand-alone publications submitted to peer-reviewed journals, with one currently in publication. This work will be presented at the upcoming 2012 American Water Resources Association Conference, and has already been presented at two international wetland conferences (Society of Wetland Scientists and INTECOL). Additionally, we were invited by St. Johns River Water Management District to share our findings with their staff during their spring 2012 district meeting. Notably, this meeting and the conference presentations initiated collaborative efforts to further investigate the importance of isolated wetlands, a current and critical issue in wetland policy.

TABLE OF CONTENTS

Section	Page
Executive Summary	2
Chapter 1. Thermal artifacts in measurements of fine scale water level variation	8
Chapter 2. Ecosystem specific yield for estimating evapotranspiration and groundwater exchange from diel surface water variation	15
Chapter 3. Realizing ecosystem services: Wetland hydrologic function along a gradient of ecosystem condition	47
Chapter 4. Landscape water storage capacitance: A nexus between isolated wetlands and downstream water bodies	70
References Cited	92

CHAPTER 1

Thermal Artifacts in Measurements of Fine Scale Water Level Variation

Abstract

Estimation of evapotranspiration (ET) from observed diurnal surface water level fluctuations may be highly sensitive to measurement errors. Available total pressure transducers (TPT) can provide requisite accuracy and precision but require atmospheric pressure compensation with equally accurate and precise barometric pressure transducers (BPT). BPT installation location determines thermal setting, and sensor sensitivity to temperature could affect compensated water levels and any analyses requiring fine scale data. We investigated effects of BPT installation location on compensated surface water levels and estimates of ET and net infiltration with the White method in four isolated forested wetlands in north Florida. Water levels compensated with two differently positioned BPTs, one in buffered thermal conditions (BPT_{buf} ; dry well at the TPT depth) and one in ambient temperatures (BPT_{amb} ; screened well head-space), resulted in markedly different diurnal signatures. Both displayed the expected diurnal pattern, but compensation with BPT_{amb} amplified diurnal variation by as much as 1.5 cm, greatly overestimated ET, and suggested net exfiltration, while BPT_{buf} compensation resulted in ET estimates similar to PET and suggested net infiltration. BPT temperature sensitivity followed diurnal temperature variation and generated systematic water level bias with the same signature as the expected trend, making these errors difficult to detect and underscoring the importance of proper BPT positioning.

Introduction

Diurnal fluctuations due to evapotranspiration (ET) have been observed in stream flow (Bond *et al.*, 2002; Wondzell *et al.*, 2009) and in other surface water bodies such as flooded wetlands (Hill and Neary, 2007). Diurnal surface water fluctuations, however, are modest compared to those observed in groundwater, attributable to aquifer specific yield differences. In surface water systems, where S_y is generally – though perhaps erroneously (Hill and Neary, 2007; Sumner, 2007) – assumed to be near 1, the magnitude of diurnal variation is the extant ET rate (e.g., 0.4 cm/day in summer). In contrast, phreatophyte transpiration of 0.4 cm/day from an aquifer with $S_y = 0.2$ will induce a water table decline of 2 cm/day, a five-fold increase.

Diurnal variation in groundwater levels has been used with the White method (White, 1932) to quantify phreatophyte transpiration (Loheide *et al.*, 2005); similar analysis of diurnal water level variation in surface water ecosystems allows simultaneous quantification of ET and groundwater fluxes (Hill and Neary, 2007). Compared with more labor intensive methods such as eddy covariance and lysimeter techniques, the White method offers a cost-effective and relatively simple alternative to measuring ET, with similar benefits for measurement of groundwater fluxes. Pressure transducers with the accuracy and precision/resolution necessary to detect and quantify diurnal surface water variation are available, but analyses requiring fine scale surface water data, such as the White method, may be particularly subject to sensitivity of sensors to varying environmental conditions.

Total pressure transducers (TPT) require compensation for barometric pressure variation, supplied by equally accurate and precise barometric pressure transducers (BPT). While vented pressure transducers (VPT) obviate this correction, vent tubes can accumulate moisture or become crimped, interrupting pressure transfer to the transducer (Freeman *et al.*, 2004)], or can

be differentially heated, creating large stage errors (> 1 cm) (Cain *et al.*, 2004). To avoid such errors, buffered vent tube thermal conditions or TPT-BPT pairs are proposed (Cain *et al.*, 2004).

Submerged TPTs are thermally buffered by the water, but installation location determines thermal buffering of the BPT. While the manufacturer of transducers used here (Solinst Canada, Ltd.) recommends BPT installation in a thermal setting similar to TPT, such as on a float in the monitoring well or in a dry well below the water surface, this is not strongly emphasized. More importantly, these recommendations are rarely followed in hydrologic studies, where BPTs are installed in ambient temperatures (e.g., in the dry head-space of a well). We evaluated the importance of BPT location, and thus effects of thermal setting, on BPT compensated water levels and the resulting inferences of ET and net infiltration using the White method.

Methods

TPTs (Solinst Gold Levelloggers[®], accuracy = 0.3 cm, precision/resolution = 0.005 cm) were deployed in surface water monitoring wells installed in the deepest part of four hydrologically isolated forested wetlands in north Florida (Sites A through D); levels were recorded at 15 minute intervals during March and April of 2010. TPT data were corrected for barometric pressure variation using data from BPTs (Solinst Barologgers[®], accuracy = 0.1 cm, resolution = 0.003 cm). For comparison, two BPTs were installed at each site. One BPT was installed in the well casing above the water level and thus in ambient temperatures (BPT_{amb}); a second BPT was installed in a dry well where the sensor was below ground level in buffered thermal conditions, but open to atmospheric pressure changes (BPT_{buf}).

Assuming ET ceases at night, allowing net groundwater fluxes to be estimated from nighttime stage changes, and that groundwater fluxes calculated in this way are diurnally constant, daily ET and exfiltration (i.e., groundwater inflow) rates (cm/day) were calculated with

$$ET = S_y (24h \pm s) \quad (1-1)$$

$$\text{Exfiltration} = S_y (24h) \quad (1-2)$$

where S_y is assumed 1.0, h is the net groundwater inflow rate (cm/hr) calculated from the slope of nighttime water level changes, and s is the net decline (+) or net rise (-) of water level over 24 hours (Fig. 1-1 insets). ET and net exfiltration were calculated with water level data separately compensated with BPT_{amb} and BPT_{buf} . Analysis was limited to periods of high stage to avoid the effects of bathymetry on S_y (Sumner, 2007) and to days with no rainfall. Calculated daily ET rates were indexed to daily PET rates determined with available climatic data and the Hargreaves method (Hargreaves and Samani, 1985).

Results

Diurnal fluctuations of water levels compensated with BPT_{buf} and BPT_{amb} were substantially different (Fig. 1-1). Water levels compensated with BPT_{amb} showed steeper daytime declines and suggested exfiltration (i.e., level increases at night). In contrast, compensation with BPT_{buf} resulted in less dramatic diurnal variation (though still evident at a finer scale), net infiltration, and lower daytime declines (Fig. 1-1).

Amplified diurnal variation of BPT_{amb} compensated data is explained by BPT sensitivity to temperature. Differences between barometric pressures recorded at the two BPT positions were highly correlated to ambient temperatures (max. difference = 1.5 cm H_2O , $R^2 = 0.95$, slope = 0.06, $p < 0.001$), with greater underestimation of barometric pressure by BPT_{amb} with decreasing temperatures. Cooling at night caused BPT_{amb} to underestimate barometric pressure, resulting in compensated water levels to be overestimated, falsely indicating exfiltration. The reverse also explains steeper water level declines with BPT_{amb} compensation during the day. These biases severely affected ET and infiltration rates calculated with the White method; BPT_{buf}

compensated data yielded ET rates near PET (mean ET:PET = 0.96 ± 0.13), whereas BPT_{amb} compensation resulted in rates up to four times greater (mean ET:PET = 3.88; Fig. 1-2a). Further, BPT_{amb} compensation suggested net groundwater flows reversed in sign (i.e., exfiltration versus infiltration) and of greater magnitude compared to BPT_{buf} compensation (Fig. 1-2b).

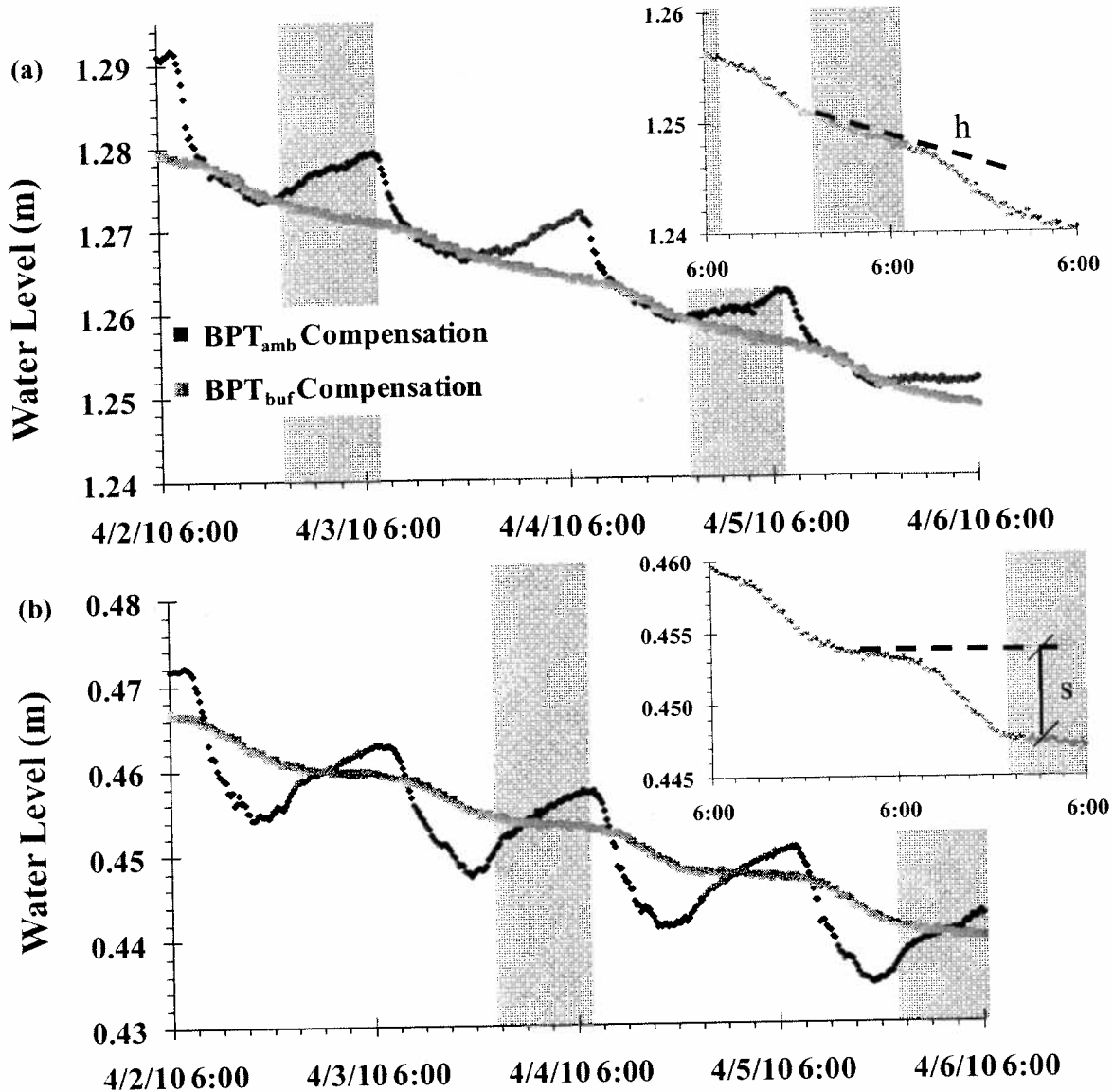


Figure 1-1. Water level data compensated with BPT_{amb} and BPT_{buf} data for Site C (a) and Site D (b). Insets display finer scale data with BPT_{buf} compensation along with parameters used in equation 1-1. Gray bars denote nighttime hours.

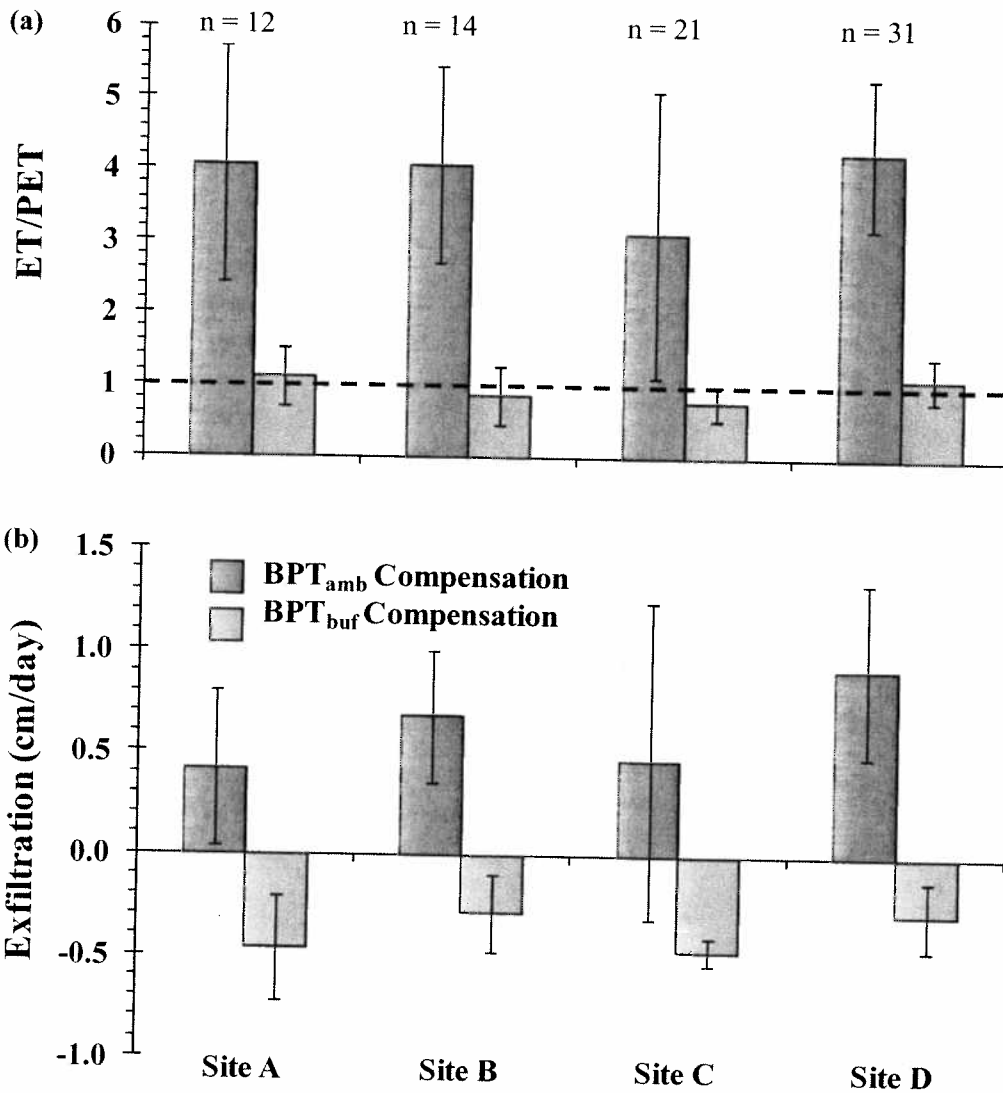


Figure 1-2. Mean (± 1 S.D.) ratios of ET to PET (a) and mean (± 1 S.D.) exfiltration (b) calculated with the White method using water level data with BPT_{buf} compensation and BPT_{amb} compensation. Dashed line denotes values where calculated ET equals estimated PET. Sample size refers to the number of analyzed days (i.e., days with high stage and without rain).

Conclusion

Water levels from TPT data compensated with differently positioned BPTs resulted in markedly different diurnal signatures due to BPT temperature sensitivity. Bias in water levels with BPT_{amb} compensation was systematic, following diurnal variation in temperature and

amplifying expected ET-induced diurnal water level fluctuations. Applying the White method with BPT_{buf} compensated water levels resulted in ET rates near PET and net infiltration, while compensation with BPT_{buf} dramatically overestimated ET and yielded net exfiltration.

Presently available pressure transducers provide the necessary accuracy and precision to quantify diurnal fluctuations in surface water levels, allowing application of the White method to simultaneously estimate ET and infiltration. These modest water level variations, however, are vulnerable to small but systematic errors (up to 1.5 cm H_2O) induced by the sensitivity of BPT sensors to temperature variation. Potential implications of this sensitivity extend to other applications such as stream discharge measurements in low flow conditions (e.g., 1 cm head overestimation results in up to 45 % error in low flow estimates with a standard v-notch weir (Grant and Dawson, 2001) and inferences of basin transpiration with diurnal stream flow (e.g., Bond *et al.*, 2002) using such weir discharge estimates. This study illustrates the critical importance of BPT positioning in buffered thermal conditions by documenting large and systematic errors in surface water level data, whose existence may be difficult to discern, when proper positioning is not used.

CHAPTER 2

Ecosystem Specific Yield for Estimating Evapotranspiration and Groundwater Exchange from Diel Surface Water Variation

Abstract

The White method, routinely used to estimate phreatophyte transpiration from diel groundwater variation, also provides measures of total evapotranspiration (ET) and groundwater fluxes in surface waters. Such applications remain rare, however, and critically require accurate representation of stage-dependent variation in specific yield (S_y). High resolution stage data from three Florida swamps were used to evaluate different relationships between S_y and stage (ecosystem specific yield, ESY). A discretized form, ESY_D , assumes constant S_y near unity for inundated conditions, applying soil S_y for belowground stage and open water S_y ($S_{y,OW} \approx 1.0$) for aboveground stage. A mixture approach, ESY_M , applies a stage-dependent interpolation between $S_{y,Soil}$ and $S_{y,OW}$ using stage-area relationships and assumes rapid lateral equilibration between inundated and non-inundated wetland areas. Finally, an empirical formulation, ESY_{RR} , uses measured ratios of rain to rise to estimate stage-specific S_y . All formulations yielded reasonable ET rates ($ET \approx PET$) at high stage; ESY_D markedly overestimated ET ($ET/PET > 3$) at intermediate stage, whereas ESY_M and ESY_{RR} maintained ET/PET near 1.0. Estimated groundwater fluxes using ESY_M and ESY_{RR} correlated well with Darcy-estimated flows, but were larger, likely due to uncertainties in Darcy parameters. Well transects across wetlands documented equal water elevation and diel variation across inundated and non-inundated areas, verifying rapid equilibration that reduces S_y and explaining overestimation by ESY_D . However, equilibration area varied within and among wetlands, explaining observed differences between ESY_M and ESY_{RR} , and suggesting ESY_{RR} may be preferred. Stage histograms followed the shape of ESY_{RR} , highlighting reciprocal influences of ESY on stage stability.

Introduction

White method in surface waters

Quantifying evapotranspiration (ET) and groundwater exchange in surface water systems (e.g., wetlands, lakes) is critically important for understanding and predicting ecosystem and watershed function. However, they are the most difficult fluxes to measure, and are often estimated as water budget residuals (Winter, 1981; Smithers *et al.*, 1995). Accurate estimation of water use and exchange is of particular importance in wetlands, where those fluxes regulate carbon sequestration, nutrient biogeochemistry, and groundwater recharge (Mitsch and Gosselink, 2007). Research on wetland ET has documented substantial deviation from open water evaporation (Ingram, 1983; Drexler *et al.*, 2004; Mitsch and Gosselink, 2007) due to variability in hydrology, nutrient availability, successional state, and surrounding land use. Rates have been reported that are both markedly higher (Gavin and Agnew, 2004; Moro *et al.*, 2004; McLaughlin *et al.*, 2011) and lower (Lafleur and Roulet, 1992; Campbell and Williamson, 1997; Peacock and Hess, 2004) than potential ET (PET) estimated with climatic models, underscoring the utility of direct empirical estimates.

Methods to estimate ET include: climate models of varying complexity; analysis of diel water level variation; micrometeorological techniques; lysimeters; water balances; and sap-flow transpiration measurements. Lysimeters and micrometeorological methods (e.g., eddy covariance and Bowen ratio techniques) provide direct estimates of ET but are only applicable at a small spatial scale, and are equipment- and labor-intensive (Drexler *et al.*, 2004). Climate-based models estimate ET at a larger scale, but results depend strongly on model selection (Mao *et al.*, 2002; Lu *et al.*, 2005), introducing significant uncertainty and potential bias. Further, without empirically derived coefficients, models do not directly account for water stress (Jacobs *et al.*, 2002) or variable plant growth characteristics (Mao *et al.*, 2002). Direct measures of

transpiration (e.g., thermal dissipation and ventilated chambers; Wullschleger *et al.*, 1998) are accurate but require biometric data to scale measurements to the stand level (Cermak *et al.*, 2004) and only measure transpiration, not the entire ET flux.

The White (1932) method, which is now routinely used for direct measurement of phreatophyte transpiration via analysis of diel variation in groundwater levels (Engel *et al.*, 2005; Loheide *et al.*, 2005; Butler *et al.*, 2007; Schilling, 2007; Lautz, 2008; Zhu *et al.*, 2011), has been proposed as a method to obtain total ET estimates in inundated wetlands (Mitsch and Gosselink, 2007). However, the method has yet to be broadly adopted in such systems and other surface waters despite several advantages, including that it: 1) yields direct spatially integrated values that approximate total ET (via diel surface water variation response to open water evaporation and community transpiration); 2) provides those estimates across heterogeneous environmental conditions; and 3) is relatively low-cost with high temporal resolution, allowing more detailed exploration of ecohydrologic controls on ET (e.g., surrounding land use, water table conditions, vegetation composition, and ecosystem maturity; Butler *et al.*, 2007).

In addition to providing spatially integrated and direct empirical ET estimates in surface water systems, the White method simultaneously yields estimates of net groundwater exchange. As with ET, groundwater exchange varies substantially both among and within systems, ranging in water budget importance from negligible to dominant (Winter, 1999). Groundwater flows are typically estimated using piezometer networks and local estimates of hydraulic conductivity (K_{sat}); however, spatial and temporal variation in K_{sat} introduces significant uncertainty, and even dense piezometer networks may fail to accurately account for all water fluxes (Winter, 1981).

The White method makes two central assumptions: 1) ET ceases at night, allowing estimation of net groundwater flow rates from nighttime water level changes, and 2) groundwater

fluxes calculated in this way are constant throughout the day. With these assumptions, ET (cm/day) and exfiltration (cm/day) are calculated with:

$$ET = S_y (24h \pm s) \tag{2-1}$$

$$\text{Exfiltration} = S_y (24h) \tag{2-2}$$

where h (cm/day) is the rate of water level change at night which defines net groundwater inflow (uncorrected for S_y); s (cm/day) is the 24-hour net water level decline (+) or rise (-); and S_y is the specific yield of the aquifer or water body (dimensionless) (Fig. 2-1). S_y is defined as the volume of water released or taken into storage by a matrix divided by the matrix volume (Healy and Cook, 2002). On an area basis, S_y is input (rain) or output (ET) depth divided by the induced water level change.

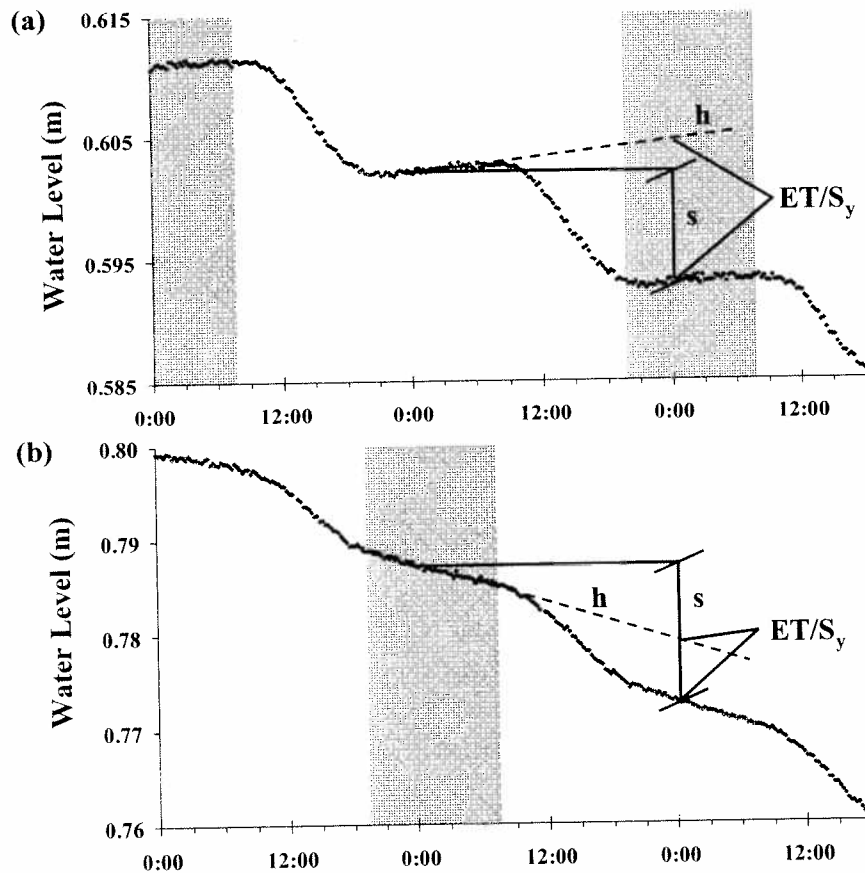


Figure 2-1. Diurnal surface water variation showing exfiltration (a) and infiltration (b) along with parameters used in equation 2-1. Gray bars denote nighttime hours.

Despite the methodological advantages, only five studies have used the White method to quantify ET in surface water systems (all inundated wetlands: Heimburg, 1976; Ewel and Smith, 1992; Liu, 1996; Rushton, 1996; Hill and Neary, 2007), compared to more common use in non-inundated wetland systems (Dolan *et al.*, 1984; Gerla, 1992; Smithers *et al.*, 1995; Lott and Hunt, 2001; Schilling and Kiniry, 2007; Mould *et al.*, 2010) and the routine application for phreatophyte transpiration in more arid settings. One reason for this discrepancy is that resolving ET-driven diel variation in surface water levels requires measurements of greater accuracy. Where S_y is near 1, which is generally, though perhaps at times erroneously (Hill and Neary, 2007; Sumner, 2007), assumed for inundated situations, the magnitude of stage fluctuation is near the extant ET rate (e.g., 0.4 cm/day in summer). In contrast, 0.4 cm/day ET uptake from a soil with $S_y = 0.2$ will induce a water table decline of 2 cm/day, far easier to detect with less accurate recorders. However, pressure transducers with necessary accuracy and resolution to quantify diel surface water variation are presently available, eliminating this operational constraint.

Specific yield of flooded wetlands

A more important constraint on broad application of the White method is uncertainty in determining site-appropriate values of S_y , and accounting for variation in S_y with stage. Estimating soil S_y ($S_{y,soil}$) is a well-known source of uncertainty in groundwater applications of the White method (Loheide *et al.*, 2005), and the assumption that $S_y = 1.0$ for all standing water conditions also warrants scrutiny, particularly in inundated wetlands. Here, S_y is likely reduced by biovolume displacement and rapid equilibration of surface water with exposed areas (e.g., elevated microsites or hummocks) (Sumner, 2007). Ignoring this may overestimate ET, particularly at lower stages, when biovolume effects increase and more wetland surface is

exposed. As a result, rigorous implementation of the White method requires an estimate of “effective S_y ” (*sensu* Liu, 1996; Sumner, 2007) that couples open water S_y (i.e., 1.0 less biovolume displacement; hereafter referred to as $S_{y,OW}$) for inundated areas with $S_{y,Soil}$ for non-inundated areas that rapidly equilibrate. This relationship between stage and S_y is determined by site bathymetry, basal area, surficial soil properties, and degree of equilibration (spatial and temporal) (Fig. 2-2). We give the function describing this relationship the term ecosystem specific yield (ESY), and, as our main objective, evaluate three different methods for its estimation.

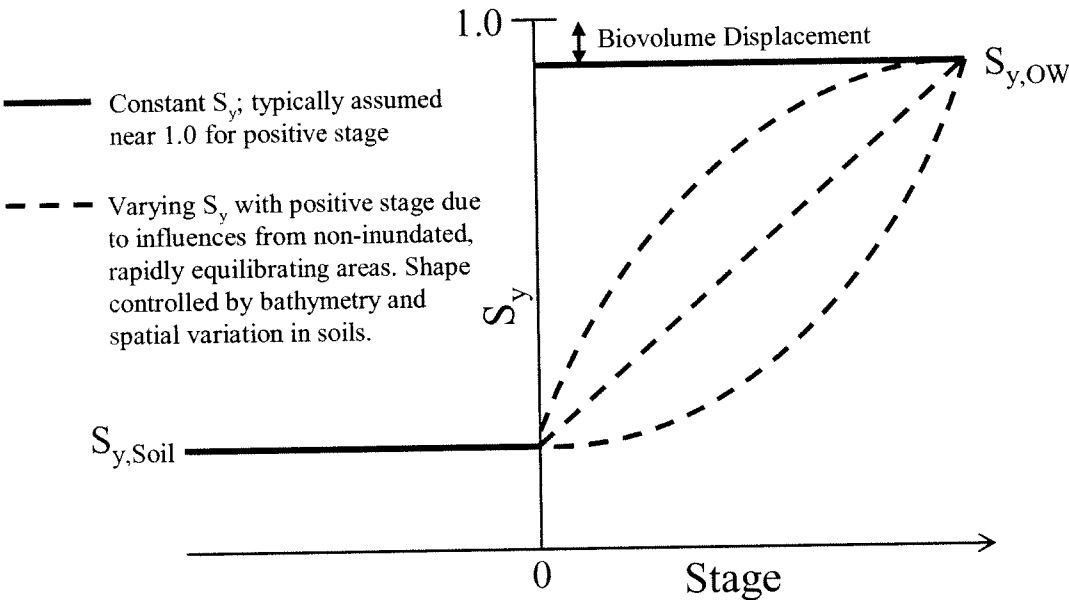


Figure 2-2. Conceptualization of the relationship between specific yield (S_y) and stage (ecosystem specific yield-ESY).

A simulation study (Sumner, 2007) showed that different assumptions about ESY resulted in dramatically different water level responses to ET. The simplest ESY form applies one value for open water conditions ($S_{y,OW}$) when stage is above a threshold land elevation, and uses $S_{y,Soil}$ for

stage below this elevation (solid line, Fig. 2-2). This discretized approach (ESY_D) implicitly assumes that water level declines observed in inundated areas are due only to ET from that inundated area. In other words, this approach assumes that ET in adjacent non-inundated areas, where $S_{y,Soil} < S_{y,OW}$ and ET-induced declines are amplified (Fig. 2-3a), does not affect the diel variation in the inundated pool, presumably because lateral water level equilibration is assumed to be slow. However, if water level equilibrates rapidly (i.e., at far less than a daily time step) between the inundated pool and adjacent non-inundated areas, then observed stage declines in the inundated area will be augmented by the lateral water subsidy necessary to maintain equal water levels in the non-inundated area (Fig. 2-3b), and using ESY_D will overestimate White method ET rates.

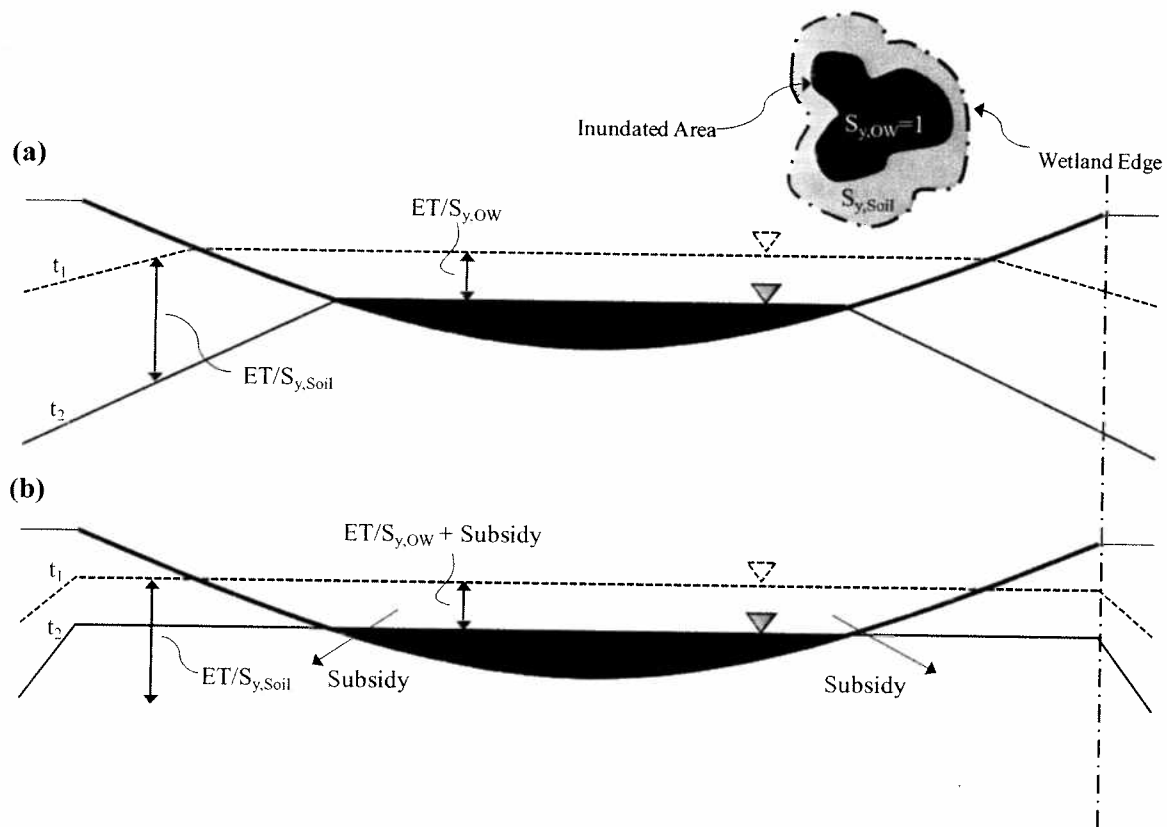


Figure 2-3. Conceptualizations of rapidly equilibrated area limited to inundated areas (a) and extending to non-inundated areas (b).

Another ESY formulation assumes that the entire wetland area rapidly equilibrates regardless of stage. As such, the reduced $S_{y,Soil}$ in exposed areas influences the effective S_y at each stage and thus the magnitude of diel surface water variation in response to ET (Fig. 2-3b). This approach considers stage-dependent variation in inundated wetland area, applying $S_{y,OW}$ for inundated areas and $S_{y,Soil}$ for non-inundated areas; this creates a smoothed transition between high stage (when $S_{y,OW}$ dominates) and dry conditions (when $S_{y,Soil}$ dominates) (dotted lines; Fig. 2-2). This mixture approach (ESY_M) is appropriate if the assumption holds that water level changes between inundated and non-inundated areas are immediately equilibrated across the entire wetland area (Fig. 2-3b). In short, the occurrence and extent of water level equilibration between non-inundated and inundated areas determines which ESY is most appropriate.

While a function similar to ESY_M was intended by Sumner (2007) to handle effects of local microtopography on diel variation, it may also apply in small, hydrologically isolated wetlands studied here that have bowl-shaped morphology (Fig. 2-3). Here, the inundated pool area declines continuously with stage, compounding effects of microtopography. Evaluating whether the water table in these isolated systems maintains rapid lateral equilibration informs whether ESY_D or ESY_M is the appropriate form for applying the White method. We hypothesized that water levels and diel fluctuations in non-inundated regions of the wetland will match surface water levels, providing a rationale for using ESY_M . However, we recognize that lateral equilibration may actually occur between extremes assumed in the ESY_D and ESY_M approaches. That is, lateral equilibration may occur over some fraction of the non-inundated wetland area, but not over the entire non-inundated area. In this case, site-specific determination of the spatial extent of equilibration would be needed to refine the accuracy of the ESY_M approach.

Additional refinements beyond investigating the spatial extent of lateral equilibration may be warranted. One likely refinement is to recognize that both $S_{y,OW}$ and $S_{y,Soil}$, treated as constants in ESY_M , may themselves vary with water depth because of differences in how biovolume is vertically distributed (for the former) and how $S_{y,Soil}$ varies spatially and with water table depth (Loheide *et al.*, 2005) (for the latter). One approach is to develop spatially disaggregated models of ESY that embed such variation in biovolume and $S_{y,Soil}$ (Sumner, 2007). However, parameterizing such a model would invoke new uncertainties that are unlikely to be resolved with reasonable data collection. Alternatively, the relationship can be obtained empirically by relating ratios of rain input (less interception) to resulting water level rise, and evaluating these rain:rise (RR) ratios across wetland stage (ESY_{RR}). This approach is often used to determine $S_{y,Soil}$ in groundwater applications (Dolan *et al.*, 1984; Schilling, 2007). While the approach is data intensive, requiring numerous storms over a range of stage conditions, it empirically describes ESY without assumptions or knowledge of influencing mechanisms (e.g., extent of equilibration area, variability of $S_{y,Soil}$, biovolume displacement).

Here we compare inferred ET and groundwater flow rates with the White method using three different ESY relationships (ESY_D , ESY_M , and ESY_{RR}) and high resolution surface water, bathymetric, and rainfall data collected at three isolated north Florida wetlands. Calculated ET and groundwater flow rates were compared among sites, across stage, and to independent estimates (i.e., potential ET via climatic data and Darcy-calculated groundwater fluxes via groundwater data). Additionally, we monitored water table dynamics across wetlands to evaluate concordance of water level variation across inundated and non-inundated wetland areas, and thus lateral extent of immediate equilibration.

Methods

Water level and bathymetric data collection

Surface water (SW) wells were installed in the deepest area of three hydrologically isolated forested wetlands (specifically cypress domes; small circular depressions dominated by *Taxodium distichum* var. *nutans*) in north Florida (Sites 1-3). Sites 1 and 2 were surrounded by fire-maintained pine flatwood forests, and Site 3 was within a low-density residential area. Sites ranged in size from 0.4 to 1.05 ha and were characterized by ~1 m sandy soil profiles overlain with an organic layer and confined below by thick clay. The sites were isolated in the sense that there were no observed surface water connections; connectivity via the subsurface was unknown when the sites were selected. SW wells were constructed of 5.08-cm diameter, Sch. 40 PVC pipe, screened above and below the ground surface and installed to a depth of 90 cm below ground; the annular space within boreholes was backfilled with sand. Total pressure transducers (Solinst Gold Leveloggers[®], accuracy = 0.3 cm, resolution = 0.005 cm) were deployed to record total pressure (m H₂O) at 15-min intervals. Total pressure was corrected for barometric pressure variation collected at equal intervals with barometric pressure transducers (Solinst Barologgers[®], accuracy = 0.1 cm, resolution = 0.003 cm). Barometric pressure transducers were installed in a dry well open to atmospheric pressure variation but below ground to buffer thermal conditions, limiting temperature sensitivity (see Chapter 1). Direct stage measurements at SW wells were made during site visits to calibrate transducer data.

Bathymetry surveys were performed at all sites at full pool (i.e., maximum inundation when flooding reached the vegetation transition between wetland and facultative upland species) to construct stage vs. inundated area relationships. Water depths were measured on a 5x2 m grid that covered the site (yielding 160 to 410 data points per site); sampling locations that fell on a

tree were noted. Measured water depths were converted to relative land elevations using the water depth measured at the SW well, where elevation was defined as zero. Wetland area was determined using GPS surveying of flooded perimeter at full pool. Stage-area relationships were developed using frequency histograms of measured relative elevations, and strong fits between stage and area ($R^2 \geq 0.95$) allowed estimation of inundated fraction at each stage.

Ecosystem specific yield (ESY)

We explored three approaches to constructing ESY curves (i.e., S_y vs. stage). A discretized ESY (ESY_D), following the common assumption of constant S_y (near 1.0) for all positive stages, applied $S_{y,OW}$ for stage > 0 and $S_{y,Soil}$ for stage < 0 . $S_{y,OW}$ was slightly less than 1.0 to account for biovolume displacement, computed by subtracting from 1.0 the areal fraction of tree and shrub basal area (estimated to be near 5 % for all three sites). $S_{y,Soil}$ was estimated for each site with ratios of rain:rise (RR) when water levels were below ground (described below). The mixture model (ESY_M) assumes rapid lateral equilibration between inundated and non-inundated wetland areas. To construct ESY_M curves, we used an approach similar to Sumner (2007) that spatially averages $S_{y,OW}$ (inundated areas) and $S_{y,Soil}$ (non-inundated areas) using site specific stage-area relationships to determine S_y at a given stage:

$$S_y [\text{stage}] = S_{y,OW} (A_I[\text{stage}]/A_T) + S_{y,Soil} (A_T - A_I[\text{stage}])/A_T \quad (2-3)$$

where A_I is the inundated area at a given stage, and A_T is the total wetland area at full pool.

We used the rain:rise (RR) ratios in two ways. First, during periods when water levels were below ground at SW wells, we used the mean RR to estimate $S_{y,Soil}$ for use in ESY_D and ESY_M (Equation 2-3). Second, under inundated conditions, RR yields S_y at a given stage. Measured RR across a range of stages yielded an empirical form of ESY (ESY_{RR}).

To estimate RR, continuous precipitation data were collected using Onset[®] RG2 data-logging tipping bucket gauges (Onset Computer Corporation, Bourne, MA) at each site. These data were converted to accumulated rainfall depths since storm initiation at 15 minute increments. Rain data were corrected for interception since any observed water level rise occurs only after interception storage is filled. Mean interception depths were empirically determined by identifying the rainfall amount at which water levels begin to rise in plots of induced rise in aboveground SW data vs. rain accumulations (i.e., the x-intercept; Heimburg, 1976). This interception depth was subtracted from all storms. Analyses of interception were performed separately for growing and non-growing season, which was necessary because all three sites were dominated by *Taxodium distichum* var. *nutans*, a deciduous species. Interception-corrected rainfall was divided by observed change in water levels over time increments ranging from 15 to 180 minutes since storm initiation to take maximum advantage of temporal variation in rainfall intensity (i.e., one event potentially resulted in multiple RR data). Calculations of RR were limited to: 1) storms when no rain had fallen during the preceding 24 hours (to limit effects of short residence time subsurface flows); 2) storm events 3 hours or less (to limit event-induced subsurface and runoff flows); and 3) accumulated rainfall depths > 3 mm. Surface runoff was negligible since these isolated systems were surrounded by flat vegetated terrain with well-drained sandy soils. The relationship between RR and stage yielded $S_{y, \text{Soil}}$ for belowground stage and provided data for fitting empirical relationships between S_y and all stages (ESY_{RR}).

White method estimation of ET and groundwater flows

ET and exfiltration were calculated using the White method (Equations 2-1 and 2-2) for days with no rain using barometrically corrected water level data. The slopes of ordinary least squares best-fit lines between nighttime water level and time (between 0:00 and 5:00 am) before and

after each day were averaged to determine h. ET and exfiltration rates were calculated with each of the three ESY relationships.

Calculated ET rates were indexed to daily PET estimated with climate data (Real-time Observation Monitor and Analysis Network; <http://raws.wrh.noaa.gov/roman>) from weather stations within 5 miles of each site using the Hargreaves method (Hargreaves and Samani, 1985). Indexing calculated rates with PET excluded temporal and spatial variability in climatic conditions, allowing comparisons across sites and time, and offered a consistent benchmark for comparing rates using the different ESY relationships. Available data precluded use of the Penman (1948) method at all three sites. However, at one site with requisite Penman data, a comparison between methods revealed no significant bias (linear $R^2 = 0.85$, slope = 1.02, y-intercept = -0.008, $p < 0.005$). Indexed ET rates (ET/PET) for each ESY formulation were compared across observed stages to discern which method yields the most valid results.

Leaf area index (LAI) was measured using the grid developed for bathymetry surveying with a Sunfleck[®] Ceptometer (Decagon Devices, Pullman, WA, USA). This instrument estimates LAI using radiation transmittance (Chen *et al.*, 1997) vis-à-vis open canopy conditions, automatically averaging discrete LAI measurements and providing a mean value for each wetland. Site mean LAI was used to explain differences in indexed ET among sites.

Estimates of net exfiltration from the White method were compared to surficial groundwater fluxes estimated using three groundwater monitoring wells (GW_A-GW_C) at each site. GW wells were installed 30-50 m away from the delineated wetland edge to triangulate groundwater fluxes, and well materials and transducers were similar to SW wells. GW wells were screened across the surficial aquifer to confinement depth, and the borehole annular space was backfilled with sand pack and capped with bentonite clay. Wells were surveyed relative to the SW well ground

elevation, and relative elevations were used to quantify the hydraulic gradient controlling exchange between upland and wetland systems. Three slug tests were performed in each GW well to determine lateral saturated soil hydraulic conductivity (K_{sat}) using the Hvorslev (1951) method resulting in mean values (m/day) (\pm SD) of 1.13 (\pm 0.72), 6.42 (\pm 4.73), and 1.87 (\pm 0.96) for Sites 1, 2, and 3, respectively. It should be noted that this method yielded K_{sat} estimates only for the saturated soil profile above confinement at time of measurement, and it was assumed that resulting values were representative of entire the surficial soil profile.

Confinement depth, mean K_{sat} , lateral and perimeter distance of exchange, and hydraulic gradients were used to calculate daily groundwater fluxes for each well via Darcy's equation. The lateral distance for each GW well was its distance from the wetland edge. The cross-sectional area of exchange was determined based on the water elevation relative to clay confining depth and the exchange perimeter, calculated at the wetland edge for groundwater inflow and at the GW well for groundwater outflow. Note that the exchange perimeter could not be considered constant for these circular depressions. Exchange perimeters at wetland edge and GW well were determined by the relative position of GW wells to each other and to wetland edge. Groundwater exchange (exfiltration = groundwater flow into the wetland) was calculated for each GW well, and summed to one site value representing net exchange. Comparison to rates determined using the White method provided insight similar to indexed ET estimates.

Wetland water table dynamics and lateral equilibration

Additional groundwater monitoring was performed at Sites 1 and 2 to document water table dynamics across the wetland center-to-upland margin during periods of wetland drying. Four wells (GW1-GW4) were installed along a transect beginning approximately 20 m away from the SW well and extending across the wetland edge to within 20 m of one of the triangulated wells

(GW_A). Three of four transect wells were installed in the wetland (hereafter: in-wetland wells) with the farthest just within the wetland edge; the fourth well was installed just outside the wetland edge. Well ground surface elevations were surveyed relative to the ground surface at the SW well. Diel variation and relative elevation of water levels across the well transects were evaluated to observe if, and at what distance, immediate water table equilibration occurred within the wetland basins, which informs selection of the most appropriate ESY formulation.

Results

Estimated ET and sensitivity to ESY

Strong diel fluctuations in surface water levels at all sites were evident over the entire study period, interrupted only on days with significant rainfall, with daily signatures of exfiltration and infiltration (similar to those in Figs. 2-1a and 2-1b, respectively). From site bathymetry surveys, biovolume displacement due to tree and shrub basal area was estimated to be 5%, yielding $S_{y,OW}$ values of 0.95 for all three sites. From mean (\pm SD) RR when water levels at SW were below ground, we estimated $S_{y,Soil}$ to be 0.13 (\pm 0.06) for Site 1, 0.11 (\pm 0.04) for Site 2, and 0.13 (\pm 0.06) for Site 3. Applying the White method using ESY_D , where S_y takes one of two extremes ($S_{y,OW}$ for stage > 0 and $S_{y,Soil}$ for stage ≤ 0), yielded reasonable indexed ET values (i.e., ET/PET near 1.0) at high stage across all three sites (open symbols, Fig. 2-4). However, at intermediate stage, use of ESY_D substantially overestimated ET (e.g., ET/PET > 12 at Site 3). Using ESY_M , where S_y is an area-weighted mixture of $S_{y,OW}$ (inundated area) and $S_{y,Soil}$ (non-inundated wetland area), yielded results similar to those using ESY_D at both very high and negative stage, but much more reasonable (ET/PET closer to 1.0) at intermediate stage (black squares; Fig. 2-4).

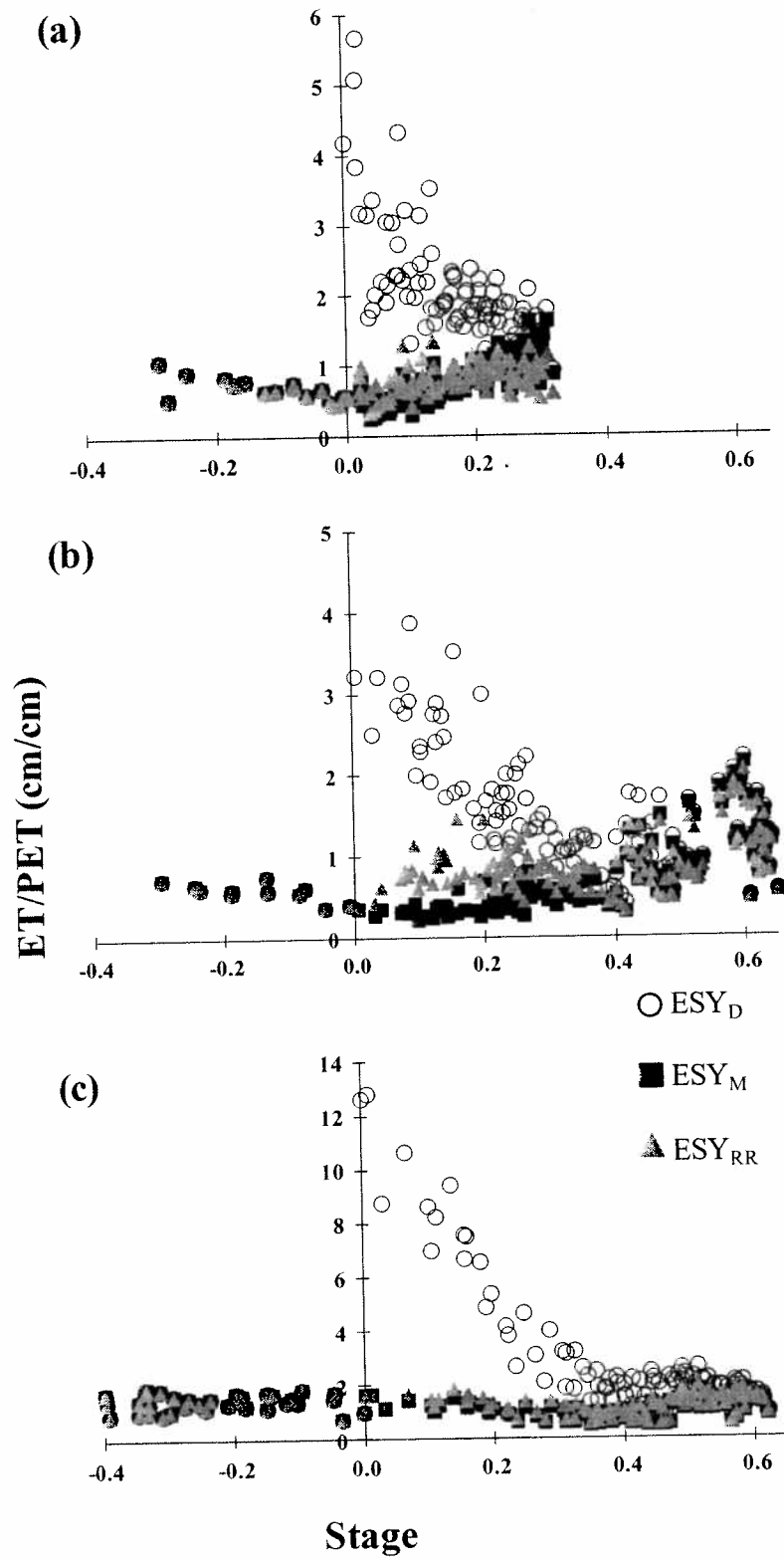


Figure 2-4. ET/PET for Sites 1 (a), 2 (b), and 3 (c) using ESY_D , ESY_M , and ESY_{RR} . ESY s resulted in equal values at negative stage since all apply $S_{y,soil}$ for belowground stage.

The ESY_{RR} formulation was empirically obtained from RR as a function of stage. Raw RR data (Fig. 2-5) for each site followed the expected trend with low S_y at belowground stage ($S_{y,Soil}$) increasing to slightly less than 1.0 at high stage, but were relatively noisy, particularly for Site 1. However, the expected variation in $S_{y,Soil}$ with water table depth (i.e., due to capillary fringe effects; Healy and Cook 2001) was not observed, though data density was relatively low. Multiple functional forms (e.g., Monod equation, saturating exponential) were evaluated to fit RR data under inundated conditions; the best fit function for all sites was a quadratic equation, which was constrained to a maximum of $S_{y,OW}$ and yielded ESY_{RR} for each site (grey dashed lines; Fig. 2-5). Notably, these ESY_{RR} curve shapes differed from the mixture model curves (ESY_M ; black line) at Sites 1 and 2, with ESY_{RR} concave-down and ESY_M concave-up. At Site 3, both ESY curves were concave-up and remarkably similar. ESY_{RR} resulted in indexed ET values near 1.0 across all stages for all sites (grey triangles; Fig. 2-4). Deviation between indexed ET rates calculated with ESY_{RR} and ESY_M was observed at high stage at Site 1 (ESY_D yielded higher values) and at intermediate stage at Site 2 (ESY_D yielded lower values; Fig. 2-4), when the two ESY curves similarly disagree to the greatest extent (Fig. 2-5).

Site mean indexed ET values under inundated conditions are shown in Table 2-1 for each ESY formulation over the entire study; we omitted ET estimates under non-inundated conditions because they were identical across ESY formulations. Values obtained using ESY_M and ESY_{RR} were near 1.0, whereas values using ESY_D were unrealistically high. Measured LAI (m^2/m^2) was variable among sites (Table 2-1), and this variation appears to explain observed differences in indexed ET, particularly when using ESY_{RR} .

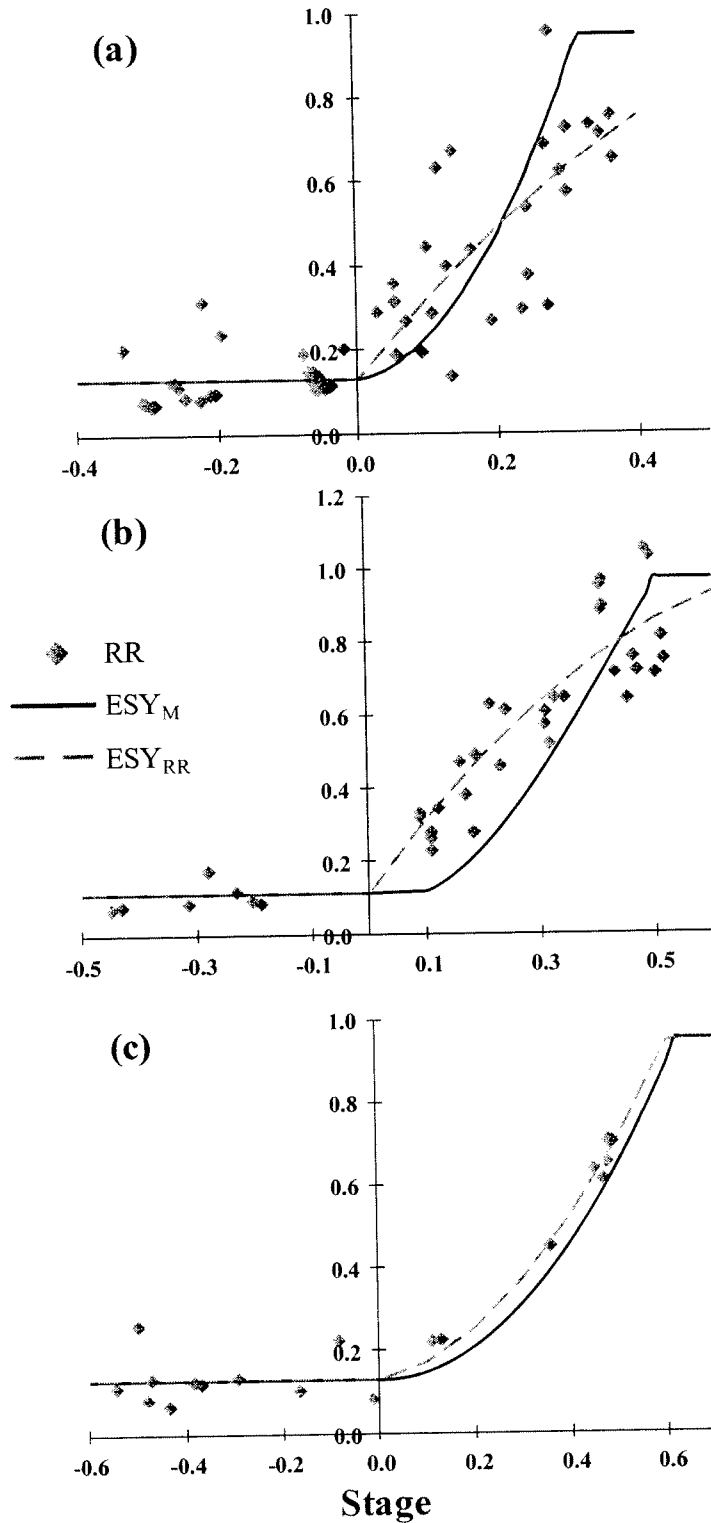


Figure 2-5. RR data, ESY_M , and ESY_{RR} for Sites 1 (a), 2 (b), and 3 (c). ESY_{RR} relationships were best-fit with quadratic equations resulting in R^2 's of 0.46, 0.72, and 0.98 for Sites 1, 2, and 3, respectively.

Table 2-1. Mean (\pm S.D.) ET/PET using ESY_D , ESY_M , and ESY_{RR} along with leaf area index (LAI).

	Site	ET/PET (cm/cm)			LAI
		ESY_D	ESY_M	ESY_{RR}	
BAONF1	1	2.07 ± 0.83	0.80 ± 0.31	0.83 ± 0.21	1.32
CLJENN2	2	1.47 ± 0.70	0.76 ± 0.45	0.91 ± 0.35	2.58
DUFROG	3	2.61 ± 2.02	1.11 ± 0.33	1.24 ± 0.36	5.06

Wetland-groundwater exchange

Observed nighttime water level changes indicated net groundwater exchange switching from exfiltration to infiltration (e.g., Fig. 2-1); flow direction matched the sign of the hydraulic gradient between upland ($GW_A - GW_C$) and wetland (SW) (Site 1 – Fig. 2-6; other sites were similar). Notably, the stage vs. time association at night informs the validity of assuming that groundwater fluxes from the White method are diurnally constant. In all cases the best fit was linear with no systematic deviation from zero in the 2nd derivative; the coefficient of determination (R^2) took values either near 1 (mean = 0.76) or 0 (mean = 0.14; indicating negligible flow).

As with ET estimates, ESY_D yielded higher net groundwater fluxes than ESY_M and ESY_{RR} at intermediate stage (data not shown). In all three sites, indexed exfiltration rates (i.e., ratios of White-exfiltration relative to values calculated with upland groundwater data [$GW_A - GW_C$] and Darcy’s equation) were well above unity for all positive stage conditions and across all ESY formulations (mean ratios using ESY_{RR} = 6.69, 2.84, and 2.71 for Sites 1, 2, and 3, respectively). Note that Darcy-calculated rates for Site 1 (Fig. 2-6) are magnified 10-times to be visible. Despite this disagreement in the absolute magnitude of groundwater fluxes, there was reasonable concordance in the relative magnitude and direction of exfiltration between Darcy-calculated rates and White estimates (i.e., positively correlated; Pearson r = 0.66, 0.41, and 0.61 for Sites 1-3 using ESY_{RR} , $p < 0.001$). The disagreement in absolute magnitude between estimates with

Darcy's equation and the White method (even when using more appropriate ESY) may be explained by large uncertainties in the former due to spatial heterogeneity of K_{sat} (vertically and laterally), confinement depth, and hydraulic gradient. Multiplying measured K_{sat} estimates by the indexed exfiltration values would yield broad concordance between the two methods, and the implied magnitude of K_{sat} values from doing that are plausible, falling both within the range of values measured in our wells, and within a broader survey of hydraulic properties of upland sandy soils in north Florida (Obreza and Collins, 2008).

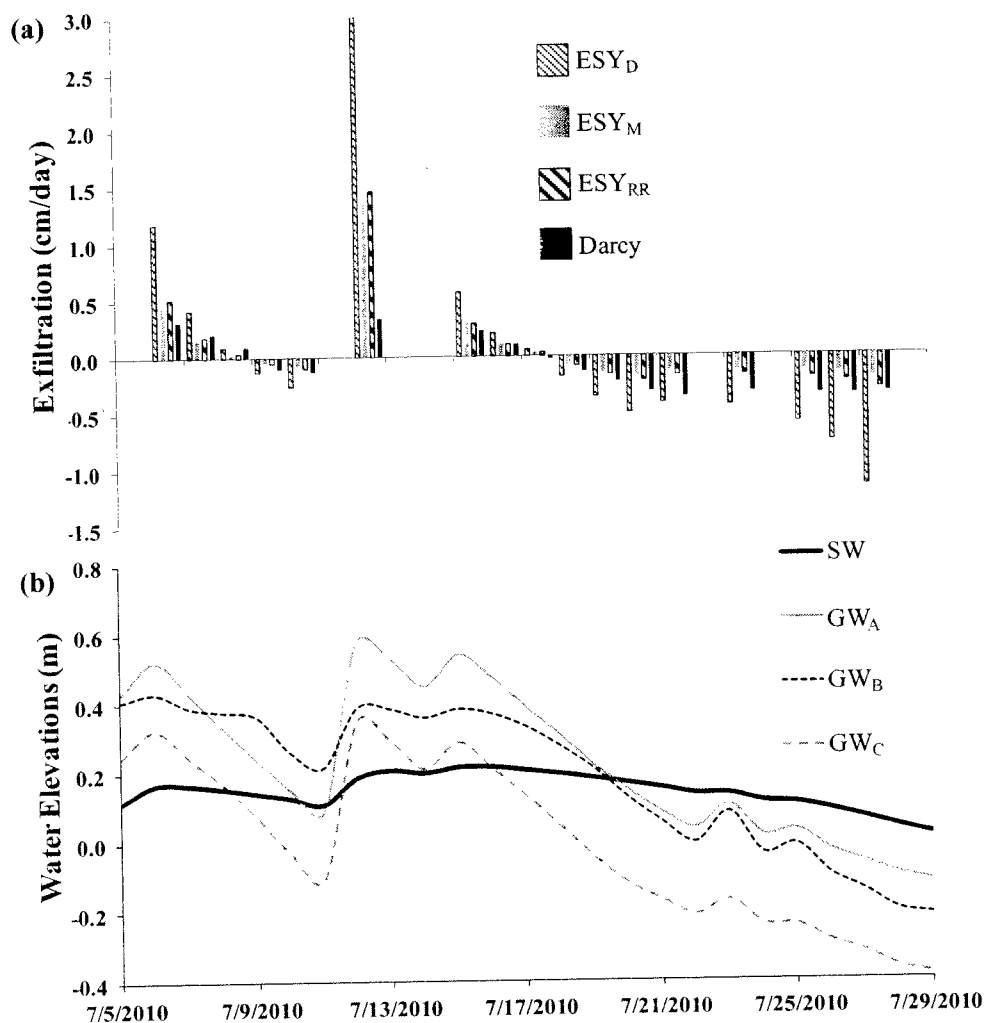


Figure 2-6. White-calculated exfiltration (cm/day) with ESY_D, ESY_M, and ESY_{RR}, along with exfiltration calculated with Darcy and groundwater data at Site 1 (a). Darcy rates are scaled by a factor of 10 to be visible. Groundwater elevations relative to surface water elevations at Site 1 over the same time period (b).

Wetland water table dynamics and lateral equilibration

Wells (GW1-GW4) between surface water (SW) and upland wells (GW_A) at two sites (Fig. 2-7) help explain why S_y falls between $S_{y,OW}$ and $S_{y,Soil}$ at intermediate stage (Fig. 2-5), and thus why ESY_M yielded more reasonable rates than ESY_D (Fig. 2-4). At Site 1, when water levels were below ground at all wells except the SW well (i.e., when SW = 0.14 m), there was strong concordance between water levels (elevation and signature of diel fluctuations) in the inundated (SW) and non-inundated (GW1, GW2, GW3) portions of the wetland (Fig. 2-7a); this is clearly evident with finer scale data (Fig. 2-7a; inset). Water levels outside the wetland edge (GW4, GW_A), however, experienced an amplified diel signature and more rapid decline. Together, these observations suggest that water levels equilibrate immediately within the wetland basin between inundated and non-inundated areas, but that this rapid exchange does not occur with upland groundwater (Fig. 2-7a).

It follows that the daytime drop observed at the SW well occurs in response to ET from both the inundated and non-inundated portions. As such, diel variation at SW under intermediate stage conditions is due, in part, to water delivered to adjacent non-inundated areas to maintain water table equilibration (Fig. 2-3b), supporting the ESY_M formulation. Note, however, that GW3 (the farthest in-wetland well) deviated from SW with decreasing stage (Fig. 2-7a), while GW1 and GW2 continued to match SW with complete wetland drying (data not shown), suggesting stage-dependent variation in the area over which lateral equilibration occurs.

This stage-dependent variation in equilibration area is more evident at Site 2, which has a steeper elevation gradient between the wetland and adjacent uplands (note elevation offsets in Fig. 2-7b). At this site, GW1 levels were above ground until SW levels fell below 0.28 m; all other wells were below ground during the period shown (Fig. 2-7b). The signature and elevation

of GW1 levels matched SW levels closely throughout the period presented, but deviated markedly when SW stage was below 0.08 m (data not shown). Matching also occurred between GW2 and SW until SW levels fell below 0.28 m, at which point GW2 declined more rapidly and with increasing diel fluctuations, indicating that rapid lateral equilibration had ceased. Water levels at GW3 showed large diel fluctuation throughout, suggestive of variation controlled by local ET and $S_{y,Soil}$ (i.e., no rapid equilibration with the inundated pool). GW4 water levels, which varied between 0.46 and 0.84 m below ground, also recorded large diel fluctuation, but less than GW3, possibly because of higher local $S_{y,Soil}$ or decreased use of groundwater for ET.

The upland well (GW_A) at Site 2 showed a relatively constant decline, with a weak diel signature likely due to reduced phreatophyte uptake during this period when water table depths ranged from 0.78 to 1.02 m (Fig. 2-7b). Moreover, water elevations at GW_A were lower than those near the wetland center (GW1 and GW2) but higher than those at the wetland edge (GW3 and GW4) (Fig. 2-7b). These relative elevations indicate a groundwater trough developed at the wetland edge where water elevations (GW3 and GW4) were lower than those at upland (GW_A) and more in-wetland wells (SW, GW1, GW2). This likely occurs due to phreatophyte pumping of groundwater at the wetland edge (i.e., GW3 and GW4 diel variation; Fig. 2-7b), while that process is absent in the uplands where the water table lies outside the root zone.

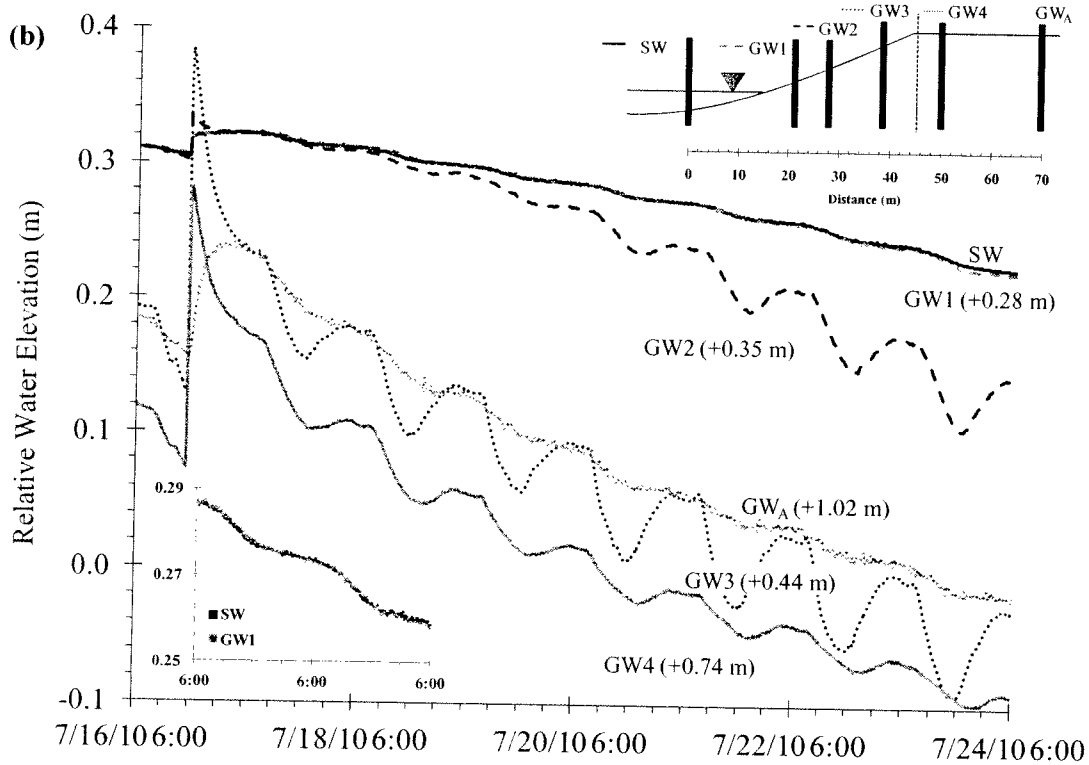
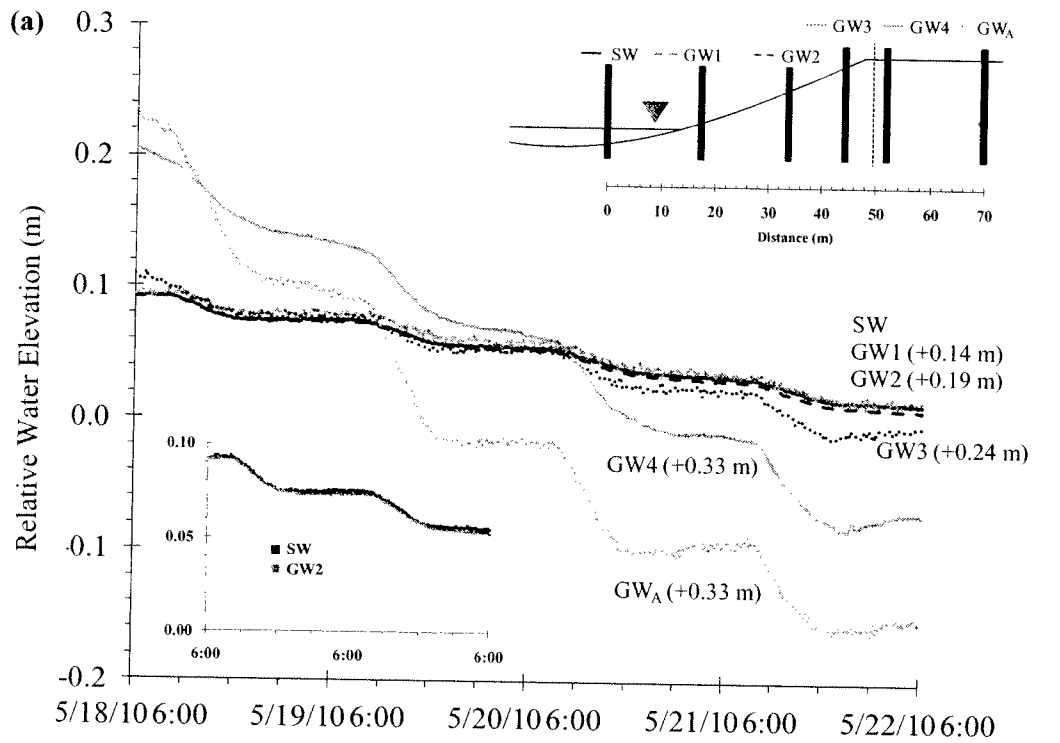


Figure 2-7. Well transect data for Sites 1 (a) and 2 (b) showing groundwater elevations relative to surface water elevation. Insets show well installation locations and finer-scale data. Values in parentheses represent ground elevation differences between groundwater wells and the surface water well (i.e., offsets from actual water table depth).

Discussion

The broad applicability and advantages of the White method for surface water balances are hard to overstate: the method is inexpensive, empirical, and spatially integrated, providing estimates of the two most challenging and important components of an ecosystem water budget (Winter, 1981). Accurate determination of both groundwater exchange and ET can help inform ecosystem management and restoration, and provides direct evidence of ecological feedbacks on local hydrologic behavior. Increasing utilization of the method to estimate phreatophyte transpiration, a sub-component of ecosystem water budgets, from diel variation in groundwater levels (Loheide, 2005) is evidence that expanding the range of systems (e.g., wetlands, lakes) in which the method can be applied will improve inference of how land use, community composition, and environmental conditions control ecosystem productivity and water use.

Our study demonstrates that the issues that have constrained application in surface waters, namely accuracy requirements and use of appropriate S_y , can be readily overcome. The constraint of inadequate accuracy, precision, and resolution to reliably detect diel variation in surface waters (Liu, 1996) is clearly no longer a limitation, though transducer deployment considerations are of critical importance (see Chapter 1). Highly accurate and precise data allow quantification of diurnal variation (often < 1 cm) in wetland surface water levels; White method inferences of ET and exfiltration rates from these data, however, critically depend on using an appropriate S_y value. This second limitation required more attention because our results confirmed that S_y was stage-dependent, necessitating a site-specific function to describe S_y variation with water level. Our work compared three approaches to describe the stage-dependent S_y function at the system scale – that is, ecosystem specific yield (ESY). Two of these approaches embedded the extremes regarding the nature of rapid lateral hydrologic equilibration

within the wetland (ESY_D assumes none, and ESY_M assumes it occurs over the entire wetland basin); the third (ESY_{RR}) provided an empirical description with no requisite assumptions.

The first approach, ESY_D , used two discrete but constant S_y values, $S_{y,Soil}$ for belowground stage and $S_{y,OW}$ for aboveground stage. The latter was estimated to be slightly less than 1.0 (0.95), with the departure from unity created by biovolume (Sumner, 2007) estimated from field bathymetry measurements. Similar results were observed in Liu (1996), where biovolume displacement in similar north Florida cypress domes was estimated to be 1%. At high stage, ESY_D resulted in reasonable indexed ET rates (i.e., ET/PET near 1.0), but yielded increasingly implausible values with decreasing stage, with extreme values exceeding 10 (i.e., an order of magnitude higher than the Hargreaves estimate of ET; Fig. 2-4). We argue that this approach is intrinsically oversimplified, strongly reject the plausibility of the assumption that $S_y = 1.0$ for all inundated conditions, and conclude that significant rapid lateral exchange between inundated and non-inundated regions of the wetland must be occurring.

The second approach, where ESY is a stage-varying mixture of the two discrete values $S_{y,Soil}$ and $S_{y,OW}$ (ESY_M), assumes lateral exchange between inundated and non-inundated areas occurs over the entire wetland area, meaning that ET from the entire wetland basin contributes to the diel stage signal in the inundated pool. This approach yields better estimates in these small isolated basins. Indexed ET rates were plausible at all stages using ESY_M , unlike with ESY_D (Fig. 2-4).

In practice, the appropriateness of the ESY_M approach is determined by the extent of rapid lateral equilibration. While we observed effectively immediate equilibration between water levels in inundated and non-inundated wetland areas, the extent of the rapid lateral equilibration area appears to be stage- and site- dependent (Fig. 2-7). Hill and Neary (2007) assumed that this

equilibrated area is confined to the flooded edges that are exposed by day-to-day water level decline, and accounted for this with a composite S_y that includes $S_{y,soil}$ for edge water losses. This composite S_y , which is conceptually similar to our ESY_M , though far more limited in spatial extent, yielded modest reductions (10 to 25%) in ET rates estimated at intermediate stage (0.15 to 0.25 m). However, these reductions would be insufficient to reduce our indexed ET rates to plausible values at all stages (Fig. 2-4), and Hill and Neary (2007) did not provide a comparison of their values to other estimates of ET. We conclude that the contributing area for diel surface water variation is larger than previously assumed, but cannot generalize to all sites that it contains the entire wetland basin at all stages. Site-specific measurements of water level divergence between wells within a wetland site would be needed to establish the stage-varying equilibration area.

While investigating the spatial extent of lateral equilibration will attenuate this uncertainty associated with ESY_M , other uncertainties will remain, namely vertical, horizontal, and temporal variability in $S_{y,Soil}$. Our third approach, ESY_{RR} , independently and empirically describes ESY using ratios of rain:rise (RR) across stage, and does not require knowledge of the spatial extent of equilibration, spatial variation in soil properties (Cohen *et al.*, 2008), or water table depth effects on $S_{y,Soil}$ (Loheide, 2005). Our implementation of ESY_{RR} illustrates that it requires large sample sizes of storms at varying stage. Most rain events are too small to provide reliable results, and the method assumes that runoff and event-induced subsurface flow are negligible during the period of analysis. Moreover, interception, which varies seasonally, needs to be estimated and removed from the rainfall input quantity. To address these concerns, we censored the data to relatively large three hour storms that were isolated in time and used the x-intercept of seasonal plots of rise vs. rain to estimate interception. However, this and additional censoring

compound data requirements, limiting applicability to hydrologically isolated systems with a long data record and detailed local rainfall measurements. Finally, this method yields relatively noisy estimates that will benefit greatly from even longer data sets than were available to us.

In spite of these constraints the results were informative. The ESY_{RR} curves varied with stage in a way that was broadly similar to ESY_M (Fig. 2-5), supporting the use of the latter in similar settings (e.g., conductive surficial soils that permit rapid lateral equilibration) where RR data are limited. However, there was also evidence of site-specific disagreement between ESY_{RR} and ESY_M at some stages. In particular, ESY_{RR} at Site 2 yielded much higher S_y values and markedly different concavity at intermediate stage (Fig. 2-5b), which increased ET estimates (Fig. 2-4b). A major reason for this disagreement may be that the lateral equilibration area evident at Site 2 (Fig. 2-7b) was smaller than the wetland basin, which means that ESY_M underestimates S_y and resulting ET estimates at intermediate stage. This site specificity of the association between ESY_M and ESY_{RR} is also made clear by the nearly perfect fit between ESY_M and ESY_{RR} for Site 3 (Fig. 2-5c); no lateral equilibration area data were collected at this site.

One of the advantages of the White method is that it permits a more finely resolved investigation into the effects of land use (e.g., fire history, nutrient loading) and environmental drivers (e.g., water depth) on ET and groundwater exchange. Surrounding land use for the sites here included fire-maintained pine flatwoods at Sites 1 and 2 and a fire-suppressed, low-density residential at Site 3. LAI responded to these influences, with the highest LAI by far in the fire suppressed cypress dome (Table 2-1). These values were consistent with previous cypress dome measurements; Liu (1996) and Brown (1978) measured growing season LAI in north Florida cypress domes ranging from 2.0 to 7.3, with minimum values corresponding with active fire history. The effects of LAI variation on ecosystem water use and presumably productivity

through influences on ET (Gholz *et al.*, 1989) were evident (i.e., increasing mean ET/PET with increasing site LAI; Table 2-1), particularly when using the ESY_{RR} approach.

The White method estimates of net groundwater exchange, which combine lateral and vertical exchange, revealed several insights regarding wetland surface water-groundwater interactions. First, while the direction of groundwater exchange (i.e., infiltration vs. exfiltration) and relative magnitude was strongly concordant between the White method and Darcy estimates, the latter were much lower (e.g., Fig. 2-6a). There are several possible reasons. The most likely is due to the significant uncertainties associated with the application of Darcy's equation (e.g., large heterogeneity in confinement depth, soil conductivities, and preferential flow paths; Winter, 1981). Using our highest measured K_{sat} values as opposed to the means, or values reported for similar upland soils of the region (Obreza and Collins, 2008), yields Darcy-calculated flows much closer to White estimates, underscoring the sensitivity of the former to a parameter that may not be fully represented with point measurements (i.e., slug tests). Another possibility, albeit unlikely, is that exchange is occurring vertically with the Upper Floridan Aquifer, which lies below these systems and is separated by a thick, though frequently fractured, clay confining unit. This underscores the difference between the White method inference (which yields the combined vertical and horizontal net groundwater exchange) and Darcy estimates (which measures only lateral exchange unless deep piezometers are also installed).

A second important observation is that groundwater exchange exhibited frequent sign reversals. Exfiltration occurred for several days following large rainfall events, but switched to infiltration between these large resetting rainfall events; the wetland was a source of water to the adjacent surficial aquifer for the vast majority of days. This switching behavior (Fig. 2-6) derives in part from S_y differences between the upland and wetland environments, whereby

wetland water levels change less in response to the same depth of vertical water losses and gains (Lu *et al.*, 2009). We note that this ultimately dampens local vertical water table variation in the surrounding uplands by decreasing rain-induced rise (via discharge to wetland areas) and subsequent drying (via recharge from wetland areas). At the landscape scale, this represents a potentially important hydrologic service (i.e., buffering baseflow to streams) that accrues in spite of the fact that these systems are referred to as hydrologically isolated.

While we observed stage-dependent variation in S_y when water levels were above ground, most research has focused on variation in S_y when the water table is below the surface (Duke, 1972; Loheide, 2005). $S_{y,Soil}$ has been shown to decrease with water table rise, approaching zero at the ground surface where highly magnified water level changes ensue from small rainfall inputs (i.e., reverse Wieringermeer effect) or ET losses (Healy and Cook, 2001; Duke, 1972). We observed no such behavior, either in the ET signal as water levels approached the ground elevation (Fig. 2-4), or in observations of RR ratios as a function of stage (Fig. 2-5). We reconcile these divergent observations by recalling that rapid lateral equilibration integrates S_y across the wetland basin. As such, the inferred S_y (via RR data or ESY_M) at a given stage is not for a discrete location but a spatially weighted average across the site. Because of the characteristic bowl-shaped basin morphology of these cypress domes, at any given stage there are land elevations at, above, and below water elevation that all exert influence on the effective S_y via rapid equilibration. As such, the phenomenon wherein S_y approaches zero when the water level is at the ground surface may still be occurring, but only in a small fraction of the wetland basin at any given stage, and this effect is masked via the effects of spatial aggregation with sites where water levels are higher and lower.

A point model by Tamea *et al.* (2010), where $S_{y,Soil}$ varies with water table depth but S_y is constant (1.0) for water levels aboveground, predicts a bimodal probability density function (pdf) for wetland stage. The combination of stochastic rainfall and daily ET with this ESY (i.e., $S_y = 1.0$ for positive stage, $S_y \approx 0$ at zero stage, and $S_{y,Soil}$ that increases with increasing water table depth) yields two high probability modes (one above and one below ground); this prediction was validated with empirical data from a landscape with bimodal soil elevations. A low probability saddle between modes is created at ground elevation because water level becomes highly sensitive to minor inputs and outputs as S_y approaches zero. Higher S_y increases stability of both aboveground and more belowground water levels.

The shape of the ESY function consequently regulates water level stability. Our observed ESY patterns, in contrast to those used in Tamea *et al.* (2010), do not predict a high probability mode at negative stage because constant belowground S_y creates equal stability and thus a more uniform pdf across all negative stages. Moreover, our observed stage-dependent variation in S_y at positive stage, which contrasts to the assumption of constant $S_y = 1.0$, would augment the aboveground mode. That is, increasing S_y with stage means that higher water levels are less affected by hydrologic flows, increasing stability. Histograms of daily stage (Fig. 2-8) show a mode at positive stage in all three sites, no evidence of a second high probability mode at negative stage, and a histogram geometry that matches the shape of the empirical ESY_{RR} . As such, the shape of ESY in turn influences stage stability.

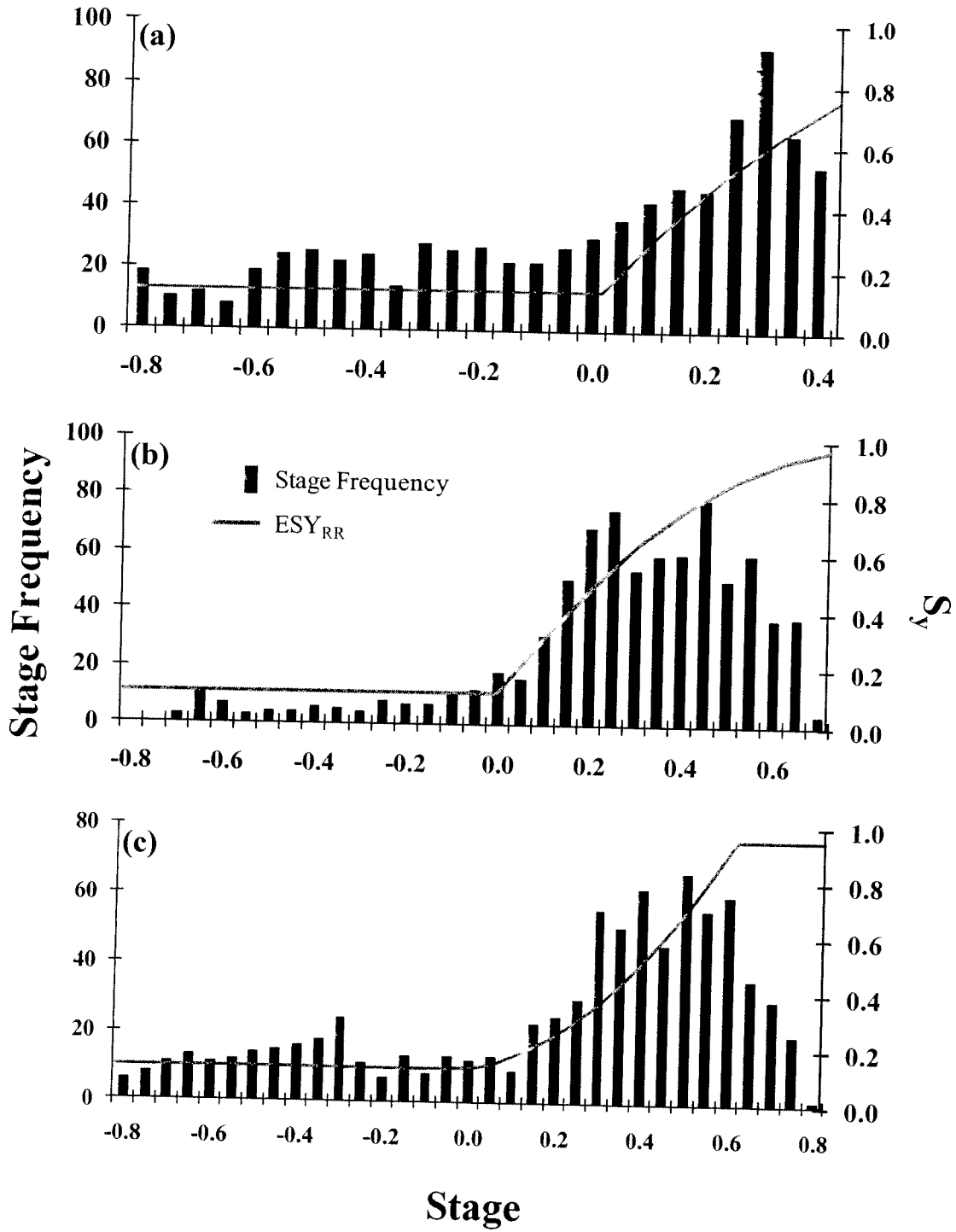


Figure 2-8. Histograms of daily stage along with ESY_{RR} for Sites 1 (a), 2 (b), and 3 (c).

ET and groundwater exchange are related to important ecosystem services and control water budgets both locally and regionally. The White method is a viable, low-cost, and empirical approach to estimating both these rates, and can do so in a manner that expands the plausibility of investigating the complex feedbacks between surface water hydrology and ecosystem structure, composition, and succession. Crucially, however, it requires an improved understanding of the variation of S_y with stage. The broad assumption that $S_y = 1$ for all ponded conditions is clearly not tenable, and creates large errors in inferred ET and groundwater exchange rates except perhaps under deeply flooded conditions (e.g., deep water swamps and lakes) where S_y approaches one. Where reasonable approximations of ESY can be obtained, the method has the clear potential to be a significant tool in service of understanding surface water ecohydrology and improving the management and restoration of these systems.

CHAPTER 3

Realizing Ecosystem Services: Wetland Hydrologic Function along a Gradient of Ecosystem Condition

Abstract

Land use influences to ecosystem condition and function affect the provisioning of ecosystem services. Because habitat-related services are particularly vulnerable to disturbance, assessments of ecosystem condition (via biological integrity) are often used to infer impairment of ecosystem function. However, there may exist a critical disconnect between the provision of ecosystem services (derived from a range of functions that extend beyond habitat) and enumeration of ecosystem value (based solely on condition). Hydrology regulates many of the functions that wetlands may continue to provide despite impaired ecosystem condition (e.g., latent heat exchange, biogeochemical cycles, and regional hydrologic buffering). To investigate the relationship between ecosystem condition and hydrologic functions, we monitored eleven north Florida cypress domes that spanned a wide gradient of land use intensity to evaluate assessed ecosystem condition, hydrologic regime, groundwater exchange, and evapotranspiration (ET). No systematic variation in hydrologic regime (i.e., mean and variance in stage, daily stage change) was observed across a gradient of assessed condition. In contrast, vegetation structure (via leaf area index) and its regulation of ET fluxes were clearly affected by disturbance, with higher ET rates in agriculture and urban landscapes. Amplification of ET increases latent exchange and local climate regulation via cooling, a function especially needed in urban heat islands, as well as indicates higher productivity in these forested wetlands. Frequent reversals in the direction of groundwater exchange in response to wet and dry cycles were observed at all sites. Regardless of ecosystem condition, this sink/source behavior buffers regional hydrology, with wetlands providing water storage capacitance within the landscape. Comparing hydrologic functions with assessed condition highlights that the latter, which is largely determined by biological integrity, does not fully capture the full suite of ecosystem functions supplied by wetlands. Surrounding land use affects wetland condition and function while also determining which ecosystem services are realized and valuable. While increased disturbance may impair habitat-related services, other ecosystem services that are particularly needed within disturbed landscapes may remain and may even be amplified in these “working” wetlands.

Introduction

Ecosystem services accrue from ecological functions, which are frequently impaired by anthropogenic disturbance. One common effect of human disturbance is to impair the ability of an ecosystem to provide habitat that sustains local and regional biodiversity. Because of the central prominence of the loss of biodiversity functions, ecosystem condition is often evaluated by comparing a sites' biological assemblage vis-à-vis minimally impacted reference settings (Karr and Chu, 1997). While other functions such as carbon sequestration, adjacency effects on pollination (Ricketts *et al.*, 2008), hydrologic buffering (i.e., infiltration, storage and slow release), microclimate regulation, and contaminant removal are acknowledged as important, they are more challenging to enumerate at appropriate temporal and spatial scales. This raises the question of whether ecosystem functions are predicted by measures of ecosystem condition (Hruby, 2001; Fennessy *et al.*, 2004). If not (e.g., Ehrenfeld, 2004), a potentially critical disconnect may exist between the provision of ecosystem services (derived from functions) and enumeration of ecosystem value (based on condition).

Wetlands are an informative setting in which to examine the general question of the association between ecosystem condition and function (Stander and Ehrenfeld, 2009). Wetlands provide a well-known array of services (MEA, 2005), and Federal Clean Water Act mandates that target no net regional loss have resulted in significant maturation of conditional assessment tools that support compensatory mitigation efforts. Wetland functions are, as in other ecosystems, difficult to quantify, especially at their characteristic temporal scale (Stander and Ehrenfeld, 2009). As such, rapid assessments of condition (not function) are routinely used to prioritize conservation and compensatory mitigation (Hruby, 2001; Fennessy *et al.* 2004; Cole, 2006). This creates the institutionally implicit assumption (Fennessy *et al.*, 2004) that condition

(assessed via indicators of species composition, structure, water quality, flooding regime) is correlated with function, and thus ecosystem service provisioning. Because conditional assessment is calibrated to quantify departure from reference (i.e., minimally impacted) conditions, this further embeds the assumption that all wetland functions are maximized under reference conditions (Hruby, 2001; Stander and Ehrenfeld, 2009). Not surprisingly, conditional assessments yield low scores for wetlands within high intensity land uses (e.g., urban and agriculture; Lopez and Fennessy, 2002; Reiss, 2006; Mack, 2007), resulting in reduced compensatory mitigation requirements for their loss. However, many services that wetlands are thought to provide (water quality improvement, flood water storage, microclimate regulation) are unlikely to be *realized* except in contexts where water quality and quantity, and thus ecosystem condition, are impaired (Reiss, 2006).

Hydrology is the central determinant of wetland type, habitat, and process (Mitsch and Gosselink, 2007), and thus the core control on the differential realization of wetland functions across land uses. Land use influences to hydrologic regime (e.g., changes in depth, duration, and/or spatial extent of flooding) can reduce habitat quality via controls on ecosystem structure and species composition at multiple trophic levels. However, wetland hydrologic functions extend beyond habitat effects to also regulation of downstream flooding, controls on important biogeochemical cycles responsible for improving water quality, local groundwater recharge, and latent heat exchange via evapotranspiration (ET); these functions are not, a priori, reduced when hydrologic regime is disturbed and/or biological condition declines. Indeed, nutrient loading, reduced fire regime, and introduction of invasive species can reduce biological condition but increase ecosystem productivity (Keddy, 2010) and its regulation of ET, with commensurate increases in associated hydrologic functions. Moreover, alteration of catchment physical

conditions (e.g., soil compaction, impervious surfaces, and drainage networks) can influence wetland and watershed hydrology (Winter, 1988), and the role of wetlands in mitigating these disturbances is most important in landscapes where they have occurred. Despite recent work highlighting the importance of direct measurement of site specific hydrology to assess function, rather than solely using integrative indicators (e.g., redoximorphic features, seasonal high water lines, buttressed tree trunks) (Cole, 2006; Stander and Ehrenfeld, 2009; Gebo and Brooks, 2012), information about wetland flooding dynamics and exchanges (e.g., ET and groundwater exchange) remains surprisingly scarce.

Exchanges of water between wetlands and adjacent aquifers and the atmosphere are among the most important wetland functions. The role of wetlands in regulating aquifers through groundwater-surface water exchange has been long recognized (Winter, 1999; Sophocleous, 2002), despite persistent challenges in enumerating this exchange process. Less frequently cited are functions related to ET (Peters et al, 2011), such as latent heat exchange, which regulates temperature at local to global scales (Ban-Weiss *et al.*, 2011). Urban vegetation is known to partially alleviate heat island effects (Taha, 1997), and persistent water availability (i.e., oasis effect; Drexler *et al.*, 2004), dense vegetation structure (the “clothesline” effect; Drexler *et al.*, 2004) and lateral advection of sensible heat (Spronken-Smith *et al.*, 2000) make urban wetlands optimal locations for this function to be realized relative to other land covers in urban landscapes. Moreover, ET and primary productivity are tightly coupled, suggesting that spatial and temporal variation in productivity and related functions (e.g., C sequestration) may be inferred from measured ET rates, especially in forested systems with comparable communities (i.e., where transpiration dominates the ET flux and with similar water use efficiencies; Law *et al.*, 2002).

Despite the strong rationale for direct measurements of hydrologic fluxes to assess wetland function, spatial and temporal variation makes such measurements difficult to obtain (Winter, 1999; Drexler *et al.*, 2004). For example, groundwater-surface water exchange is typically estimated using multiple piezometers and measured soil hydraulic properties, but spatial and temporal heterogeneity in groundwater levels and soil type and texture can introduce large uncertainties in calculated rates (Sophocleous, 2002). Similarly, ET rates are either estimated from climate-based models, which estimate potential ET (PET) not actual ET and do so with large variation among models (Lu *et al.*, 2005), or are measured with resource-intensive methods (e.g., eddy covariance, sap flow methods, and weighing lysimeters) that limit their utility. The White (1932) method, a tool developed and now widely used to estimate phreatophyte transpiration from diurnal variation in groundwater levels (Loheide *et al.*, 2005), provides a low cost, spatially integrative, empirical approach that can, in surface water systems, yield estimates of both ET and groundwater fluxes. Despite numerous advantages of the approach, applications in surface water systems have been limited, primarily due to two operational constraints: accurate instrumentation and stage-dependent variation in specific yield, a key parameter required of the method. These constraints have been recently alleviated (see Chapters 1 and 2), broadening applicability to aquatic ecosystems, and for the first time providing an opportunity to assess wetland hydrologic functions at spatial and temporal scales commensurate with their delivery.

In this work, we measured physical and biotically-mediated hydrologic responses (including high resolution White method estimates of ET and groundwater fluxes) in wetland systems spanning a human disturbance gradient to test the hypotheses that: 1) assessed ecosystem

condition covaries with alteration of hydrologic regime, but that 2) certain hydrologic functions (ET and groundwater exchange) remain and are even amplified as measured condition declines.

Methods

Site Descriptions

Eleven cypress domes (small circular depressions dominated by *Taxodium distichum* var. *nutans*; Ewel, 1990) were selected across north Florida; these sites were selected from the larger set of domes previously used to calibrate the Florida Wetland Condition Index (FWCI; Reiss 2006). All sites were hydrologically isolated with no observable surface water connections, and ranged in size from 0.2 to 1.24 ha (Table 3-1). While the dominant soil series varies among sites (Table 3-1), all were characterized by ~1 m sandy soil profiles overlain with an organic layer and confined below by a clay aquitard. Sites were selected from an a priori human disturbance gradient; land uses ranged from minimal human disturbance (i.e., reference) to silviculture, agriculture (improved pasture and row crops), to urban (Table 3-1).

Table 3-1. Site locations with land use, area, soil series, and condition scores using the uniform mitigation assessment method (UMAM) and Florida wetland condition index (FWCI).

Site	Land Use	Location	Area (ha)	Soil Series ¹	UMAM ²	FWCI ²
R1	Protected Park	30.47229 -81.49923	1.06	Evergreen-Wesconnett Complex	0.933	49.0
R2	Conserved Forest	30.17871 -81.93942	1.05	Plummer Fine Sand	0.833	43.0
R3	Conserved Forest	30.16982 -81.93639	1.24	Plummer Fine Sand	0.833	44.0
R4	Protected Park	30.30300 -82.41403	0.33	Mascotte Fine Sand	0.833	46.2
S	Silviculture	29.47003 -83.09615	0.67	Clara, Oktown, and Meadowbrook	0.800	37.4
A1	Ag_Row Crops	29.80023 -82.41417	0.48	Pomona Sand	0.767	17.4
A2	Ag_Row Crops	29.79495 -82.41924	0.36	Pomona Sand	0.633	36.5
U1	Urban	30.20991 -82.64868	0.65	Surrency Fine Sand	0.600	30.1
U2	Urban	30.11208 -81.62379	0.52	Adamsville Fine Sand	0.567	37.9
U3	Urban	30.20305 -81.76350	0.81	Surrency Loamy Fine Sand	0.433	19.9
A3	Ag_Pasture	29.74165 -82.26923	0.2	Pomona Sand	0.300	9.7

¹ Natural Resources Conservation Service Soil Survey (NRCS 2012).

² Deimeke (2009)

Ecosystem Condition

Conditional assessment estimates (Table 3-1) were previously determined (Deimeke 2009) using Florida's Uniform Mitigation Assessment Method (UMAM) and FWCI. FWCI is an intensive assessment method (Level III) that provides a multi-metric index of biological integrity (Reiss, 2006), whereas UMAM is a rapid assessment method (Level II) and the Florida mandated method for determining mitigation requirements and success (Florida Statute 373.414 (18); Chapter 62-345 F.A.C.). The resulting scores from both methods reflect the systems' surrounding land uses, with high values reported for reference sites, and decreasing values associated with increasing disturbance.

Hydrologic Regime

To test the hypothesis that land use intensity systematically alters prevailing hydrologic regime, we compared mean and variance of daily stage and flooding duration across sites. We also calculated the frequency and magnitude of daily positive and negative stage changes as a metric of site hydrologic regime (Richter *et al.* 1996). Wetland stage (relative to ground surface) was continuously measured for two years (2009 – 2011) with total pressure transducers (Solinst Gold Leveloggers[®], accuracy = 0.3 cm, resolution = 0.005 cm) deployed in monitoring wells at the deepest area of each wetland. Wetland wells were installed to a depth of 90 cm below ground; well casings were screened above and below ground surface, and constructed of 5.08-cm diameter, Sch. 40 PVC. Total pressure (m H₂O) was measured at 15-min intervals and corrected for barometric pressure variation collected at equal intervals with barometric pressure transducers (Solinst Barologgers[®], accuracy = 0.1 cm, resolution = 0.003 cm). Barometric pressure transducers were installed in a dry well below the ground surface, but open to atmospheric pressure variation, to buffer thermal conditions and avoid known temperature

sensitivity (see Chapter 1). Barometrically corrected stage data were checked and calibrated with direct stage measurements made during site visits.

ET and Groundwater Exchange

We compared measured ET and groundwater fluxes across sites to test the hypothesis that certain hydrologic functions remain despite decline in ecosystem condition. The White method was used to calculate daily ET and net groundwater flow rates from high resolution stage data for days with no rain. The method assumes ET fluxes are negligible at night, allowing net groundwater flows to be inferred from nighttime stage changes; groundwater flow rates are assumed diurnally constant. ET is inferred from 24-hour stage changes (s , where positive values indicate net stage decline; cm) corrected for groundwater exchange (h ; cm/day) and adjusted by specific yield (S_y ; dimensionless):

$$ET = S_y(24h \pm s) \tag{3-1}$$

$$\text{Exfiltration} = S_y(24h), \tag{3-2}$$

The linear slope of nighttime stage vs. time (between 0:00 - 5:00 am) for the night before and after each day were averaged to determine h . S_y is defined as the water volume released or taken into storage by a matrix divided by the matrix volume (Healy and Cook, 2002); on a unit area basis, S_y represents the input (rain) or output (ET) depth divided by the induced change in water level. S_y applies to aquifer and soil media (soil $S_y \ll 1$) or surface water systems (water $S_y \sim 1$). High S_y values under flooded conditions, which mute the ET signal vis-à-vis what is observed in groundwater applications, necessitate the high resolution pressure transducers used here.

S_y can also vary with stage, necessitating site-specific functions that describe stage dependent variation in S_y (ecosystem specific yield—ESY). We empirically determined the relationship between stage and S_y (ESY) for each site from the observed ratio of rainfall inputs to

induced stage rise (rain:rise) as a function of stage (see Chapter 2). Onset[®] RG2 data-logging tipping bucket gauges (Onset Computer Corporation, Bourne, MA) were installed at each site to collect continuous rain data from which we extracted accumulated rainfall in 15 minute increments since storm initiation. The x-intercept of rise vs. rain plots yields interception storage (Hiemburg, 1976), which was subtracted from rain accumulations; we estimated interception storage for both growing and non-growing seasons. To isolate the effects of S_y from those of catchment subsidies, we calculated rain:rise values (interception-corrected rainfall depths divided by measured stage increases) only for storm events that met the following criteria: 1) > 3 mm cumulative depth, 2) three hours or less in duration, and 3) not within 24 hours of a preceding storm event. Of the multiple functional forms (e.g., Monod equation, saturating exponential) evaluated, quadratic equations provided the best fit between S_y and stage for all sites and the site-specific ESY functions used to set S_y in Equations 3-1 and 3-2. Methodological details for construction of ESY functions are in Chapter 2.

Calculated ET rates were indexed to estimated daily PET to control for climatic variability across sites and time. Climate data from weather stations (Real-time Observation Monitor and Analysis Network; <http://raws.wrh.noaa.gov/roman>) within 5 miles of each site were used to estimate PET based on the Hargreaves method (Hargreaves and Samani, 1985). Mean indexed ET rates (ET/PET) during flooded and shallow water table (stage > -30 cm) were compared between sites. Rates determined for drier conditions diverge from ecosystem ET and only indicate the proportion of that flux that is met with groundwater uptake, introducing error when comparing indexed rates between sites; we used -30 cm as a cautious threshold to avoid such errors.

Ecosystem ET can be strongly regulated by vegetation structure, which is often affected by land use and disturbance. To test the hypothesis that vegetation structure controls ET, we compared site mean ET/PET with measured mean leaf area index (LAI) for each site. A Sunfleck[®] Ceptometer (Decagon Devices, Pullman, WA, USA) was used to measure LAI based on radiation transmittance (Chen *et al.*, 1997) vis-à-vis open canopy conditions. Discrete LAI measurements were made at each node of a 5 x 2 m grid spanning the entire wetland area at 75 cm above ground surface, capturing leaf structure of canopy and subcanopy strata; the instrument automatically averaged discrete LAI measurements and yielded mean LAI for each site.

Groundwater exchange from the White method is available only for days without rain since the method assumes constant groundwater flow and does not account for rain inputs. This constraint limits the continuity of the data set and systematically underestimates the frequency of groundwater inflow events, which are more likely to occur during and following rain events. To correct for this bias, groundwater flows on rainy days were estimated from the residuals of the daily water balance using measured 24-hour stage change (corrected for S_y), estimated ET rates, and measured precipitation. However, since ET also cannot be measured on rainy days using the White method, this flux was estimated as the product of PET on each rainy day and the site-specific mean ET/PET measured on days without rain. Daily exfiltration on rainy days was then calculated by subtracting rain depths and adding estimated ET to 24-hour stage change (corrected for S_y). We note that exfiltration rates calculated in this way include any overland flows resulting from storm events. These exfiltration data were merged with estimated groundwater flows on non-rainy days, resulting in a complete dataset of catchment-wetland exchange. This was used to evaluate whether a site is a net sink or source of water within the landscape, and the frequency, direction, and magnitude of the implied exchanges.

Hydrologic regime (mean and variance in stage, flooding duration, and daily stage change) and ET and groundwater exchange were compared across sites using the UMAM conditional assessment score as the abscissa; UMAM scores were used since the method is the mandated method in Florida for wetland mitigation. This allowed relationships between ecosystem condition, hydrologic regime (flooding dynamics), and certain hydrologic functions (ET, groundwater exchange) to be evaluated; inferences of the effects of land use intensity were facilitated along this condition gradient because of the apparent influence of land use on assessed condition (Table 3-1).

Results

Ecosystem Condition

FWCI and UMAM condition scores were strongly correlated (linear $R^2 = 0.62$, p -value < 0.005), indicating UMAM, a rapid assessment method, is a good predictor of measured biological condition via an intensive, Level III method (FWCI). Both methods reflected land use intensities, but UMAM scores more clearly grouped sites by land use category. Site A3 was the only site not to be grouped within its representative land use (agriculture) due to active grazing activities, which resulted in the lowest measured condition.

Hydrologic Regime

Despite substantial differences across sites in mean water depth (mean stage ranging from 1.1 to -0.1 m) and variation (stage standard deviation ranging from 0.25 to more than 1.0 m), we observed no clear trend with ecosystem condition/disturbance (Figs. 3-1a and 3-1b). Of particular note is the observation that stage variation in urban sites was generally low, even compared with reference sites (Fig. 3-1b). Similarly, there was no systematic variation in

flooding duration (hydroperiod) with measured condition (Fig. 3-1c), though we note that the period of stage record reported was anomalously dry (cumulative rainfall ~30 cm below normal).

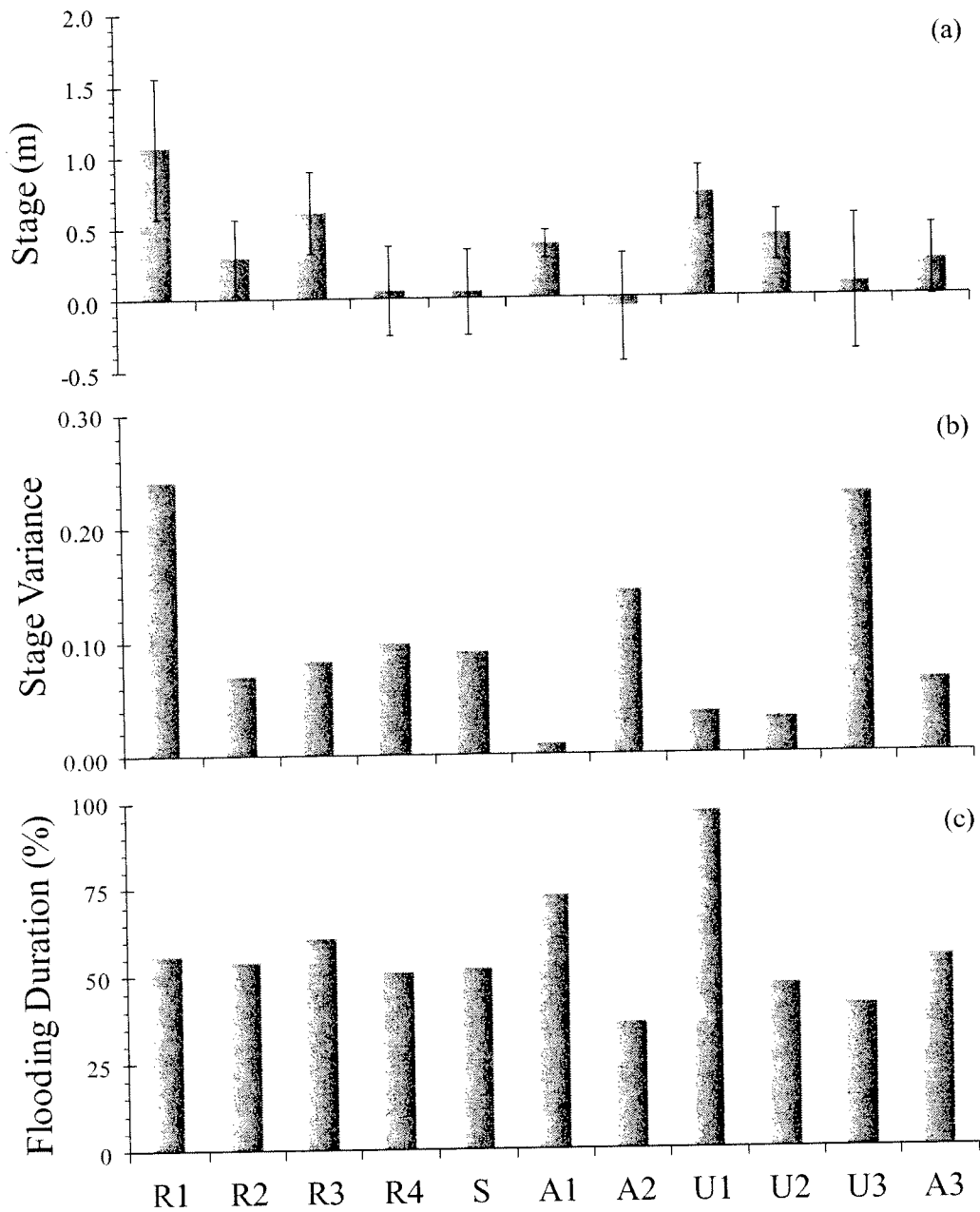


Figure 3-1. No systematic variation in (a) mean (\pm std. dev.) wetland stage, (b) variance of wetland stage, or (c) percent of time flooded is evident across a condition gradient.

Mean positive and negative daily stage changes, a more robust measure of water level ‘flashiness’ than stage variation alone, revealed no clear trend in storm responsiveness (mean positive stage change) or drying rate (mean negative stage change) with disturbance (Fig. 3-2). These results do, however, illustrate a fundamental feature of isolated wetland hydrology, with large differences between the magnitude and frequency of stage increases vs. decreases. In all cases, mean positive increases were higher in magnitude (by a factor ranging from 1.74 to 2.58) but occurred less frequently ($\leq 25\%$ of the study period). This asymmetry derives from discrete rain events that induce runoff (including subsurface flows) and create large, but low frequency, stage increases compared to smaller, but extended drying via ET and infiltration; this general behavior was remarkably consistent across all sites.

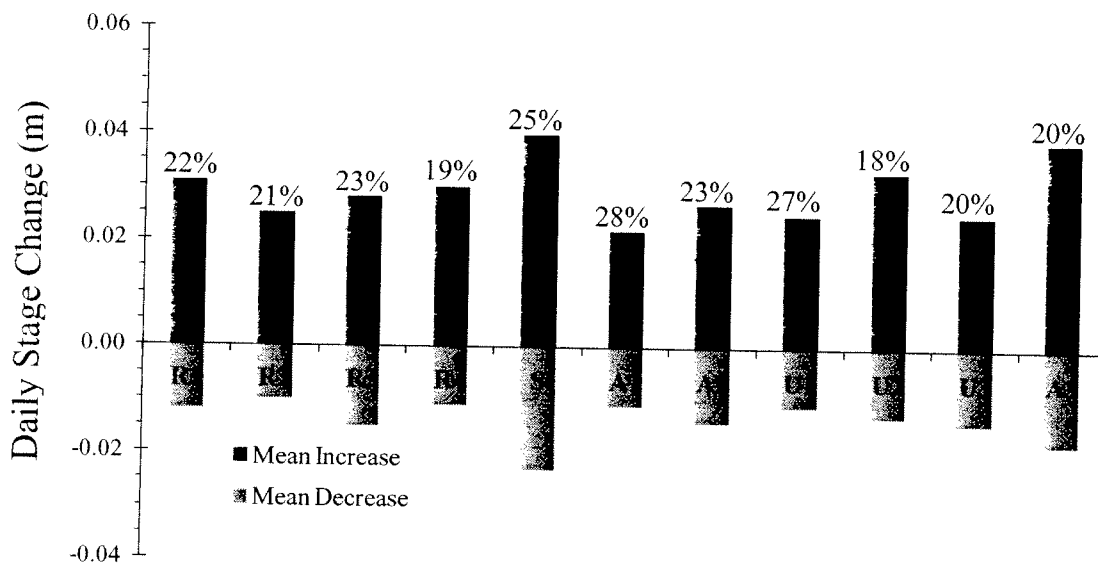


Figure 3-2. Daily stage change shows no systematic variation in mean magnitude or relative frequency of increases or decreases in stage across a disturbance gradient. The relative frequency of positive stage changes are shown as percentages of days during the study period when stage increased.

ET and groundwater exchange

Site-specific relationships between S_y and stage (ESY; Table 3-2) allowed the White method to be applied at all stages; we limited our inference to a minimum stage of -0.3 m because of uncertainty with the assumption that ET fluxes were predominantly from the saturated zone below this depth. Mean indexed ET rates (ET/PET) suggest a strong amplifying effect of disturbance on wetland ET fluxes (Fig. 3-3a). ET rates of agriculture (A) and urban (U) sites were near or above PET estimates. The exception (Site A3) is in a heavily grazed cattle pasture, which clearly affected vegetation structure via reduced LAI (Fig. 3-3b); field observations suggest the near total absence of mid-story and under-story vegetation. In contrast, the other agricultural (including silviculture) and urban sites had increased LAI relative to the reference sites, which led to the observed elevated ET rates (Fig. 3-3). Linear regression of ET/PET versus LAI yielded a strongly predictive ($R^2 = 0.78$) and significant (p-value < 0.001) relationship; the resulting slope (0.09; data not shown) suggests a 9 % increase in ET per unit increase in LAI.

Table 3-2. Quality of fit for ecosystem specific yield (ESY) relationships, along with soil S_y ($S_{y,Soil}$), which represents site-specific minimum S_y values, and the S_y value ($S_{y,Max}$) at maximum observed stage.

Site	R^2	$S_{y,Soil}$	$S_{y,Max}$
R1	0.73	0.11	0.72
R2	0.72	0.11	0.96
R3	0.50	0.16	0.84
R4	0.46	0.13	0.78
S	0.61	0.09	0.78
A1	0.73	0.25	0.71
A2	0.75	0.15	0.81
U1	0.74	0.11	0.79
U2	0.74	0.17	0.73
U3	0.98	0.13	0.99
A3	0.53	0.22	0.76

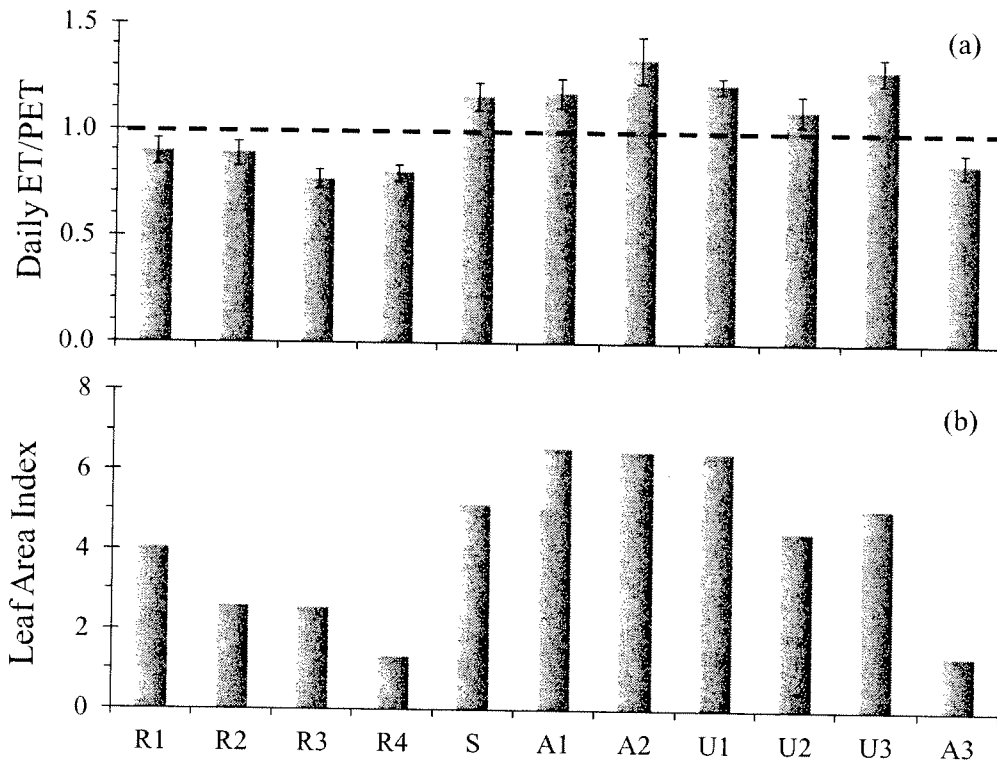


Figure 3-3. (a) Measured mean daily ET rates indexed to PET (error bars denote 95% confidence intervals) and (b) leaf area index (LAI).

The frequency and mean rates of exfiltration (inflow) and infiltration (outflow) events (Fig. 3-4) are similar to mean daily stage changes (Fig. 3-2): exfiltration events were less frequent (with the exception of A1; Fig. 3-4a) but with higher mean rates (by a factor from 1.06 to 2.61; Fig. 3-4b) compared to infiltration events. All sites, however, experienced episodic switching between net recharge and discharge (Fig. 3-4a). In contrast to metrics of flooding dynamics, ratios of cumulative exfiltration to infiltration showed systematic variation across the disturbance gradient (Fig. 3-4c). Reference sites, along with the silviculture site, had higher infiltration totals than exfiltration and acted as net recharge systems over the period of study. In contrast, sites with lower condition, with the exception of A3, were closer to being balanced (i.e., ratio = 1; dotted line in Fig. 3-4c) or served as net discharge systems. Low LAI and ET in site A3 likely explain that site's role as a net source, since less of the stored water is lost to the atmosphere.

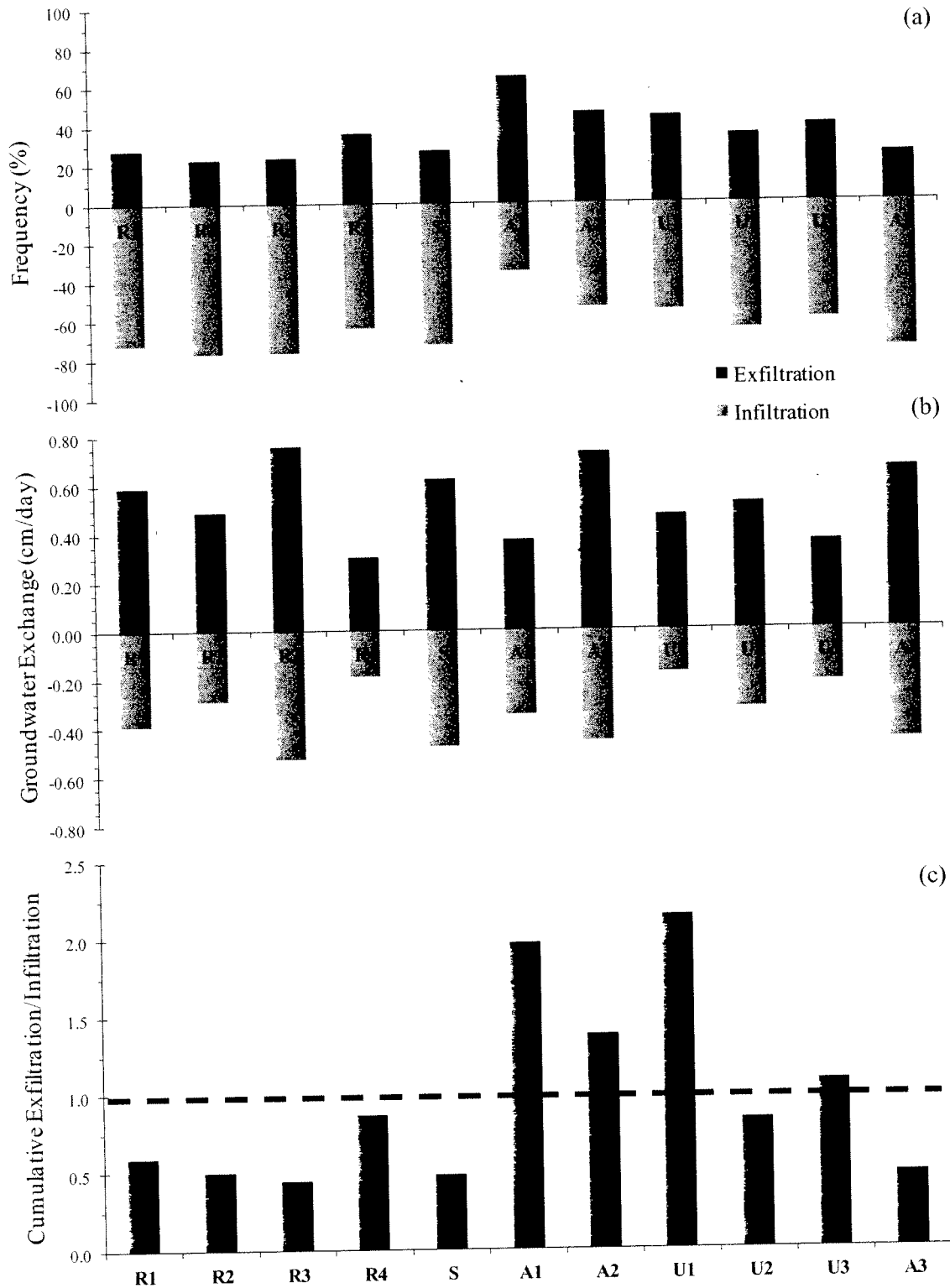


Figure 3-4. (a) Frequency (%) and (b) mean rates of daily net exfiltration and infiltration events. (c) Ratios of cumulative exfiltration to infiltration; dotted line denotes neutrality between cumulative exfiltration and infiltration.

Discussion

Hydrology, which regulates wetland habitat and process (Mitsch and Gosselink, 2007), can be strongly affected by land use (Winter, 1988; Ehrenfeld, 2000), and understanding subsequent consequences to ecosystem condition and function necessitates comprehensive hydrologic monitoring (Cole, 2006; Stander and Ehrenfeld, 2009; Gebo and Brooks, 2012). We collected high resolution wetland stage data within 11 north Florida cypress domes, allowing us to evaluate variation in hydrologic regime across a wide gradient of land use intensity and for systems within a single hydrogeomorphic subclass. Additionally, these data uniquely provided direct estimates of hydrologic function. As such, this work is novel in that it is among the few to document wetland hydrologic regime (e.g., Stander and Ehrenfeld, 2009) or hydrologic function (e.g., Siegel, 1988) across land use intensities, and to our knowledge the first to evaluate variation in both across a gradient of ecosystem condition. Wetland value largely accrues from hydrologic functions, and a complete assessment of these functions requires the type of collected data assembled here.

Hydrologic Regime

Alteration of hydrologic regime (e.g., changes in the mean and variance of depth and duration of flooding) from human disturbance has been observed across aquatic ecosystems (Richter *et al.*, 1996), and such shifts in hydrologic regime can severely affect habitat suitability for vegetation, macroinvertebrates, and fishes. A priori evaluations of human disturbance, however, may not accurately predict hydrologic alteration (Standar and Ehrenfeld 2009), underscoring the need for site-specific hydrologic evaluation (Gebo and Brooks, 2012). Widely available river stage data allows hydrologic regime to be interpreted from long-term data sets, and frequently with records of pre- and post-disturbance regimes (Richter *et al.*, 1996, Richter *et*

al., 1997). Such data sets from wetland systems are limited, leading to the routine use of reference sites and synoptic indicators to estimate a site's departure from reference hydrologic regime. Wetlands, however, are largely diverse in their geomorphic positioning, which introduces complexity when identifying reference sites; the hydrogeomorphic classification system (HGM; Brinson, 1993) accounts for this variation, allowing comparisons between sites and reference sites with similar geomorphic controls.

Alteration of hydrologic regime in our sites was not predicted by a priori identification of disturbance or evident with comparisons to reference site conditions. Our sites were all cypress domes, a specific HGM subclass, in north Florida, but contrary to our expectation, no clear effect of land use on hydrologic regime was observed (Figs. 3-1 and 3-2). These findings reinforce those of Stander and Ehrenfeld (2009), who also observed poor correlation between hydrologic regime and a priori-determined disturbance within HGM classes. Moreover, we found no characteristic reference regime within our HGM subclass. In fact, the largest differences in mean stage between sites occurred within the reference category, which surprisingly included the site with the highest stage variance (i.e., flashiness commonly associated with urbanization; Ehrenfeld *et al.*, 2003). Land use intensity resulted in impaired habitat quality and ecosystem condition (via UMAM and FWCI assessments), but the impacts to hydrologic regime were less clear in these isolated wetlands where local soil and topographic variation may exert primary controls on flooding dynamics.

Hydrologic Function

Functions related to hydrology extend beyond habitat suitability and include ecosystem services regulated by groundwater and ET flows. While these flows have remained difficult to directly measure, methods presented here, together with data with requisite resolution and

accuracy (see Chapters 2 and 3), provide empirical, low cost quantification of these fluxes in inundated conditions. As such, applications of the White method can be extended to surface water systems (e.g., lakes, wetlands), where empirical assessments of ET and groundwater flows provide salient insights regarding ecohydrologic controls on functions related to ecosystem water use and exchange.

Abiotic drivers (e.g., fire, nutrient loading, and hydrology) strongly control ecosystem productivity and water use (Keddy, 2010), with these two tightly coupled processes influencing multiple ecosystem functions. As such, measured ET informs inferences of local climate regulation, ecosystem productivity, C-sequestration, and biogeochemical functions. ET directly indicates the rate of latent heat exchange that regulates local temperatures (Taha, 1997), and particularly in forested systems where transpiration dominates the ET flux, provides a relative measure of productivity (Law *et al.*, 2002). Amplified ET is highly suggestive of commensurate increases in productivity and the associated organic carbon for sequestration and to enhance biogeochemical processes responsible for improved water quality (e.g., denitrification—[Hernandez and Mitsch, 2007]; dehalogenation of toxins—[Mohn and Tiedje, 1992]).

Opposite to our measured metrics of hydrologic regime, there was a clear effect of land use on vegetation structure and its regulation of ET fluxes. Urbanization and agriculture land uses result in reduced, if not complete removal, of fire regime while typically increasing nutrient loading (Ehrenfeld, 2000), leading to augmentation of vegetation structure (Keddy, 2010). We observed increased vegetation structure as LAI in more disturbed sites, suggesting the impact of land use on ecosystem productivity and water use (Fig. 3-3). LAI may be the most informative of various metrics of vegetation structure when estimating productivity and water use rates since it is a direct measure of the surface exchange area for carbon and water (Vose *et al.*, 1994; Law

et al., 2002). The relationship between White-measured indexed ET rates (ET/PET) and LAI was strong and significant (Fig. 3-3), explaining the increased ET rates in more disturbed sites and supporting the inference of productivity from measured ET rates in our forested systems.

Although wetlands are commonly, and often erroneously, recognized as locations for groundwater recharge (Winter, 1999), it is their ability to buffer aquifer dynamics that may be most important. Depressional wetlands have been observed to regularly switch in groundwater flow direction (Winter, 1999; Riekerk and Korhnak, 2000) due to different fluctuations in groundwater and surface water levels in response to ET and rain fluxes. Sign reversals in groundwater exchange result in wetlands that alternate between serving as a sink and source of water; this behavior ultimately buffers surficial aquifer dynamics within the landscape, where wetlands provide water storage capacitance to decrease water table response to dry and wet conditions.

All of our sites demonstrated regular sign reversals and thus the ability to buffer aquifer dynamics, regardless of their surrounding land use intensity (Fig. 3-4). Ratios of cumulative of exfiltration to infiltration, however, suggest that wetlands surrounded by forested uplands (i.e., reference and silviculture land uses) may act more as net recharge systems, whereas higher land use intensities tend to increase the flows a wetland receives (Fig. 3-4c). During periods with no rain, transpiration in forested uplands maintains a greater gradient for wetland infiltration, whereas exfiltration following rain events may be amplified in higher land use intensities due to increased impervious surfaces, soil compaction, and drainage networks. Both groundwater recharge to support upland productivity and water storage of stormwater flows represent important hydrologic functions of systems that range in ecosystem condition.

Condition versus Function

The relationship between ecosystem condition, hydrologic regime, and hydrologic function provides new insights regarding the distinction between condition and function. The emerging awareness that ecosystem condition and function are not necessarily equivalent (Hruby, 2001; Stander and Ehrenfeld, 2009) leads to a disconnect between what we value (i.e., a diverse set of functions that create ecosystem services) and how we commonly assess that value (i.e., departure from reference conditions). This disconnect is a particular challenge for wetland management and mitigation, which are motivated by the myriad ecosystem services wetlands provide. It is imperative to validate that impaired wetland quality (i.e., via synoptic indicators of hydrologic condition, biological and structural integrity, and disturbance; Fennessy *et al.*, 2004) means diminution in total functionality if we are to successfully realize “no net loss” of wetland function.

This study of isolated wetland hydrology further reinforces the contention that function and condition are poorly correlated, at least with regard to the hydrologic functions that are identified as among the core services wetlands provide. The ability of wetlands to buffer surficial aquifer dynamics remained despite variation in ecosystem condition. Furthermore, LAI and ET increased with decreasing condition, indicating amplified latent heat exchange and productivity in agriculture and urban settings, where increased productivity may augment C-sequestration and biogeochemical cycles.

Location is critically important in regards to which functions are realized as opposed to those that remain as potential (Hruby, 1999). Minimally altered landscapes benefit more from habitat quality (i.e., ecosystem condition) than from temperature regulation, water quality, and water storage services that are valuable, realized, and possibly amplified in disturbed landscapes. We

measured higher ET rates in urban landscapes, which uniquely benefit from latent heat exchange and cooling land covers (Taha, 1997). Furthermore, amplified productivity in urban and agriculture systems suggests increased potential for water quality functions. Elevated denitrification rates have been measured in more disturbed wetlands (Jordan *et al.*, 2007; Stander and Ehrenfeld, 2009), supporting our inferences from measured ET and LAI. Similarly, wetlands in higher land use intensities acted more as water sinks, likely attenuating stormwater flooding in such landscapes. In undeveloped landscapes, however, reduced ET and water conservative ecosystems may result in increased recharge to aquifers. Notably, stimulation of an ecosystem process (e.g., ET) may represent an ecosystem service in one landscape setting (alleviation of urban heat island effects) but unfavorable in another (decrease in regional water yield).

Amplification of certain functions (e.g., latent heat exchange, C-sequestration, and water quality improvements) may be at the expense of others (e.g., habitat), representing a tradeoff between ecosystem services. It is this tradeoff that is not fully addressed with current wetland regulation and mitigation, which heavily weights habitat and underestimates the value of “working wetlands”. We note that not all assessment methods are restricted to biological condition, with some, namely the federally preferred HGM functional assessment method (Hauer and Smith, 1998), targeted at directly assessing function (Brinson and Rheinhardt, 1996). Similar to other assessment methods, however, the HGM method relies on reference sites for calibration of structural indicators to infer function, meaning that a priori determination of disturbance defines what represents maximum functionality (Stander and Ehrenfeld, 2009). The assumption, however, that function is maximized under reference conditions is clearly not tenable for all ecosystem functions.

Our intent is not to question the importance of ecosystem condition (e.g., biodiversity and habitat functions), but rather question the correlation between condition and function and ultimately the way in which we value impaired systems. This argument is central to wetland mitigation but is general to ecosystem management. Conservation and restoration of critical habitats should remain a principal priority, but it is also imperative to better recognize the importance of “working” ecosystems proximate to disturbance, where the consequences of human actions are most realized and potentially minimized.

CHAPTER 4

Landscape Water Storage Capacitance: A Nexus between Isolated Wetlands and Downstream Water Bodies

Abstract

Recent U.S. Supreme Court Case rulings have limited the federal protection over isolated wetlands, and now documentation of a significant nexus to a navigable water body is required for federal jurisdiction. Despite geographic isolation, however, isolated wetlands likely influence regional hydrology, including surficial aquifer dynamics and baseflow to surface water systems. Isolated wetlands have been observed to switch between recharge and discharge systems; this sink/source behavior buffers water table response to both storm events and drought. As such, wetlands with no direct surface or groundwater connection to other water bodies may still regulate the surficial aquifer that supports downstream systems. To demonstrate the importance of this wetland function at the landscape scale, we integrated models of daily fluctuations of soil moisture, upland water table, and wetland stage to simulate the effect of isolated wetland area and spatial distribution on regional water table dynamics. Increasing wetland area or density reduced water table variability and the frequency of both high and low water table events. Considering the strong influence of regional water table on downstream systems, loss of isolated wetland area or mitigation of this loss at the expense of wetland density (i.e., large mitigation banks versus small distributed systems) may increase the vulnerability of downstream water bodies to both flooding and drought conditions. Isolated wetlands buffer surficial aquifer dynamics by providing water storage capacitance at the landscape scale and ultimately exert hydraulic regulation of regional surface waters through an indirect, but still significant nexus.

Introduction

The hydrologic continuum integrates the dynamics of surface water and groundwater systems, with alterations in one system impacting the other (Winter, 1988). As such, this continuum links geographically isolated wetlands (i.e., surrounded by uplands; Tiner, 2003) to the surficial aquifer and its baseflow contribution to downstream water bodies. However, recent U.S. Supreme Court Case rulings (*Solid Waste Agency of Northern Cook County v. U.S. Army Corps—SWANCC* [2001], *Rapanos v. U.S.* and *Carabell v. U.S.* [2006]) have resulted in reduced federal jurisdiction of isolated wetlands, and now a documented “significant nexus” to navigable or interstate waters is required for a wetland to be considered as a water of the U.S. (EPA and US. Army Corps of Engineers, 2008). Significant nexus is defined as measurable influences to the “chemical, physical, or biological integrity of traditional navigable waters or interstate waters”, and is often considered for jurisdiction of wetlands adjacent to drainage features (EPA and US. Army Corps of Engineers, 2008). More recently, federal guidance has explicitly recognized that geographically isolated waters could fall under jurisdiction if a significant nexus is demonstrated, while also stressing the difficulty in such demonstration and providing little guidance (EPA and US. Army Corps of Engineers, 2011). Significant nexus was first introduced in SWANCC, and the need to better understand the offsite influences of isolated wetlands on traditional waters of the U.S. was soon emphasized (Leibowitz and Nadeau, 2003) and still remains.

With current federal regulation predicated on the interpretation and demonstration of a significant nexus, it is imperative that we question if geographic isolation means hydrologic isolation (Leibowitz, 2003). There is an obvious nexus for exchange of water and its constituents between floodplain, estuarine, and lake fringe wetlands and their adjacent surface

water bodies, as well as between headwater wetlands and tributaries; these wetlands have long been known to store flood waters (overland and stream flows) and provide baseflow to their adjacent water bodies (e.g., Carter, 1986; Ogawa and Male, 1986). The role of isolated wetlands to reduce runoff amounts and store flood waters has also been recognized (Tiner, 2003; Leibowitz and Nadeau, 2003; Lane and D'Amico 2010), though the absence of a connecting drainage network (except during extreme flooding and connections via sheetflow) may limit this hydrologic function. However, isolated systems interact with, and may significantly influence, the surficial aquifer. Baseflow to water bodies can be largely controlled by surficial aquifer dynamics (Winter, 1999), meaning any regulation of the surficial aquifer by isolated wetlands is propagated to downstream water bodies. Here we explore this potential nexus, where small isolated systems across the landscape may regulate regional water table dynamics through distributed water storage capacitance.

While wetlands are often referred to as discharge and recharge systems, groundwater exchange between wetlands and upland surficial aquifers has been shown to regularly reverse in direction in response to wet and dry cycles (Winter, 1988; Winter, 1999, Riekerk and Korhnaak, 2000). This behavior is likely most pronounced in depressionnal, low relief landscapes where local groundwater patterns are highly variable and dominant (Winter, 1988). We previously observed sign reversals in hydraulic gradients between isolated forested wetlands and surrounding uplands in north Florida (Chapter 2), and these observations were concordant with calculated wetland infiltration (groundwater outflow) and exfiltration (inflow) rates (Chapter 3), demonstrating that groundwater flow reversals characterize these depressionnal systems. The switching between exfiltration and infiltration occurs due to specific yield (S_y) differences between groundwater aquifers ($S_{y,Soil} \approx 0.1 - 0.35$) and surface water ($S_{y,sw} \approx 1.0$), where

groundwater response to both rain and evapotranspiration (ET) is amplified relative to surface water fluctuations (Chapter 2). As such, wetlands act as a sink during wet cycles (via wetland exfiltration) and a source (via infiltration) to the surficial aquifer during drier times (Fig. 4-1).

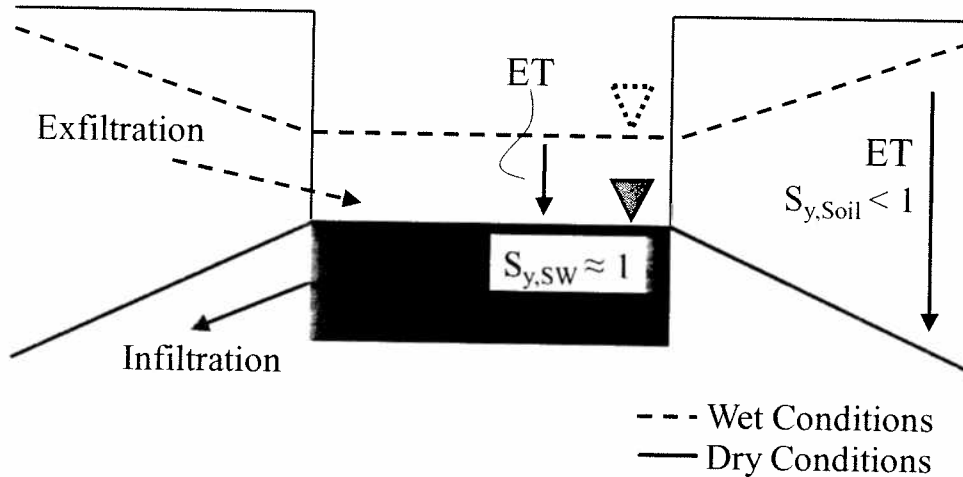


Figure 4-1. Conceptualization of groundwater exchange between an isolated wetland and its surrounding uplands. Switching between exfiltration and infiltration from wet to dry conditions, respectively, occurs due to specific yield (S_y) differences between surface water ($S_{y,SW} \approx 1.0$) and the groundwater aquifer (e.g., $S_{y,Soil} \approx 0.2$), where responses to both rainfall and ET are amplified in the upland water table.

The local sink/source patterns of wetlands due to S_y differences between aquifers and wetlands likely buffer water table fluctuations at local to regional scales, with the latter dependent on wetland area and density across the landscape. Previous research has demonstrated the strong influence of $S_{y,Soil}$ on shallow water table dynamics (Laio *et al.*, 2009), as well as stage-varying S_y effects on wetland water levels (Sumner, 2007); such efforts, however, have not investigated the integrated influences to water table dynamics that result from different S_y values between uplands and wetlands. Moreover, the cumulative area and spatial distribution of isolated wetlands likely determines the degree to which these systems provide a sink/source, or

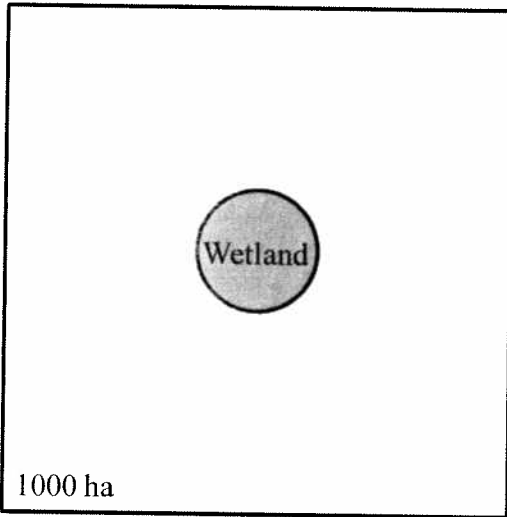
capacitance, function beyond local scales. Quantifying this function improves our understanding of the potential for isolated wetlands to buffer the regional water table and ultimately downstream water bodies. Here, we integrate existing models of shallow water table and soil moisture dynamics with a wetland water balance model to simulate the effects of wetland area and density on surficial aquifer fluctuations.

Methods

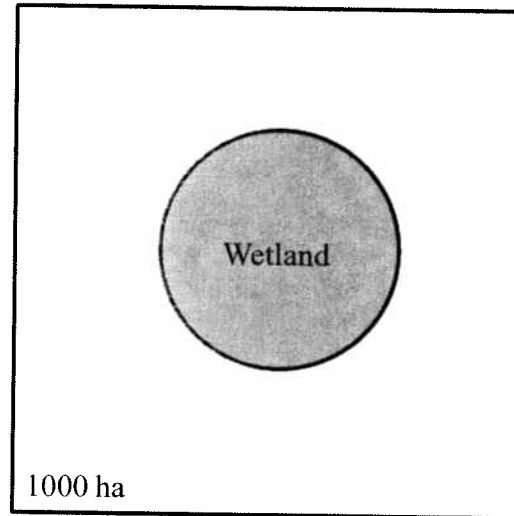
Model Description

Existing models of water table (Laio *et al.*, 2009) and soil moisture (Laio *et al.*, 2001) dynamics were integrated with modeled wetland stage fluctuations to simulate daily water table fluctuation in a generic landscape (area = 10 km²) where the area and density of isolated wetlands were varied (Fig. 4-2). The simulated landscape broadly represented the upland-wetland matrix characteristic of forested flatwood systems of the southeastern coastal plain (via soil parameters and rooting depths used; Table 4-1), where depressional, and often isolated, wetlands comprise ~30% of the landscape (Marois and Ewel, 1989). Variation in upland or wetland topography was not considered. All wetlands were cylindrical with bottom elevations 1.25 m below the mean upland soil elevation (upland elevation: $z = 0$); clay depth (i.e., confinement depth of the surficial aquifer) was set at $z = - 2.0$ m (Fig. 4-3). Wetland, and thus watershed, density was increased by factors of four, where watersheds and their wetlands remained equally distributed across the landscape and with equal areas (Fig. 4-2).

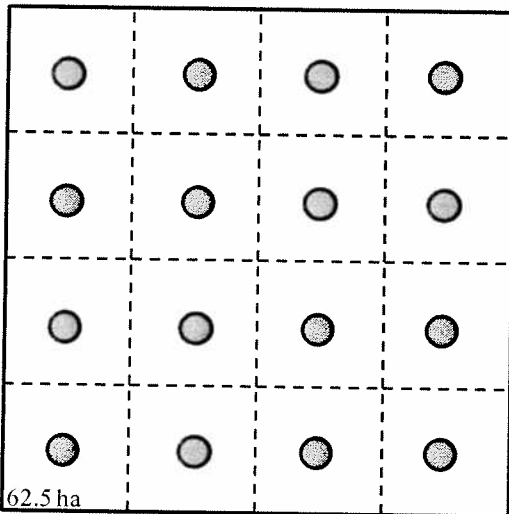
(a) Wetland Area = 10%; Density = 1



(b) Wetland Area = 30%; Density = 1



(c) Wetland Area = 10%; Density = 16



(d) Wetland Area = 30%; Density = 16

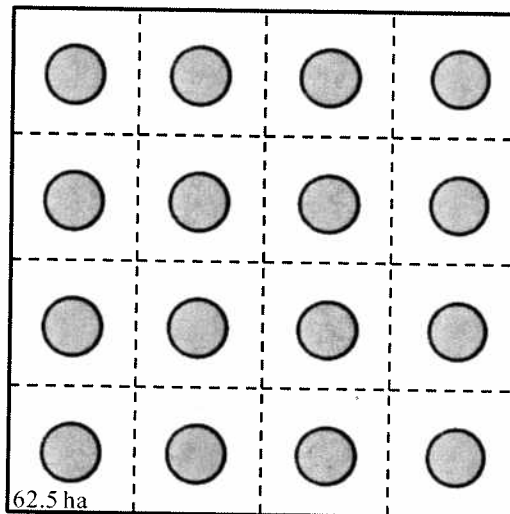


Figure 4-2. Simulated landscape where wetland area and density is varied but with wetlands being equally distributed and with equal areas. (a) One watershed with wetland area 10% of the watershed area results in wetland and upland areas of 100 ha and 900 ha, respectively; (b) 30% wetland area with one watershed increases wetland area to 300 ha, while reducing upland area to 700 ha. (c) A wetland area of 10% and 16 watersheds (each 62.5 ha) results in wetland area of 6.25 ha with an upland contributing area of 56.25 ha within each watershed. (d) 16 watersheds and wetland area of 30% results in wetland and upland areas of 18.83 ha and 43.75 ha, respectively.

Table 4-1. Soil parameters and mean rooting depth used in water table and soil moisture modeling. See text for definitions of parameters.

Parameter	Value	Source
k_{sat} (m/day)	15.2	Obreza and Collins (2008)
ψ_s (-m)	0.19	Clapp and Hornberger (1978)
s_{fc}	0.35	Laio et al. (2001)
s^*	0.33	"
s_w	0.11	"
n	0.35	Dingman (2002)
y_c	0.6	Laio et al. (2009)
b (m)	0.4	Van Rees and Comerford (1986)

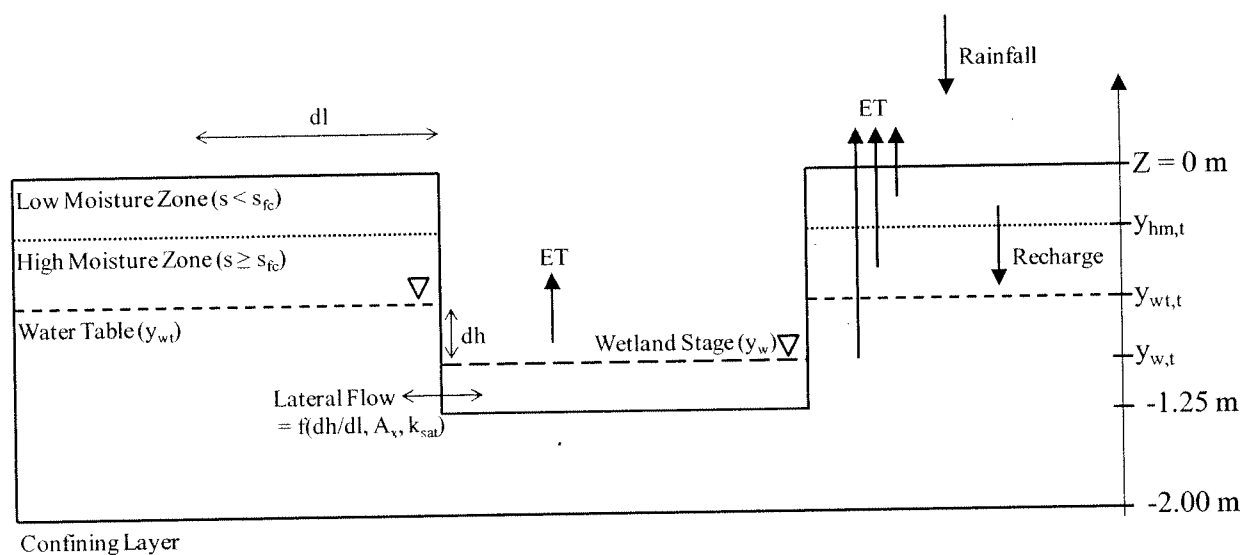


Figure 4-3. Simulated watershed with a centered, cylindrical wetland and surrounding uplands. The soil profile in the upland can be fully saturated (i.e., $y_{wt} = 0$ m) or have some unsaturated depth, separated by soil moisture (s) into high moisture and low moisture zones. Recharge to the water table is equal to rainfall when the soil profile is fully saturated or when there is no low moisture zone; soil water storage capacity in the low moisture zone reduces water table recharge. The wetland experiences ET rates equal to PET, whereas ET in the upland may be reduced with decreasing water table elevation. Lateral flow occurs along the entire wetland perimeter and is a function of saturated hydraulic conductivity (k_{sat}), dh/dl with dl as the distance between the upland's centroid and the wetland edge, and cross sectional area of exchange (A_x).

Daily rainfall and climatic data from 2000 to 2009 were obtained from the Florida Automated Weather Network (www.fawn.ifas.ufl.edu), and climatic data were used to estimate daily potential evapotranspiration (PET) with the Hargreaves method (Hargreaves and Samani, 1985). Daily rain and PET were assumed constant over the landscape and these created different fluctuations in wetland stage and upland water table due to S_y differences (Fig. 4-1), as well as soil moisture storage and the potential for $ET < PET$ in the uplands. Different fluctuations to equal rain and PET created the gradient for groundwater exchange between wetlands and uplands; overland drainage (i.e., runoff) was not considered. Only groundwater exchange between a watershed and its wetland was permitted, with no flow between other watersheds or outside of the landscape; vertical flow between surficial and deeper aquifers was also excluded.

Simulation of Wetland Stage Dynamics

Wetland stage within each simulated watershed responded to ET, rain, and lateral groundwater exchange; overland flows were excluded. Daily stage (m) was simulated with:

$$y_{w,t+1} = y_{w,t} + \frac{dy_w}{dt}; \quad (4-1)$$

$$\frac{dy_w}{dt} = \frac{1}{S_{y,sw}} (P + GW_w - ET) \quad (4-2)$$

where y_w is wetland stage elevation (m), $S_{y,sw}$ is specific yield of surface water equaling 1.0 (dimensionless); P is rain (m/day), GW_w is groundwater inflow (m/day) received (positive, exfiltration) or lost (negative, infiltration) by the wetland, and ET equals PET (m/day).

Previously, we showed that isolated wetlands can have reductions in S_y below unity with stage decrease (Chapter 2); here we excluded this effect and assumed that $S_{y,sw} = 1.0$ is reasonable for flooded systems at the landscape scale. Volumetric groundwater flow (m^3/day) was determined using Darcy's equation, the hydraulic gradient between stage and upland water table (dh), flow length (dL) equal to the distance between upland centroid and wetland edge, hydraulic saturated

conductivity (k_{sat} ; Table 4-1), and the cross sectional area for exchange (A_x) (Fig. 4-3). The latter was determined using wetland circumference and the elevation difference between wetland stage and confinement depth. Increasing wetland density and/or area increased A_x (via increase to the wetland perimeter) and decreased dl , both of which increased volumetric flow rates. Daily groundwater flow was divided by wetland area to determine GW_w as m/day (i.e., wetland exfiltration and infiltration rates). In the case where wetland stage dropped below the wetland surface ($z = -1.25$ m; Fig. 4-3), stage was set equal to the upland water table elevation.

Simulation of Upland Water Table Dynamics

Upland water table was simulated using a shallow water table model by Laio *et al.* (2009), which separates the soil profile into three zones (Fig. 4-3): 1) the saturated zone that extends $|\psi_s|$ above the water table, where ψ_s is the (negative) air entry pressure head (Table 4-1); 2) the high moisture unsaturated zone, which is above the saturated zone where soil moisture content (s) is above the soil moisture value at field capacity (s_{fc} ; Table 4-1) and bounded above by y_{hm} ; and 3) the low moisture zone above y_{hm} where $s < s_{fc}$. The low moisture zone develops only when the water table is at or below some critical depth (y_c ; Table 4-1), with this depth as a function of soil type and rooting depth (see Laio *et al.*, 2009). The water table exerts no influence on the low moisture zone through capillary rise because of the negligible unsaturated hydraulic conductivity at $s < s_{fc}$; therefore, this zone is modeled as a separate system (see below), which influences the high moisture zone and water table through its soil water storage capacity and thus reduction of water table recharge from rain events.

Daily upland water table was simulated using a daily water balance equation:

$$y_{wt,t+1} = y_{wt,t} + \frac{dy_{wt}}{dt} \quad (4-3)$$

$$\frac{dy_{wt}}{dt} = \frac{1}{S_{y,Soil}} (R + GW_{wt} - ET_{wt}) \quad (4-4)$$

where y_{wt} is water table elevation (m), $S_{y,Soil}$ is soil specific yield (dimensionless), R is recharge (m/day) from rain, GW_{WT} is groundwater flow (m/day) the water table receives (positive) or loses (negative), and ET_{wt} is the ET flux from the water table. $S_{y,Soil}$ is known to vary with water table depth (Loheide *et al.*, 2005), which is explicitly modeled for plot-scale (e.g., 1- 100 m²) water table dynamics by Laio *et al.* (2009). We assumed, however, that topographic differences over a landscape scale limits these effects and here applied a constant $S_{y,Soil}$ for all water table depths using the equation in Laio *et al.* (2009) for a constant value not influenced by water table depth:

$$n(1 - s_{fc}) \tag{4-5}$$

where n is porosity and s_{fc} is soil moisture at field capacity; values for these soil parameters (Table 4-1) resulted in a $S_{y,Soil} = 0.22$, which is in the range of fine and medium sandy soils (Healy and Cook, 2002).

Following Laio *et al.* (2009), we assumed that the unsaturated hydraulic conductivity in the high moisture zone is large enough so that water redistribution is instantaneous at the daily timescale and that recharge (R) to the water table equals the depth that reaches the high moisture zone. Therefore, when $y_{wt} > y_c$ (i.e., no low moisture zone), recharge equals the rain depth, and when $y_{wt} \leq y_c$, recharge equals rain depth less the vadose storage in the low moisture zone (see below). Volumetric groundwater flow (m³/day) was calculated as before, but here divided by upland area and reversed in sign to determine GW_{wt} as (m/day).

Similar to recharge, ET fluxes from the high moisture zone were assumed to be instantaneously met from capillary rise from the water table. Therefore, ET_{wt} is the sum of root uptake and soil evaporation from both the water table and high moisture zone, and when $y_{wt} > y_c$, ET_{wt} equals PET. However, when $y_{wt} \leq y_c$, root uptake from both the high moisture zone and

water table is reduced, because, in this case, some percentage of the total root biomass exists in the low moisture zone. The reduction in ET_{wt} with $y_{wt} \leq y_c$ was modeled as exponential decline function as done in Laio *et al.* (2009) assuming an exponential distribution of root biomass (Schenk and Jackson; 2002) and using:

$$ET_{wt} = PET \times e^{y_{hm}/b} \quad (4-6)$$

where y_{hm} is the elevation of the upper boundary of the high moisture zone and b is the mean rooting depth of all upland vegetation (value used here represented coastal plain flatwood ecosystems; Table 4-1).

The water table elevation was bounded by elevations of confinement depth and ground surface (i.e., $-2 \leq y_{wt} \leq 0$). The former represented the case of complete drying of the surficial aquifer, which remained until R resulted in rewetting. The ground surface limit was imposed to reflect that flooding of uplands (i.e., $y_{wt} > 0$) results in overland flows that effectively drain any standing water, with fully saturated upland soils remaining (i.e., $y_{wt} = 0$).

Simulation of Soil Moisture in the Low Moisture Zone

At a water table below y_c , a low moisture zone develops where $s < s_{fc}$. Following Laio *et al.* (2009), the elevation of the boundary (y_{hm}) between the high moisture and low moisture zones was modeled as a function of y_{wt} , y_c , b , ψ_s , and s_{fc} (Table 4-1; see Laio *et al.* [2009] for model details). A soil moisture modeling approach similar to Laio *et al.* (2001) was applied to simulate the dynamics of the low moisture zone using a volume-balance equation applied to determine average soil moisture content (s) over the low moisture zone profile:

$$s_{t+1} = s_t + \frac{ds}{dt} \quad (4-7)$$

$$n|y_{hm}| \frac{ds}{dt} = P - L(s) - ET_{lm}(s) \quad (4-8)$$

where n is porosity (Table 4-1), $|y_{hm}|$ is the absolute value of upper boundary of the high moisture zone (i.e., the thickness of the low moisture zone profile; Fig. 4-3), P is rain (m/day), L is leakage (m/day) to the high moisture zone, and ET_{lm} is the ET flux from the low moisture zone; both L and ET_{lm} are a function of antecedent soil moisture content (s_t). As before, unsaturated hydraulic conductivities at $s > s_{fc}$ are assumed large enough for instantaneous water redistribution. Therefore, vadose storage of the low moisture zone is equal to $n |y_{hm}| (s_{fc} - s)$, and any excess water infiltrates to the high moisture zone through leakage (L). As such, $P - L$ represents vadose storage, with L recharging the water table (i.e., R in equation 4-4 when $y_{wt} \leq y_c$).

The difference between PET and ET_{wt} was applied as potential ET uptake from the low moisture zone (PET_{lm}), with water availability (s_t) determining the degree to which this potential flux is met through ET in the low moisture zone (ET_{lm}). Similar to Laio *et al.* (2001), we assumed that ET_{lm} equals PET_{lm} when $s > s^*$, where s^* (Table 4-1) represents the threshold soil moisture at which point ET_{lm} is reduced relative to PET_{lm} because of lower water availability and plant water stress. Below s^* , ET_{lm} linearly decreases to zero at a soil moisture content representing the permanent wilting point (s_w ; Table 4-1) with:

$$ET_{lm} = PET_{lm} \frac{(s - s_w)}{(s^* - s_w)} \quad (4-9)$$

This approach slightly departs from Laio *et al.* (2001), where some loss via soil evaporation occurs when $s_h < s < s_w$, with s_h as the hygroscopic soil moisture; we assumed that these losses are negligible and excluded consideration here.

Simulated daily fluctuations in soil moisture, water table, and wetland stage were integrated via vadose storage effects to water table recharge, ET_{wt} control on ET_{lm} , and lateral exchange between wetlands and uplands. The integrated models were applied over a 10 year period (1999-

2009) using daily rain and PET to simulate the effects of isolated wetland area and density on water table dynamics.

Results

Increasing wetland area (as % of the landscape), but with constant wetland density ($n=256$), reduced water table responses to both wetting and drying periods (Fig. 4-4a). Wetland area maintained at 30%, but with decreased wetland density ($n=4$), resulted in water table fluctuations (Fig. 4-4b) similar to low wetland area (5%) with high density ($n=256$; Fig. 4-4a), revealing the strong influence of wetland distribution on water table regulation (Fig. 4-4b). The effects of wetland area and density are more evident in frequency histograms of upland water table elevation; higher areas or densities tightened the histograms with less frequent high and low water table events (Fig. 4-5). Comparing simulated elevations of wetland stage and upland water table, along with daily wetland groundwater flows (GW_w), demonstrates the mechanism creating the buffering effect from wetland area and density (Fig. 4-6). Upland water table responds more to rain and ET fluxes than wetland stage (Figs. 4-1 and 4-6a), creating the gradient for wetland exfiltration and infiltration, respectively (Fig. 4-6b).

Summary statistics of simulated upland water table elevation across a range of wetland areas, but with constant wetland density ($n=256$), are shown in Table 4-2. Increasing wetland area has marginal, and not unidirectional, effects on mean water table elevation. However, the influence of wetland area on water table variability is clear, with a linear decrease in standard deviation from 0.46 m with no wetlands to 0.32 m with a wetland area of 40%. Similarly, increasing wetland density, but with a constant wetland area (30%), resulted in decreased water table variability, but with negligible effects to mean water table (Table 4-3).

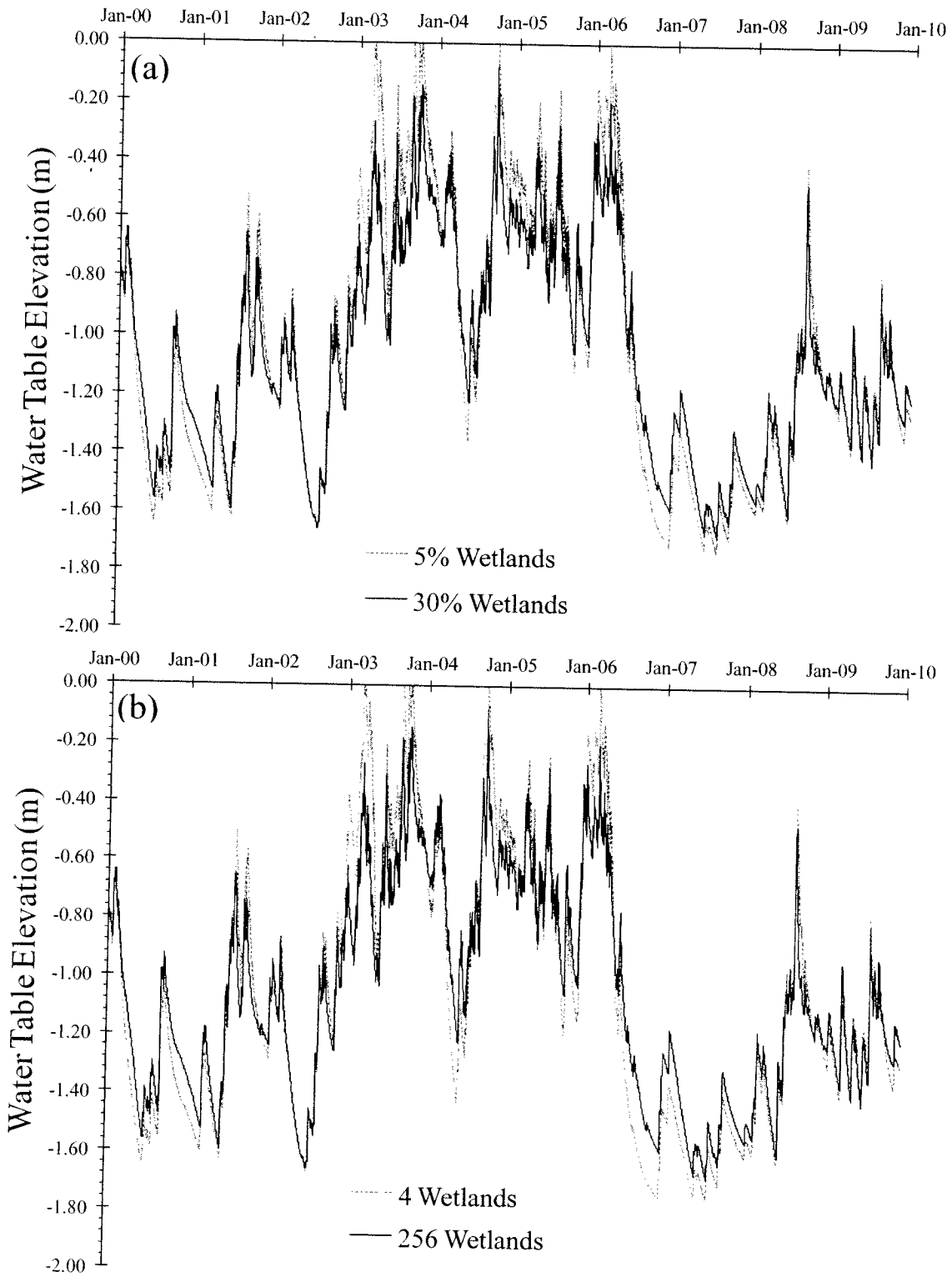


Figure 4-4. (a) Increasing wetland area from 5 to 30% of the total landscape area but with equal wetland density ($n=256$) results in more buffered responses to extreme wet and dry time periods. (b) Increasing wetland density, while keeping total wetland area at 30% of the landscape, also results in increased buffering.

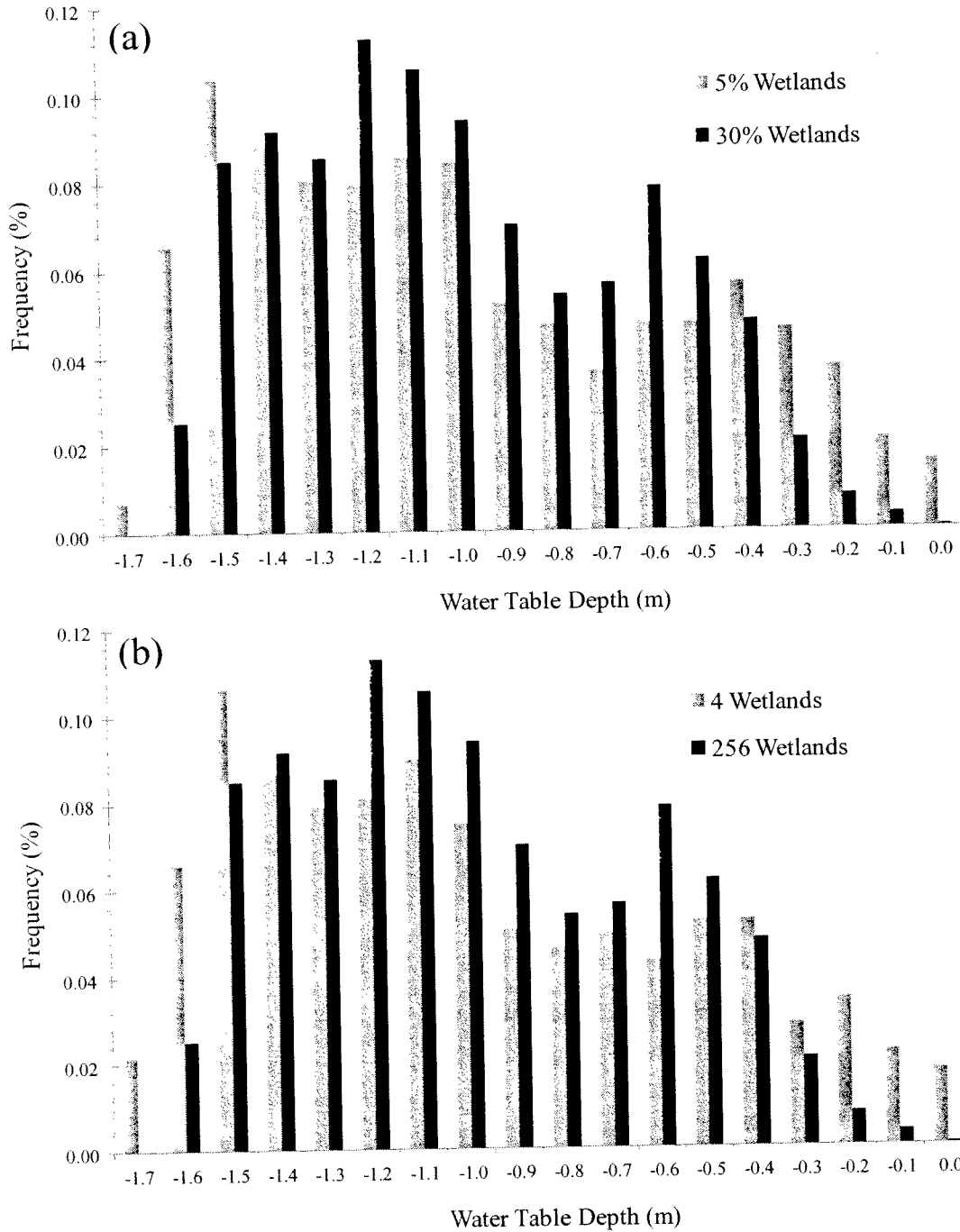


Figure 4-5. Frequency histograms of upland water table depth with (a) wetland areas of 5 to 30% but with equal wetland density (n=256) and (b) wetland densities of 4 and 265 with constant wetland area of 30% show less frequent high and low water table events with increasing area or density of wetlands.

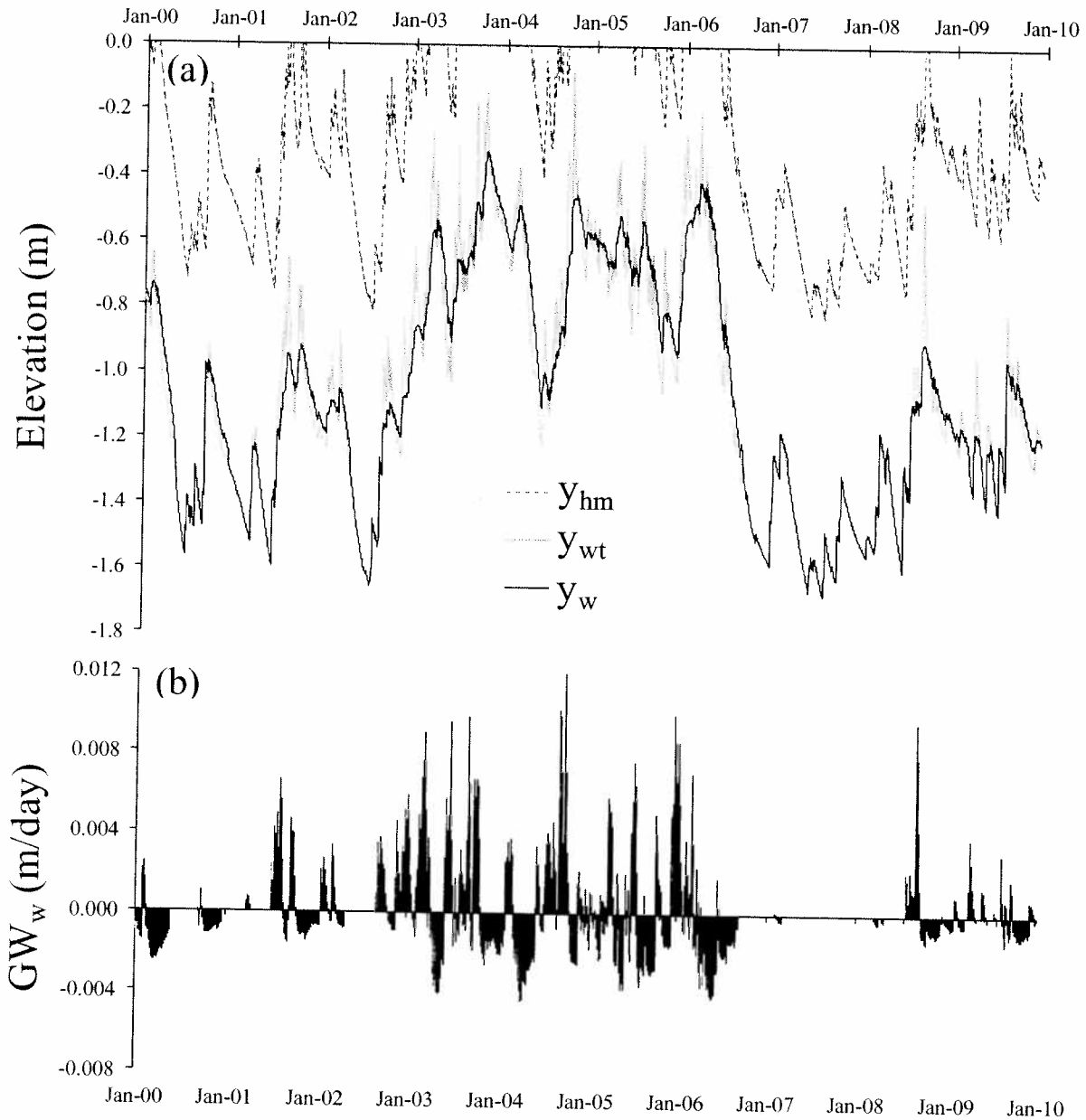


Figure 4-6. (a) Wetland stage (y_w) and water table (y_{wt}) elevations with wetland area of 30% ($n=256$) show reversals in hydraulic gradient, which is realized in (b) switching between exfiltration (positive GW_w) and infiltration (negative GW_w) events. The elevation of the upper boundary (y_{hm}) of the high moisture zone is also shown (a), indicating the transient presence and depth of a low moisture zone.

Table 4-2. Summary statistics of simulations with increasing wetland area at constant wetland density (n=256)

Wetland Area (%)	Mean	Water Table (m)			Groundwater Exchange		
		S.D.	Min.	Max.	+ GW _w (cm/day)	-GW _w (cm/day)	Flow (m ³ /day)
0	-1.04	0.46	-1.75	0.00	0.00	0.00	0
5	-1.03	0.45	-1.73	0.00	0.40	-0.27	1058
10	-1.03	0.44	-1.71	0.00	0.32	-0.22	1764
20	-1.03	0.40	-1.69	0.00	0.26	-0.17	2850
30	-1.05	0.36	-1.68	-0.08	0.23	-0.13	3541
40	-1.07	0.32	-1.68	-0.19	0.20	-0.11	4000
50	-1.10	0.29	-1.68	-0.28	0.18	-0.09	4248

Table 4-3. Summary statistics of simulations with increasing wetland density at constant wetland area (30%).

Wetland Density	Mean	Water Table (m)			Groundwater Exchange		
		S.D.	Min.	Max.	+ GW _w (cm/day)	-GW _w (cm/day)	Flow (m ³ /day)
1	-1.05	0.46	-1.75	0.00	0.003	-0.001	45
4	-1.05	0.45	-1.75	0.00	0.010	-0.004	165
16	-1.06	0.43	-1.73	0.00	0.03	-0.02	568
64	-1.05	0.39	-1.69	0.00	0.10	-0.06	1661
256	-1.05	0.36	-1.68	-0.08	0.23	-0.13	3541
1024	-1.05	0.35	-1.68	-0.12	0.52	-0.22	6306

Also shown in Tables 4-2 and 4-3 are mean daily wetland exfiltration (+GW_w) and infiltration (-GW_w) rates, along with mean daily volumetric flows cumulatively exchanged across the landscape. Increasing wetland area at constant density from 0 to 10% increased mean wetland exfiltration and infiltration rates, but these rates declined with further increases in wetland area (Table 4-2). Mean volumetric flow rates, however, continued to increase with increasing wetland area (Table 4-2). Increasing wetland area increases the perimeters for exchange, increasing landscape volumetric flows, but also increases the denominator (i.e., wetland area) used to determine daily exchange as depth that the wetland receives (exfiltration) or loses (infiltration). Increasing wetland density, but with constant wetland area, increased volumetric flow, wetland exfiltration, and wetland infiltration rates (Table 4-3).

We further investigated the effect of wetland area and density on water table response by evaluating the cumulative frequency of extreme water table events. The percentage of time upland water table elevation was lower than -1.5 m (extreme low water table) was calculated across a range of wetland areas but with constant wetland density ($n=256$), and for a range of densities with constant wetland area (30%); this was also performed for the percentage of time that the water table exceeded -0.25 m (extreme high water table). The frequency of extreme low water table events decreased by approximately 10% as wetland area approached 40%, but then slightly increased with further increases in wetland area (Fig. 4-7a), due to increased landscape storage confounding the effects of landscape capacitance. The frequency of extreme high water table decreased from 7% with no wetlands to near zero with wetland area at or above 30% (Fig. 4-7a). Similarly, increasing wetland density decreased the frequencies of extreme low and high water table events (Fig. 4-7b). Notably, wetland densities of one or four, with a wetland area of 30% (Fig. 4-7b), have frequencies that are near those of a landscape with no wetlands (i.e., the y-intercept of Fig. 4-7a), again highlighting the strong influence of wetland distribution.

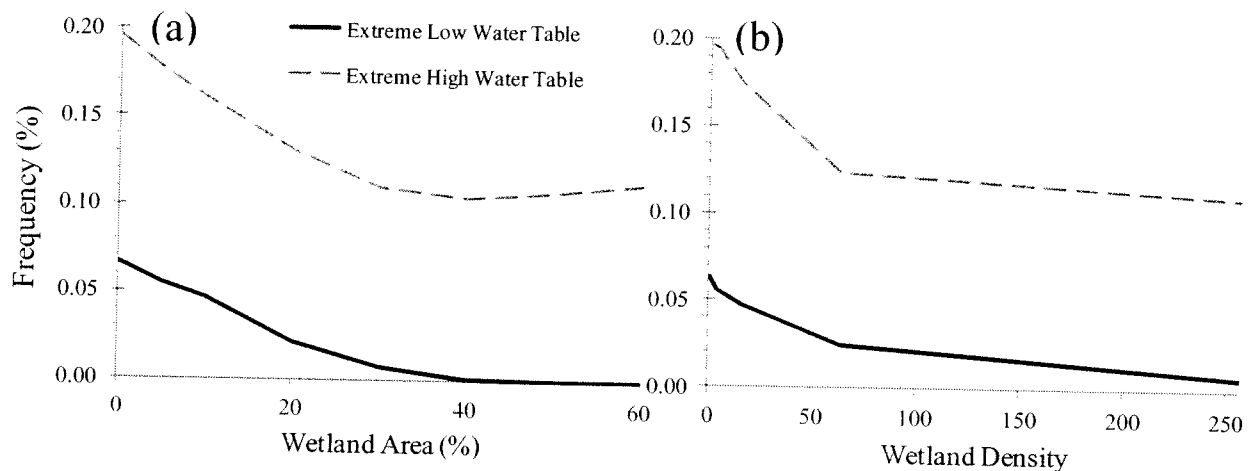


Figure 4-7. Frequencies of extreme low ($y_{wt} < -1.5$) and high ($y_{wt} > -0.25$) water table events decrease with increasing wetland area at constant density (256 wetlands) and increasing wetland density at constant wetland area (30%).

Discussion

The decreased regulation of isolated wetlands calls for a better understanding of the role of these systems within the landscape, particularly to what degree geographic isolation restricts influences to regional hydrology (Leibowitz, 2003). To evaluate the effect of surface morphology on regional groundwater necessitates evaluation of water table dynamics, which are influenced by both regional and local topography (Winter, 1988). In low relief depressional landscapes, water table dynamics are controlled by local groundwater flow patterns, and to less extent by regional topographic position (Winter, 1988). Here, we applied models of soil moisture, water table elevation, and wetland stage within a depressional landscape that demonstrated the effect of wetland area and density to regulate the regional water table through local groundwater flow patterns.

Regional groundwater connections between isolated wetlands and distant water bodies can range from effective to negligible (Winter and LaBaugh, 2003); the former case clearly suggests significant nexus (e.g., influences to stream water quality and flows), while the latter questions the importance of local groundwater patterns on regional water table regulation. Specific yield (S_y) differences between surface water and groundwater systems amplifies upland water table fluctuations relative to wetland stage in response to both rain events and ET fluxes (Fig. 4-6a), resulting in a gradient for local groundwater exchange between wetlands and uplands (Fig. 4-6b). We previously measured groundwater exchange between isolated forested wetlands and their surrounding uplands (Chapters 2 and 3), where switching between wetland exfiltration and infiltration frequently occurred. Simulations here resulted in similar groundwater flow rates (Tables 4-2 and 4-3) and sign reversals (Fig. 4-6) as to those measured in Chapter 3, and

demonstrated that this alternating sink/source action of wetlands provides water storage capacitance that buffers water table dynamics (Fig. 4-4).

The influence of S_y differences between wetlands and surrounding uplands is realized through local groundwater exchange, and the cumulative magnitude and distribution of this exchange determine the degree of water storage capacitance at the landscape scale. Increasing wetland area and/or density increases the perimeters for groundwater exchange, while also decreasing flow lengths, and both of these effects increase the total groundwater volume exchanged between wetlands and uplands across the landscape (Tables 4-2 and 4-3). The increases in the volume exchanged with increasing wetland density and area had evident effects on water table dynamics; increasing wetland area or density, with the other constant, resulted in more buffered water table responses to wetting and drying (Figs. 4-4). Though the differences between simulated water table regimes may appear modest, if not marginal, the effects of wetland area and density are more evident when comparing water table variability (Tables 4-2 and 4-3) and the frequencies of extreme low and high water table events (Figs. 4-5 and 4-7).

Waters are considered under federal jurisdiction “if they, either alone or in combination with similarly situated waters in the region, significantly affect the chemical, physical, or biological integrity of traditional navigable waters or interstate waters” (EPA and US. Army Corps of Engineers, 2011). As such, demonstration of discernible downstream effects from cumulative loss of a wetland class extends jurisdiction to an individual wetland within that class (Leibowitz, 2003). A wetland area of 30% (representing typical areas within coastal plain flatwoods; Marois and Ewel, 1989) distributed across 256 wetlands resulted in individual wetland areas (ca. 1 ha) in the range of southeastern isolated systems (e.g., cypress domes; Chapter 3). Simulating these wetland areas compared to simulations with decreased wetland area underscores the implications

of wetland loss to regional hydrology. Notably, however, conserving this wetland area but with larger and less numerous wetlands substantially reduced water storage capacitance (Table 4-3 and Fig. 4-7). This effect of wetland distribution critically questions mitigating loss of wetlands that are distributed across a region with large, concentrated mitigation banks.

Our previous empirical observations of groundwater flow reversals in isolated wetlands (Chapters 2 and 3) and the modeling efforts here that those observations prompted demonstrate that there exists a “hydraulic” nexus between isolated wetlands and distant water bodies. We point out hydraulic because water within these wetlands may never reach downstream systems, but isolated wetlands, nevertheless, exert regulation on regional surficial aquifer dynamics via water storage capacitance distributed across the landscape. As such, and despite geographical isolation, there may exist an indirect, but still significant nexus between isolated and navigable waters via hydraulic regulation of regional groundwater systems.

REFERENCES

- Ban-Weiss, G.A., Bala, G., Coa, L., Pongratz, J., Caldeira K. 2011. Climate forcing and response to idealized changes in surface latent and sensible heat. *Environmental Research Letters* 6: doi: 10.1088/1748-9326/6/3/034032
- Bond, B.J., Jones, J.A., Moore, G., Phillips, N., Post, D., McDonnell, J.J. 2002. The zone of vegetation influence on baseflow revealed by diel patterns of streamflow and vegetation water use in a headwater basin. *Hydrological Processes* 16: 1671-1677, doi:10.1002/hyp.5022
- Brinson, M.M. 1993. A hydrogeomorphic classification for wetlands. U.S. Army Corps of Engineers Waterways Experimental Station, Vicksburg, MS, USA. WRP-DE-4, NTIS, No. AD A270 053
- Brinson, M.M., Rheinhardt, R.D. 1996. The role of reference wetlands in functional assessment and mitigation. *Ecological Applications* 6: 69-76
- Butler, J.J. Jr., Kluitenberg, G.J., Whittemore, D.O., Loheide, S.P. II, Jin, W., Billinger, M.A., Zhan, X. 2007. A field investigation of phreatophyte-induced fluctuations in the water table. *Water Resources Research* 43: W0204, doi:10.1029/2005WR004627
- Cain, S.F. III, Davis, G.A., Loheide, S.P. II, Butler, J.J. Jr. 2004. Noise in pressure transducer readings produced by variations in solar radiation. *Ground water* 42: 939-944
- Campbell, D.I., Williamson, J.L. 1997. Evaporation from a raised peat bog. *Journal of Hydrology* 193: 142-160
- Carter, V. 1986. An overview of the hydrologic concerns related to wetlands in the United States. *Canadian Journal of Botany* 64: 364-374
- Cermak, J., Kucera, J., Nadezhdina, N. 2004. Sap flow measurements with some thermodynamic methods, flow integration within trees and scaling up from sample trees to entire forest stands. *Trees* 18: 529-546, doi:10.1007/s00468-004-0339-6
- Chen, J.M., Rich, P.M., Gower, S.T., Norman, J.M., Plummer, S. 1997. Leaf area index of boreal forests: Theory, techniques, and measurements. *Journal of Geophysical Research* 102: 429-443
- Clapp, R.B., Hornberger, R.B. 1978. Empirical equations for some soil hydraulic properties. *Water Resources Research* 14: 601-604
- Cohen, M.J., Dunne, E.J., Bruland, G.L. 2008. Spatial variation of soil properties in cypress domes surrounded by different land uses. *Wetlands* 28: 411-422
- Cole, C.A. 2006. HGM and wetland functional assessment: Six degrees of separation from the data? *Ecological Indicators* 6: 485-493
- Deimeke, E. 2009. Efficacy of condition assessments to predict ecosystem function in isolated wetlands. M.S. Thesis, University of Florida, Gainesville, Florida

- Dingman, L. 2002. *Physical Hydrology*, 2nd Edition. Prentice-Hall, Inc: Upper Saddle River, New Jersey
- Dolan, T.J., Hermann, A.J., Bayley, S.E., Zoltek, J. Jr. 1984. Evapotranspiration of a Florida, U.S.A., freshwater wetland. *Journal of Hydrology* 74: 355-371
- Drexler, J.Z., Snyder, R.L., Spano, D., Tha Paw, K. 2004. A review of models and micrometeorological methods used to estimate wetland evapotranspiration. *Hydrological Processes* 18: 2071-2101
- Duke, H.R. 1972. Capillary properties of soils-influence upon specific yield. *Transactions of the American Society Agricultural Engineers* 15: 688-691
- Ehrenfeld, J.G. 2000. Evaluating wetlands within an urban context. *Ecological Engineering* 15: 253-265
- Ehrenfeld, J.G. 2004. The expression of multiple functions in urban forested wetlands. *Wetlands* 24: 719-733
- Ehrenfeld, J.G., Cutway, H.B., Hamilton, R. IV, Stander, E. 2003. Hydrological description of forested wetlands in northeastern New Jersey, USA—an urban/suburban region. *Wetlands* 23: 685-700
- Engel, V., Jobbágy, E.G., Stieglitz, M., Williams, M., Jackson, R.B. 2005. Hydrological consequences of Eucalyptus afforestation in the Argentine Pampa. *Water Resources Research* 41: W10409, doi:10.1029/2004WR003761
- EPA and US. Army Corps of Engineers. 2008. Clean Water Act Jurisdiction Following the U.S. Supreme Court's Decision in *Rapanos v. United States* and *Carabell v. United States*. U.S. Environmental Protection Agency and Army Corps of Engineers Guidance Memorandum
- EPA and US. Army Corps of Engineers. 2011. Draft Guidance on Identifying Waters Protected by the Clean Water Act. U.S. Environmental Protection Agency and Army Corps of Engineers Draft Guidance Document
- Ewel, K.C. 1990. Multiple demands on wetlands. Florida cypress swamps can serve as a case study. *Bioscience* 40: 660-666
- Ewel, K.C., Smith, J.E. 1992. Evapotranspiration from Florida pondcypress swamps. *Water Resources Bulletin* 28: 299-304
- Fennessy, M.S., Jacobs, A.D., Kentula, M.E. 2004. Review of rapid assessment methods for assessing wetland condition. U.S. Environmental Protection Agency Report: EPA/620/R-04/009
- Freeman, L.A., Carpenter, M.C., Rosenberry, D.O., Rousseau, J.P., Unger, R., McLean, J.S. 2004. Use of submersible pressure transducers in water-resources investigations, in Book 8, Instrumentation Sect. A, Instruments for Measurement of Water Level, USGS, Reston, V.A.

- Gavin, H., Agnew, C.A. 2004. Modeling actual, reference and equilibrium evaporation from a temperate wet grassland. *Hydrological Processes* 18: 229-246, doi:10.1002/hyp.1372
- Gebo, N.A., Brooks, R.P. 2012. Hydrogeomorphic (HGM) assessments of mitigation sites compared to natural reference wetlands in Pennsylvania. *Wetlands* 32: 321-331, doi 10.1007/s13157-011-0267-3
- Gerla, P.J. 1992. The relationship of water-table changes to the capillary fringe, evapotranspiration, and precipitation in intermittent wetlands. *Wetlands* 12: 91-98
- Gholz, H.L., Ewel, K.C., Teskey, R.O. 1990. Water and forest productivity. *Forest Ecology and Management* 30: 1-18
- Grant, D.M., Dawson, B.D. 2001. *Isco Open Channel Flow Measurement Handbook*, 5th ed., 501 pp., Isco, Lincoln, Nebraska
- Hargreaves, G.H., Samani, Z.A. 1985. Reference crop evapotranspiration from temperature. *Transactions of the American Society Agricultural* 1: 96-99
- Hauer, F.R., Smith, R.D. 1998. The hydrogeomorphic approach to functional assessment of riparian wetlands: evaluating impacts and mitigation on river floodplains in the U.S.A. *Freshwater Biology* 40: 517-530
- Healy, R.W., Cook, P.G. 2002. Using groundwater levels to estimate recharge. *Hydrogeology Journal* 10: 91-109, doi:10.1007/s10040-001-0178-0
- Heimburg, K. 1976. Hydrology of some northcentral Florida cypress domes. M.S. Thesis, University of Florida, Gainesville, FL
- Hernandez, M.E., Mitsch, W.J. 2007. Denitrification potential and organic matter as affected by vegetation community, wetland age, and plant introduction in created wetlands. *Journal of Environmental Quality* 36: 333-342, doi:10.2134/jeq2006.0139
- Hill, A.J., Neary, V.S. 2007. Estimating evapotranspiration and seepage for a sinkhole wetland from diel surface-water cycles. *Journal of the American Water Resources Association* 43: 1373-1382
- Hruby, T. 1999. Assessments of wetland functions: What they are and what they are not. *Environmental Management* 23: 75-85
- Hruby, T. 2001. Testing the basic assumption of the hydrogeomorphic approach to assessing wetland functions. *Environmental Management* 27: 749-761, doi:10.1007/s002670010185
- Hvorslev, M.J. 1951. Time lag and soil permeability in ground water observations. *U.S. Army Corps Engineering Bulletin*: No. 36
- Ingram, H.A.P. 1983. Hydrology. In *Ecosystems of the World 4A-Mires: Swamp, Bog, Fen and Moor*, Gore AJP (ed). Elsevier, Amsterdam, pp. 67-158

Jacobs, J.M., Mergelsberg, S.L., Lopera, A.F., Myers, D.A. 2002. Evapotranspiration from a wet prairie wetland under drought conditions: Paynes Prairie Preserve, Florida, USA. *Wetlands* 22: 374-385

Jordan, T.E., Andrews, M.P., Szuch, R.P., Whigham, D.F., Weller, D.E., Jacobs, A.D. 2007. Comparing functional assessments of wetlands to measurements of soil characteristics and nitrogen processing. *Wetlands* 27: 479-497

Karr, J.R., Chu, E.W. 1997. Biological monitoring: Essential foundation for ecological risk assessment. *Human and Ecological Risk Assessment: An International Journal* 3: 993-1004, doi: 10.1080/108

Keddy, P.A. 2010. *Wetland Ecology. Principles and Conservation*. 2nd Edition. Cambridge University Press, New York, New York

Lafleur, P.M., Rouglet, N.T. 1992. A comparison of evaporation rates from two fens of the Hudson Bay Lowland. *Aquatic Botany* 44: 59-69

Laio, F., Porporato, A., Ridolfi, L., Rodriguez-Iturbe, I. 2001. Plants in water-controlled ecosystems: active role in hydrologic processes and response to water stress II. Probabilistic soil moisture dynamics. *Advances in Water Resources* 24: 707-723

Laio, F., Tamea, S., Ridolfi, L., D'Odorico, P.D., Rodriguez-Iturbe, I. 2009. Ecohydrology of groundwater-dependent ecosystems: 1. Stochastic water table dynamics. *Water Resources Research* 45: W05419, doi:10.1029/2008WR007292

Lane, C.R., D'Amico, E. 2010. Calculating the ecosystem service of water storage in isolated wetlands using LiDAR in north central Florida, USA. *Wetlands* 30: 967-977, doi:10.1007/s13157-010-0085-z

Lautz, L.K. 2008. Estimating groundwater evapotranspiration rates using diel water-table fluctuations in a semi-arid riparian zone. *Hydrogeology Journal* 16: 483-497, doi:0.1007/s10040-007-0239-0

Law, B.E., Falge, E., Gu, L., Baldocchi, D.D., Bakwin, P., Berbigier, P., Davis K., Dolman, A.J., Falk, M., Fuentes J.D., Goldstein, A., Granier, A., Grelle, A., Hollinger, D., Janssens, I.A., Jarvis, P., Jenson, N.O., Katul, G., Mahli, Y., Matteucci, G., Meyers, T., Monson, R., Munger, W., Oechel, W., Olson, R., Pilegaard, K., Paw U, K.T., Thorgeirsson, H., Valentini, R., Verma, S., Vesala, T., Wilson, K., Wofsy, S. 2002. Environmental controls over carbon dioxide and water vapor exchange of terrestrial vegetation. *Agricultural and Forest Meteorology* 113: 197-120

Leibowitz, S.G. 2003. Isolated wetlands and their functions: an ecological perspective. *Wetlands* 23: 517-531

Leibowitz, S.G., Nadeau, T. 2003. Isolated wetlands: state-of-the-science and future directions. *Wetlands* 23: 663-684

- Liu, S. 1996. Evapotranspiration from cypress (*Taxodium ascendens*) wetlands and slash pine (*Pinus elliottii*) uplands in north-central Florida. Ph.D. Dissertation, University of Florida, Gainesville, FL
- Loheide, S.P. II, Butler, J.J. Jr., Gorelick, S.M. 2005. Estimation of groundwater consumption by phreatophytes using diel water table fluctuations: a saturated-unsaturated flow assessment. *Water Resources Research* 41: W07030, doi:10.1029/2005WR003942
- Lopez, R.D., Fennessy, M.S. 2002. Testing the floristic quality assessment as an indicator of wetland condition. *Ecological Applications* 12: 487-497
- Lott, R.B., Hunt, R.J. 2001. Estimating evapotranspiration in natural and constructed wetlands. *Wetlands* 21: 614-628
- Lu, J., Sun, G., McNulty, S.G., Amatya, D.M. 2005. A comparison of six potential evapotranspiration methods for regional use in the Southeastern United States. *Journal of the American Water Resources Association* 39: 621-633
- Lu, J., Sun, G., McNulty, S.G., Comerford, N.B. 2009. Sensitivity of pine flatwoods hydrology to climate change and forest management in Florida, USA. *Wetlands* 29: 826-836
- Mack, J.J. 2007. Developing a wetland IBI with statewide application after multiple testing iterations. *Ecological Indicators* 7: 864-881
- Mao, L.M., Bergman, M.J., Tai, C.C. 2002. Evapotranspiration measurement and estimation of three wetland environments in the Upper St. Johns River Basin, Florida. *Journal of the American Water Resources Association* 38: 1271-1285
- Marois, K.C., Ewel, K.C. 1983. Natural and management-related variation in cypress domes. *Forest Science* 29: 627-640
- McLaughlin, D.L., Brown, M.T., Cohen, M.J. 2011. The ecohydrology of a pioneer wetland species and a drastically altered landscape. *Ecohydrology*: doi:10.1002/eco.253
- MEA [Millenium Ecosystem Assessment]. 2005. *Ecosystems and Human Well-Being: Wetlands and Water Synthesis*. World Resources Institute, Washington, DC
- Mitsch, W.J., Gosselink, J.G. 2007. *Wetlands*. John Wiley: Hoboken, New Jersey; 582
- Mohn, W.W., Tiedje, J.M. 1992. Microbial reductive dehalogenation. *Microbiology and Molecular Biology Reviews* 56: 482-507
- Moro, M.J., Domingo, F., López, G. 2004. Seasonal transpiration pattern of *Phragmites australis* in a wetland of semi-arid Spain. *Hydrological Processes* 18: 213-227, doi:10.1002/hyp.1371
- Mould, D.L., Frahm, E., Salzman, T., Miegel, K., Acreman, M.C. 2010. Evaluating the use of diel groundwater fluctuations for estimating evapotranspiration in wetland environments: Case

studies in southeast England and northeast Germany. *Ecohydrology* 3: 294-305,
doi:10.1002/eco.108

NRCS. 2012. Natural Resources Conservation Service Soil Survey.
<http://websoilsurvey.nrcs.usda.gov/app/WebSoilSurvey.aspx>

Obrezza, T.A., Collins, M.E. 2002. Common soils used for citrus production in Florida.
University of Florida, IFAS Extension Publication, SL 193

Ogawa, H., Male, J.W. 1986. Simulating the flood mitigation role of wetlands. *Journal of Water Resources Planning and Management* 112: 114-128

Peacock, C.E., Hess, T.M. 2004. Estimating evapotranspiration from a reed bed using the Bowen ratio energy balance method. *Hydrological Processes* 18: 247-260, doi:10.1002/hyp.1373

Penman, H.L. 1948. Natural evaporation from open water, bare soil and grass. *Proceedings of Royal Soc. of London A* 193: 120-145

Peters, E.B., Hiller, R.V., Mcfadden, J.P. 2011. Seasonal contributions of vegetation types to suburban evapotranspiration. *Journal of Geophysical Research* 116: G01003, doi: 10.1029/

Reiss, K.C. 2006. Florida wetland condition index for depression forested wetlands. *Ecological Indicators* 6: 337-352

Richter, B.D., Baumgartner, J.V., Powell, J., Braun, D.P. 1996. A method for assessing hydrologic alteration within ecosystems. *Conservation Biology* 10: 1163-1174

Richter, B.D., Baumgartner, J.V., Wigington, R., Braun, D.P. 1997. How much water does a river need? *Freshwater Biology* 37: 231-249

Ricketts, T.H., Regetz, J., Steffan-Dewenter, I., Cunningham, S.A., Kremen, C., Bogdanski, A., Gemmill-Herren, B., Greenleaf, S.S., Klein, A.M., Mayfield, M.M., Morandin, L.A., Ochieng, A., Viana, B.F. 2008. Landscape effects on crop pollination services: are there general patterns. *Ecology Letters* 11: 499-515, doi: 10.1111/j.1461-0248.2008.01157.x

Riekerk, H., Korhnak, L.V. 2000. The hydrology of cypress wetlands in Florida pine flatwoods. *Wetlands* 20: 448-460

Rushton, B. 1996. Hydrologic budget for a freshwater marsh in Florida. *Water Resources Bulletin* 32: 13-21

Schenk, H.J., Jackson, R.B. 2002. The global biogeography of roots. *Ecological Monographs* 72: 311-328

Schilling, K.E. 2007. Water table fluctuations under three riparian land covers, Iowa (USA). *Hydrological Processes* 21: 2415-2424, doi: 10.1002/hyp.6393

Schilling, K.E., Kiniry, J.R. 2007. Estimation of evapotranspiration by reed canarygrass using field observations and model simulations. *Journal of Hydrology* 337: 356-363, doi:10.1016/j.jhydrol.2007.02.003

Siegel, D.I. 1988. Evaluating cumulative effects of disturbance on the hydrologic function of bogs, fens, and mires. *Environmental Management* 5: 621-626

Smithers, J.C., Donkin, A.D., Lorentz, S.A., Schulze, R.E. 1995. Uncertainties in estimating evaporation and the water budget of southern African wetland. *Man's Influence on Freshwater Ecosystems and Water Use. Proceedings of IAHS Boulder Symposium, IAHS Publication 230*

Sophocleous, M. 2002. Interactions between groundwater and surface water: the state of the science. *Hydrogeology Journal* 10: 52-67, doi:10.1007/s10040-001-0170-8

Spronken-Smith, R.A., Oke, T.R., Lowry, W.P. 2000. Advection and the surface energy balance across an irrigated urban park. *International Journal of Climatology* 20: 1033-1047

Stander, E.K., Ehrenfeld, J.G. 2009. Rapid assessment of urban wetlands: Do hydrogeomorphic classification and reference criteria work. *Environmental Management* 43: 725-742, doi:10.1007/s00267-008-9211-6

Sumner, D.M. 2007. Effects of capillarity and microtopography on wetland specific yield. *Wetlands* 27: 693-701

Taha, H. 1997. Urban climates and heat islands: albedo, evapotranspiration, and anthropogenic heat. *Energy and Buildings* 25: 99-103

Tamea, S., Muneeppeerakul, R., Laio, F., Ridolfi, L., Rodriguez-Iturbe, I. 2010. Stochastic description of water table fluctuations in wetlands. *Geophysical Research Letters* 37: L06403, doi:10.1029/2009GL041633

Tiner, R.W. 2003. Geographically isolated wetlands of the United States. *Wetlands* 23: 494-516

Van Rees, K.C., Comerford, N.B. 1986. Vertical root distribution and strontium uptake of a slash pine stand on a Florida spodosol. *Soil Science Society of America Journal* 50: 1042-1046

Vose, J.M., Dougherty, P.M., Long, J.N., Smith, F.W., Gholz, H.L., Curra, P.J. 1994. Factors influencing the amount and distribution of leaf area of pines stands. *Ecological Bulletins (Copenhagen)* 43: 102-114

White, W.N. 1932. A method of estimating ground-water supplies based on discharge by plants and evaporation from soil. Results of investigation in Escalante Valley, Utah. *US Geological Survey Water Supply Paper*: 1-105

Winter, T.C. 1981. Uncertainties in estimating the water balances of lakes. *Water Resources Bulletin* 17: 82-115

Winter, T.C. 1988. A conceptual framework for assessing cumulative impacts on the hydrology of nontidal wetlands. *Environmental Management* 12: 605-620

Winter, T.C. 1999. Relation of streams, lakes, and wetlands to groundwater flow systems. *Hydrogeology Journal* 7: 28-45

Winter, T.C., LaBaugh, J.W. 2003. Hydrologic considerations in defining isolated wetlands. *Wetlands* 23: 532-540

Wondzell, S.M., Gooseff, M.N., McGlynn, B.L. 2009. An analysis of alternative conceptual models relating hyporheic exchange flow to diel fluctuations in discharge during baseflow recession. *Hydrological Processes* 24: 686-694, doi:10.1002/hyp.7507

Wullschleger, S.D., Meinzer, F.C., Vertessy, R.A. 1998. A review of whole-plant water use studies in trees. *Tree Physiology* 18: 499-512

Zhu, J., Young, M., Healy, J., Jasoni, R., Osterberg, J. 2011. Interference of river level changes on riparian zone evapotranspiration estimates from diurnal groundwater level fluctuations. *Journal of Hydrology* 403: 381-398, doi:10.1016/j.jhydrol.2011.04.016